TU Clausthal

Doctoral Thesis

On the Coating of Mild Steel by Adherent Aluminium Layers

Amr Sayed Emam Ismail

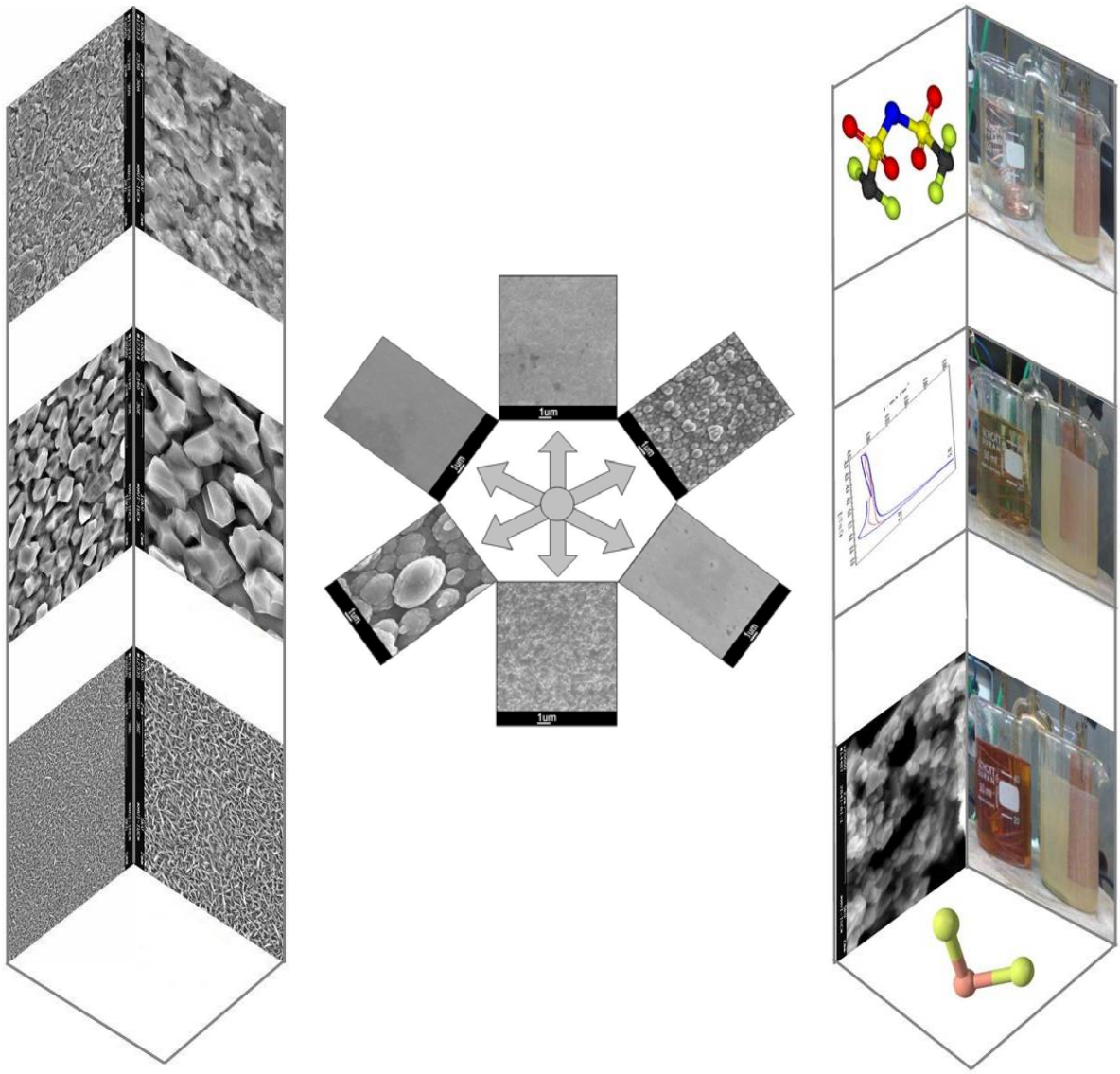

August 2010

On the Coating of Mild Steel by Adherent Aluminium Layers

Dissertation

Zur Erlangung des Grades eines Doktors
der Naturwissenschaften (Dr. rer. nat)

vorgelegt von **M.Sc.**

Amr Sayed Emam Ismail

aus Kairo / Ägypten

genehmigt von der
Fakultät für Mathematik/Informatik und Maschinenbau
der Technischen Universität Clausthal

Tag der mündlichen Prüfung
24. August 2010

Vorsitzender der Promotionskommission
Prof. Dr.-Ing. Alfons Esderts

Hauptberichterstatter
Prof. Dr. rer. nat. Frank Endres

Berichterstatter
Prof. Dr.-Ing. Ulrich Kunz

On the Coating of Mild Steel by Adherent Aluminium Layers

Doctoral Thesis

To be awarded the degree of
Doctor rerum naturalium (Dr. rer. nat)

Submitted by **M.Sc.**

Amr Sayed Emam Ismail

from Cairo / Egypt

Approved by the Faculty of
Mathematics/Computer Science and Mechanical Engineering
Clausthal University of Technology

Date of Oral Examination
24. August 2010

Chairperson of the Board of Examiners
Prof. Dr.-Ing. Alfons Esderts

Chief Reviewer
Prof. Dr. rer. nat. Frank Endres

Reviewer
Prof. Dr.-Ing. Ulrich Kunz

Acknowledgement

Primarily, I should offer my thanks, obedience and gratitude to Allah, the great from whom I receive guidance and help.

I would like to express my sincere thanks to Prof. Dr. F. Endres for his supervision, support, fruitful discussions and for offering a state of freedom in the work environment.

I also offer many thanks to Prof. Dr.-Ing. U. Kunz for reviewing my thesis and for his high morals.

I wish to express my deep thanks to Dr. S. Zein El Abedin (Professor at NRC Dokki, Cairo, Egypt) for his continued guiding and kind help in all stages of my work.

Many thanks to all our colleagues in the group for their kind help and warm feelings.

I am very grateful and thankful to Cultural Affairs and Missions Sector of the Arab Republic of Egypt for granting me the financial support for my scholarship.

Thanks also to the Egyptian Ministry of High Education and Egyptian Petroleum Research Institute (EPRI) for their interest and great help.

I am very grateful to my parents for their prayer, love, kindness and great assistances. I hope that they will be proud of me.

Finally, I would like to thank my wife Gynecologist Dr. Heba Aboutaleb for her continuous support, encouragement, patience and for taking care of our children Abdalrahman, Abdulla and Lina.

Amr Sayed Emam Ismail

Clausthal-Zellerfeld, August 2010

On the Coating of Mild Steel by Adherent Aluminium Layers

M.Sc. Amr Sayed Emam Ismail

Abstract

Due to their extra ordinary physical properties, ionic liquids stimulate a considerable interest as excellent media for chemical and electrochemical reactions. Their significantly high thermal and electrochemical stability make them of high potential for electrodeposition of several materials like metals and alloys, conducting polymers, and semiconductors which can not be obtained from aqueous solutions. In particular, it was recently shown that aluminium (Al) can be deposited from air- and water-stable ionic liquids at mild reaction conditions. Since Al has quite good resistance against corrosion, it is of interest to study "Al-coatings" from ionic liquids.

The present thesis aims to achieve this goal by investigating Al-coatings on mild steel and study the effect of changing the ionic liquids, like. e.g. changing the organic cation on the properties of the resulting Al-coatings.

- The following ionic liquids were used for this purpose: $AlCl_3$/l-ethyl-3-methyl-imidazolium chloride ($AlCl_3$/[EMIm]Cl), $AlCl_3$/l-benzyl-3-methyl-imidazolium chloride ($AlCl_3$/[BzMIm]Cl) and $AlCl_3$/l,3-dibenzyl-imidazolium chloride ($AlCl_3$/[DBzIm]Cl) ionic liquids, respectively. $AlCl_3$ was added to the liquids to provide Al-precursors. It was found that the particle size of the Al-deposites was significantly reduced from the micrometer regime down to the nanometer regime when only changing the substituents of the imidazolium cations from EMIm to DBzIm, respectively. This means; the more the aromatic rings in the cation, the finer the particle size is. Whereas the thickness and the adhesion of the Al-deposits were decreased with the presence of the aromatic rings.
- For comparison and as a first step for the Al-Cu alloy deposition, Al was also deposited on mild steel from the air- and water stable ionic liquids: 1-ethyl-3-methyl-imidazolium bis(trifluoromethylsulfonyl) amide ([EMIm]Tf_2N) and

1-butyl-1-methyl-pyrrolidinium bis(trifluoromethylsulfonyl) amide ([BMP]Tf_2N) with $AlCl_3$ concentrations of 5.5 M and 1.6 M, respectively. The results were quite similar to that obtained on Au substrates by Endres et al: microcrystalline Al from [EMIm]Tf_2N and nanocrystalline Al from [BMP]Tf_2N.

- Attempts have been performed for the electrodeposition of Al-Cu alloy on mild steel as Cu enhances the thermal and electrical conductivity of Al. For this purpose the white viscous upper phase of ($AlCl_3$/[BMP]Tf_2N) mixture was used as Al source. Because of the very low solubility of copper salts in ionic liquids, Cu ions were introduced in the system by anodic dissolution of a Cu sheet in the mentioned mixture. The results showed that no clear amount of Cu ions can be obtained even at elevated temperatures. However, anodic dissolution of Cu in the pure ionic liquids [BMP]Tf_2N and [EMIm]Tf_2N at 70 ^oC gave Cu^+ ions (as was calculated from Faraday's law by weight loss of Cu sheet) into the solution but an interesting and unexpected result was obtained which deviated the work away from the planned goal: it was found that the Tf_2N anion is subject to decomposition under extremely mild electrochemical conditions during the anodic dissolution of copper electrode in this ionic liquid at 70 ^oC, leading to the formation of CuF_2 precipitate (as was proved by XRD) which was clearly seen by naked eye. However, at room temperature no significant decomposition was obtained. Although the mechanism of this reaction is not clear at all (even raising some questions), one has to be very careful in applying ionic liquids based on Tf_2N for electrochemical experiments: the Tf_2N anion might decompose, depending on the anode material.

Motivation of the work

Owing to the quite good corrosion resistance of aluminium, this metal is of high interest as a coating material for reactive metal surfaces.

Ionic liquids have opened the door for the electrodeposition of aluminium at "mild reaction conditions". In addition to their feasible physical properties over organic solvents and molten salts like e.g. negligible vapor pressure and electrochemical and thermal stability, ionic liquids have shown quite interesting effects on the electrodeposition process: As an example, nanosized Al deposites were obtained by just changing the type of the ionic liquid.

The present thesis focuses on the feasibility of ionic liquids in the coating of mild steel by Al deposition and investigate more about the effect of changing the ionic liquid on the properties, like adhesion and particle size, of the resulting Al coatings. In addition, attempts to deposit Al-Cu alloy have been performed, as Cu enhances the thermal and electrical conductivity of Al.

Content

List of abbreviations

BMIm	1-butyl-3-methylimidazolium
BMP	1-butyl-1-methylpyrrolidinium
BzMIm	1-benzyl-3-methylimidazolium
CE	counter electrode
CV	cyclic voltammetry
DBzIm	1,3-dibenzylimidazolium
EDAX	Energy dispersive X-ray analysis
EMIm	1-ethyl-3-methylimidazolium
OPD	over potential deposition
Tf_2N	bis(trifluoromethylsulfonyl)amide
RE	reference electrode
RTILs	room temperature ionic liquids
SEM	scanning electron microscopy
UPD	under potential deposition
WE	working electrode
XRD	X-ray diffraction

1. Introduction

1.1 Ionic liquids

1.1.1 Definition

The term "ionic liquids" is used for liquids that solely consist of cations and anions, usually with melting points of 100 °C or below. They are, meanwhile, widely investigated as new solvents with a nonmolecular ionic character **[1-6]**.

1.1.2 Historical background

One of the first known low temperature ionic liquids with a melting point of 12 °C was synthesized by Walden in 1914 **[7]**. The first $AlCl_3$ based low melting salts with chloroaluminate ions were developed in 1948 by Hurley and Wier at the Rice Institute in Texas as bath solutions for low-temperature electroplating of aluminum **[8]**. As early as 1967, Swain et al. described the use of tetra-n-hexylammonium benzoate as a solvent for kinetic and electrochemical investigations **[9]**. Later, a series of ionic liquids were prepared by combining anhydrous aluminum chloride with suitable organic salts, which are based on organic cations such as 1-ethyl-3-methylimidazolium [EMIm] and 1-butyl-1-methylpyrrolidinium [BMP]. These $AlCl_3$ based ionic liquids are considered as being the first generation of ionic liquids. These systems were not further studied until the late 1970s when Osteryoung et al. and Wilkes et al. rediscovered these liquids and studied them mainly for electrochemical applications **[10,11]**. With the beginning of 1980s, Seddon and Hussey et al. began to use chloroaluminate melts as nonaqueous, polar solvents for the investigation of transition metal complexes which generally started with the electrochemical aspects **[12-14]**. At the end of 1980s Fry and Pienta **[15]** and Boon et al. **[16]** have employed ionic liquids in catalysis and organic synthesis, respectively. In 1990 Chauvin et al. and Carlin et al. reported the use of ionic liquids as solvents for homogeneous transition metal catalysts: nickel catalysts were dissolved in weakly acidic chloroaluminate melts and the resulting ionic catalyst solutions were used for the dimerization of propene and also the ethylene polymerization with Ziegler - Natta catalysts **[17,18]**.

Due to the hygroscopic nature of $AlCl_3$ based ionic liquids, they must be handled under inert gas atmosphere. For this reason, the need for air- and water-stable ionic liquids, which are considered as the second generation of ionic liquids, attracted much more interest. In 1992, Wilkes and Zawarotko reported the first class of air and water ionic liquids **[19]**. These ionic liquids consist mainly of 1-ethyl-3-methylimidazolium as a cation and either tetrafluoroborate (BF_4^-) or hexafluorophosphate (PF_6^-) as anions which can be handled under air, but it was found that the exposure of these ionic liquids to moisture for long time maybe causes some changes in their physical and chemical properties (especially at elevated temperatures) as HF gas liberated **[20,21]**. Although, these systems offer high tolerance versus functional groups which opens up a much larger range of applications especially for transition metal catalysis, more scientists have been moving away from (BF_4^-) and (PF_6^-) and towards more stable hydrophobic anions such as trifluoromethylsulfonate (CF_3SO_3), bis(trifluoromethylsulfonyl) amide [$(CF_3SO_2)_2N^-$] and tris(trifluoromethylsulfonyl) methide [$(CF_3SO_2)_3C^-$] **[22-24]**.

This new class of air- and water- stable ionic liquids have attracted more interest due to their extraordinary physical properties like the significantly high chemical, thermal and electrochemical stability **[25]**.

The molecular structure of some cations and anions is illustrated in the following table (1.1)

Cations	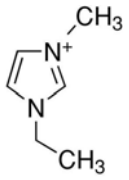	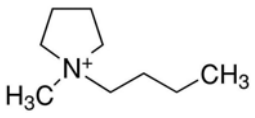	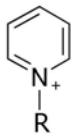	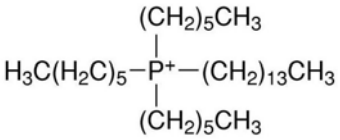
	[EMIm]	[BMP]	N-Alkyl pyridinium	[$P_{14,6,6,6}$]
Anions		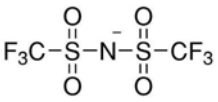		
	Chloride	[Tf_2N]	Tetrafluoroborate	Hexafluorophosphate

Table 1. 1. *Molecular structure of some of cations and anions used in ionic liquids and their abbreviations.*

1.1.3 Characteristics of ionic liquids

Ionic liquids (ILs) possess a unique array of physico-chemical properties that make them suitable in numerous task-specific applications in which conventional solvents are non-applicable or insufficiently effective. The properties of ionic liquids specifically vary over a wide range by the selection of suitable cations and anions **[26-29]**. Several methods have shown that it is possible to make predictions of the physical properties of ionic liquids which will allow the design of new ionic liquids with specific properties tailored for particular applications, without the need for time-consuming trial and error synthesis **[30,31]**. Also, the corrosivity of ionic liquids media strongly depends on the chemical structure of the cationic moiety and the nature of the anion of the ionic liquid. Several studies have been considered on the physico-chemical characteristics of ionic liquids which investigated by electrochemical and gravimetric techniques at different temperatures **[32-35]**.

The characteristics of ionic liquids are shortly discussed in the following subsection:-

1.1.3.1 Volatility

Due to their practical non-volatility (10^{-11} mbar vapour pressure at room temperature), ionic liquids have been considered as having a low impact on the environment and human health, and thus recognized as solvents for green chemistry. However, this is distinct from toxicity, and it remains to be seen how 'environmentally-friendly' ionic liquids will be regarded once widely used by industry. The extremely low vapour pressures of most ionic liquids allow the removal of water from them by simply heating under vaccum **[36]**.

1.1.3.2 Solubility

Room-temperature ionic liquids (RTILs) have been used as novel reaction solvents. They seem to behave like dipolar, aprotic organic solvents and short-chain alcohols in their interaction with organic solutes. Ionic liquid stationary phases have a dual nature for acting as a low-polarity stationary phase to nonpolar compounds and as molecules with strong proton donor groups.

Furthermore, the nature of the anion can have a significant effect on both the solvating ability and the selectivity of ionic liquid stationary phases **[37-39]**. Some factors such as dispersion, polarity, hydrogen bonding and cavity formation have also approximately equal importance in the solvating properties of ionic liquids. Furthermore, the solubility of polar compounds that contain bulky and aromatic groups can be enhanced in ionic liquids due to higher dispersion interactions in ionic liquids than in aqueous solution **[40,41]**. In contrast, the solubility of metal salts in sometimes low, due to the weak coordinating ability of the bulky cations and anions of most ionic liquids.

1.1.3.3 Melting point

In general, ionic liquids have melting points below 100 °C and most of them are liquid at room temperature. While the simplest example of a primitive molten salts is "NaCl" with a melting point of more than 801 °C **[42,43].** The melting points of 1-ethyl-3-methylimidazolium based ionic liquids, as an example, with different anions, such as $[BF_4]^-$ and $[Tf_2N]^-$ are 15 °C **[22]** and –3 °C **[23]**, respectively. Both cations and anions contribute to the low meting points of ionic liquids. Bulky asymmetric organic cations, weak intermolecular interactions (hydrogen bonding and van der Waals forces) **[41]** and good charge distribution **[44]** decrease the melting points of ionic liquids. Also, the increase in the anion size leads to a decrease in the melting point too **[45-47]**.

1.1.3.4 Density

Mostly, ionic liquids are denser than water with values ranging from 1 to 1.6 g cm $^{-3}$ at 25 ºC and their densities decrease with increasing in the alkyl chain length in the cation systemically. The densities of ionic liquids are affected by the identity of cations and anions. The order of increasing density for ionic liquids composed of a single cation is: $[CH_3SO_3]^- \approx [BF_4]^- < [CF_3CO_2]^- < [CF_3SO_3]^- < [C_3F_7CO_2]^- < [(CF_3SO_2)_2N]^-$ **[48]**. I. e, the larger the anion, the denser the ionic liquid is.

1.1.3.5 Viscosity

Ionic liquids are of higher viscosities than other molecular solvents. Their viscosities are ranging from 10 to 500 mPa s at room temperature. Furthermore, high viscosity results in low diffusion coefficients and thus leads to slow mass transfer in ionic liquid/fluid multiphase systems **[49,50]**. The influence of temperature on viscosity is much more important than on density, where a strong decrease in viscosity is observed with increasing temperature making ionic liquids easier to apply **[35,51-54]**. The viscosity of ionic liquids is determined by van der Waals forces and hydrogen bonding. Electrostatic forces may also play an important role. Alkyl chain lengthening in the cation leads to an increase in viscosity **[43]**. This is due to stronger van der Waals forces between cations leading to increase in the energy required for molecular motion. Also, the ability of anions to form hydrogen bonding plays an important role **[55]**.

1.1.3.6 Conductivity

Conductivities and viscosities of ionic liquids are inversely linked in a proportional correlation in many systems with high viscosities leading to low conductivities. Furthermore, as compared with the common organic electrolyte systems, ionic liquids have good ionic conductivities (up to 10 mS cm^{-1}) **[41]**. In some cases the conductivity value is up to 0.1 Ω^{-1} cm^{-1} at 200 °C. However, at room temperature their conductivities are usually lower than those of concentrated aqueous electrolytes. Based on the fact that the composition of ionic liquids is only ions, it would be expected that ionic liquids have rather high conductivities. However, the conductivity of any solution depends not only on the number of charge carriers but also on their mobility. For ionic liquids the ions are usually large and this reduces their mobility which, in turn, leads to lower conductivities. Furthermore, Lengthening of the chain, ion pair formation and ion aggregation lead to reduced conductivity **[2,50]**. For a given anion with a range of cations, conductivity generally decreases in the order 1-alkyl-3-methylimidazolium > N,N dialkylpyrrolidinium > tetra-alkylammonium, and this has been identified with a decrease in planarity of the cationic core **[24]**.

1.1.3.7 Thermal stability

The thermal stability of ionic liquids is limited by the strength of their heteroatom–carbon and their heteroatom–hydrogen bonds, respectively **[5]**. At least on a short time scale, ionic liquids can be thermally stable up to temperatures of 450 °C **[2]**. However, decomposition could also occur if they are exposed to high temperatures for a long time.

1.1.3.8 Electrochemical window

By definition, the electrochemical window is the electrochemical potential range over which the electrolyte is neither reduced nor oxidized at an electrode. Moreover, the electrochemical window is an important property and plays a key role in using ionic liquids in electrodeposition of metals and semiconductors. In many cases it was found, in practice, that the constituent anions are oxidized at sufficiently large potentials, and at sufficiently low ones, the organic cations undergo reduction. The potentials at which these bulky processes are initiated determine the accessible electrochemical window for each liquid. The electrodeposition of elements and compounds in water is limited by its low electrochemical window of only about 1.2 V, while in most ionic liquids more than 4 V is achievable **[24,56]**. Generally, the wide electrochemical windows of ionic liquids have opened the door to electrodeposit metals and alloys at room temperature which were formerly obtained only from high temperature molten salts.

1.1.4 Effect of impurities

From an electrochemical point of view, the trace levels of some impurities such as halide and alkali metal ions or molecular solvents in various types of ionic liquids can greatly influence electrochemical experiments. Halide and alkali metal ions are generally introduced during the synthesis of ionic liquids. Widespread studies for the influence of the purity of such reaction media on the catalytic activity and/or selectivity of the ionic liquid systems and their physical properties such as viscosity and electrochemical window were carried out **[35,57-61]**.

1.1.5 Electrodeposition of metals and alloys

In general, room temperature ionic liquids with a melting point of 100 °C or below can be employed as solvents for the electrodeposition of metals and alloys. He et al. **[62]** and Tai et al. **[63]** reported that silver and palladium-silver alloys can be electrodeposited on glassy carbon electrode using organic substituted imidazolium cations and inorganic anions, such as BF_4^- and PF_6^- **[62,63]**. Furthermore, copper and copper-Zinc alloys can be electrodeposited on tungsten and nickel electrodes in ionic liquids based on imidazolium cation and BF_4^- anion **[64,65]**. Cadmium **[66]** can also be electrodeposited in basic [EMIm]Cl/BF_4^- mixtures.

The electrodeposition of bulk antimony on glassy carbon and nickel electrodes in basic 1-ethyl-3-methylimidazolium chloride/tetrafluoroborate ionic liquid at different temperatures was investigated **[67]**. Several attempts were done for the electrodeposition of Pd–In alloys in aqueous baths because of the combination between In and Pd provides higher microhardness and wear-resistance coating than the pure Pd without sacrificing the low contact resistance of the palladium and also the Pd–In coatings can be used as replacement for Au, Ag and Pd coatings in various applications **[68–74]**. The electrochemistry and the electrodeposition of zinc and zinc alloys were studied in the Lewis acidic $ZnCl_2$/[EMIm]Cl ionic liquids **[75–77]**. Moreover, Huang and Sun have reported that the electrodeposition of Pt, Fe, Sn and Cd with/without Zn in Lewis acidic $ZnCl_2$/[EMIm]Cl ionic liquids can be achieved **[78–82]**.

Endres et al. **[83]** have reported that tantalum can be electrodeposited in 1-butyl-1-methylpyrrolidinium bis(trifluoromethylsulfonyl) amide ([BMP]Tf2N) ionic liquid at 200 °C in addition to the formation of insoluble tantalum compounds on the electrode surface. The electrochemical behavior and the electrodeposition of titanium in l-butyl-3-methyl-imidazolium bis (trifluoromethylsulfonyl) amide ([BMIm]Tf_2N) ionic liquid were reported: Ti nanowires have been deposited electrochemically, with in situ monitoring by scanning tunnelling microscopy (SEM) at room temperature. In a first step $TiCl_4$ is reacted to $TiCl_2$, which is subsequently reduced to metallic Ti. **[84,85]**

The synthesis of new moisture stable Lewis acidic ionic liquids/deep eutectic solvents made from metal chlorides and quaternary ammonium salts at or around room temperature were discussed by Abbott et al. **[86]**. Moreover, the electrodeposition of black Cr films in the nanometre regime was successfully obtained from chromium (III) chloride hexahydrate and quaternary ammonium salts. The easy preparations and the low costs of these liquids make their use in many applications possible **[87,88]**

1.1.6 Electrodeposition of aluminium

Owing to the excellent physical and chemical properties of Al coatings, it is widely used in modern industries. Furthermore, the interest in the preparation of aluminium coatings has steadily increased during the last decades as the excellent corrosion resistance of aluminium deposits provides solutions for many engineering problems such as chemical and atmospheric attack. The performance of an aluminium deposit as a protective layer was found to be superior to that of cadmium or zinc coatings. Another advantage of aluminium coating is the fact that it is readily anodized and the obtained oxide layer exhibits very good mechanical properties and an attractive aesthetic appearance which is not the case with the anodized layer formed on a number of metal alloys. For some applications, Al acts as a light material in automotive and planes as well as for decorative purposes. Several methods can be employed for the electrodeposition of aluminium on various metals - mainly on steel - such as metal spraying, hot-dipping, vacuum deposition and cladding **[89]**.

However, these techniques are considered to be expensive, as high temperatures are required for the preparation of the coating because of the high melting point of aluminium. In addition the above methods are often impractical as the specimens could be damaged by heating at high temperatures. Several studies such as inorganic, organic and metallic-organic as well as potential Al plating baths have been subjected to a variety of spectroscopic and electrochemical studies including aluminium electrodeposition **[90]**, possible electrolytes for molten salt batteries **[91]** and photoelectrochemical cell investigations **[92-95]**.

Also, aluminium can be recovered from ores by the electrolysis of cryolite (Na_3AlF_6) and aluminium in the liquid state using Hall-Héroult process but this method is not suitable to coat other metals because it is carried out at 1000 °C **[96, 97]**. Considerable efforts and researches have gone into the search for a suitable electrolyte that can be used for Al electrodeposition at ambient temperatures so as to reduce energy consumption as Al can not be deposited from aqueous solutions. In recent years, $AlCl_3$-alkylpridinium halides have been shown to be suitable stable systems with low melting points over a wide composition range. The adjustable Lewis acid-base properties of these room temperature haloaluminate salts make them excellent solvents for the electrodeposition of Al. However, reactive metals such as aluminum and aluminum alloys cannot be deposited by these traditional techniques or in any aprotic solvent, because the electrochemical window of aqueous electrolytes is too narrow and the aluminium reactivity is ($E° = –1.7$ V *vs.* NHE). The electrodeposition process in aqueous solutions: water starts to decompose, forming hydrogen and oxygen before the metals begin to deposit; consequently, aluminium can only be electrodeposited from non-aqueous aprotic electrolytes such as molten salts and organic solvents. Many of these electrolytes are sensitive to air and moisture so that the aluminium electrodeposition process must be carried out in inert atmosphere such as argon or nitrogen. The baths for Al electrodeposition should have some requirements dependent on solute/solvent interaction phase **[98,99]**.

1.1.6.1 Electrodeposition of aluminium in ionic liquids

Electrodeposition of aluminium in ionic liquids can be performed at room temperature. The aluminium deposits obtained are usually of good quality, high purity and of low porosity and heat resistance. Popular examples of such systems include the chloroaluminate ionic liquids, which are prepared by mixing anhydrous $AlCl_3$ with a suitable organic halide. This kind of ionic liquids is the simplest system from which aluminium can be easily electrodeposited. As the molar ratio of this mixture changes, the melt can be classified as basic, neutral or acidic in the sense of Lewis acidity. In the neutral 1:l melt Al precursors are present almost entirely as $AlCl_4^-$ ions, whereas in the 2:l melt it is present as $Al_2Cl_7^-$. In chloroaluminate ionic liquids ($AlCl_3$:EMImCl) having a molar ratio between 1:l and 2:1, both $Al_2Cl_7^-$and $AlCl_4^-$ ions will be present **[100,101]**.

A lot of work has been done using chloroaluminate ionic liquids to get high-quality aluminum and aluminum alloy deposits because it has a very low melting point over a wide range of compositions, high intrinsic electrical conductivity at room temperature, and a low vapour pressure **[102]**. A lot of researches carried out using different generations of ionic liquids such as $AlCl_3$/l-ethyl-3-methyl imidazolium chloride ($AlCl_3$/[EMIm]Cl), $AlCl_3$/l-ethyl-3-methyl- imidazolium bis(trifluoromethylsulfonyl) amide ($AlCl_3$/ [EMIm]Tf_2N) and $AlCl_3$/l-butyl-1-methylpyrrolidinium bis(trifluoromethylsulfonyl) amide ($AlCl_3$/ [BMP]Tf_2N) to get high quality aluminium and aluminium alloy deposits: The combination of l-ethyl-3-methyl-imidazolium chloride ([EMIm]Cl) as cationic source and anhydrous aluminium trichloride ($AlCl_3$) is widely employed as low temperature ionic liquids. Hussey and co-workers did extensive studies on the electrodeposition of aluminium and aluminium alloys in $AlCl_3$/[EMIm]Cl ionic liquid **[103-107]**. These alloys are technologically important because of their corrosion resistance, especially pitting corrosion, and in some cases, their interesting magnetic properties.

The electrodeposition, electrochemical nucleation and surface morphology of aluminium on both tungsten and aluminium electrodes from 2:1 molar ratio $AlCl_3$: [EMIm]Cl ionic liquid were studied by Jiang et al. **[108]**. The electrodeposits obtained on both tungsten and aluminium electrodes were dense, continuous and well adherent. The $AlCl_3$/[EMIm]Cl (60/40 mol.%) ionic liquid was used to electroplate mild steel by well adherent and highly corrosion resistant aluminium coatings **[109]**. However, the quality of the deposit can be greatly improved by utilizing pulse plating techniques **[110,111]** or by the addition of some organic solvents such as benzene and methyl-t-butyl ether **[111]** that improve the deposit surface morphology. It is possible that the organic molecules play the role of brighteners. Endres et al. reported that nanocrystalline aluminium can be made electrochemically in Lewis acidic ionic liquids based on $AlCl_3$ and [EMIm]Cl under galvanostatic conditions by addition of nicotinic acid **[112]**. Also the $AlCl_3$/[EMIm]Cl mixture is a viscous and transparent liquid at room temperature when the molar composition is in the range of 0.3:1 to 2:1 **[113]**.

Moreover, The mechanism of the electrodeposition and dissolution processes of aluminium in room temperature $AlCl_3$/[EMIm]Cl ionic liquid on glassy carbon was studied by Lai **[114]**. The obtained results indicated that the aluminium deposition process at the above-mentioned substrates is preceded by a nucleation step and is kinetically complicated. The deposited aluminium was found to be unstable and subject to a slow corrosion process. This is most likely due to impurities and organic cations present in the melt. Also, aluminum deposition from $AlCl_3$/[EMIm]Cl ionic liquid was studied by employing an inverted optical microscope to perform in situ optical observations during the deposition process at tungsten electrode. Thin and continuous aluminum coatings with crystal sizes below optical microscopic resolution are produced. Analysis of chronoamperograms indicated that the deposition process involves progressive nucleation with diffusion-controlled growth of the three-dimensional nuclei **[115]**.

In addition, the electrodeposition of Al in ionic liquids based on more hydrophobic anions such as Tf_2N^- anion has attracted more attention in the last years. Endres et al. **[116-118]** have investigated the electrodeposition of aluminium on Au substrates from the $AlCl_3$ salt in different air- and water-stable ionic liquids which have the same anion such as 1-butyl-1-methyl-pyrrolidinium bis(trifluoromethylsulfonyl) amide [BMP]Tf_2N, 1-ethyl-3-methyl-imidazolium bis(trifluoromethylsulfonyl) amide [EMIm]Tf_2N and trihexyl-tetradecyl phosphonium bis(trifluoromethylsulfonyl) amide [$P_{14,6,6,6}$]Tf_2N. It was found that [BMP]Tf_2N and [EMIm]Tf_2N ionic liquids show biphasic behaviour with the $AlCl_3$ concentration range from 2.5 to 5.5 M and 1.6 to 2.5 M, respectively. The biphasic mixtures become monophasic at temperatures $\geq$ 80 ^oC. In [EMIm]Tf_2N ionic liquid, microcrystalline aluminium can be electrodeposited as coarse cubic-shaped microcrystallines in the upper phase of the biphasic $AlCl_3$/[EMIm]Tf_2N mixture. However, uniform, dense, shining and adherent aluminium particles of sizes in the nanometer range were obtained in the $AlCl_3$/[BMP]Tf_2N mixture.

2. Experimental

2.1 Chemicals

Anhydrous aluminium chloride ($AlCl_3$) salt (Fluka, 99%) was used as a source of aluminium ions in the ionic liquids. In the present thesis, the following ionic liquids were employed: 1-ethyl-3-methylimidazolium chloride [EMIm]Cl, 1-ethyl-3-methyl-imidazolium bis(trifluoromethylsulfonyl) amide [EMIm]Tf_2N and 1-butyl-1-methyl-pyrrolidinium bis(trifluoromethylsulfonyl) amide [BMP]Tf_2N, in ultrapure quality. Prior to use, the 1-ethyl-3-methylimidazolium chloride salt [EMIm]Cl (99.9%) and the other two ionic liquids were dried under vacuum at 70°C and 100°C, respectively, for 12 hours to remove residual moisture. The solution preparation and all electrodeposition experiments were performed under inert gas condition (H_2O, O_2 < 2 ppm) inside an argon-filled glove box (OMNI-LAB from Vacuum-Atmospheres). The structures and physical properties of the employed ionic liquids are shown in table (2.1).

Ionic liquid		**[EMIm]Cl**	**[EMIm]Tf_2N**	**[BMP]Tf_2N**
Structure	Cation	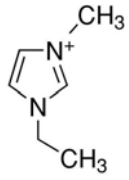	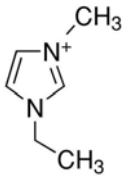	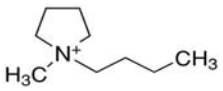
	Anion	Cl^-	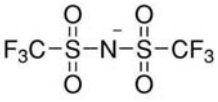	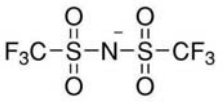
Molar Mass (g/mol)		146.62	391.31	422.41
Melting point (°C)		80*	-15 [119]	-18 [23]
Density (g/ml)		1.12*	1.46 [43]	1.41 [23]
Viscosity (mPa.s)		47.4*	27 [120]	60 [120]
Conductivity (mS/cm)			7.63 [121]	3.4 [120]

* at 80 ºC

Table. 2.1. *The structures and physical properties of the employed ionic liquids (Sigma- Aldrich.com/ionic liquids).*

2.2 Compositions

The chemical compositions of $AlCl_3$ in the three ionic liquids [EMIm]Cl, [EMIm]Tf_2N and [BMP]Tf_2N, used for aluminium deposition are listed in table (2.2).

Ionic liquid	[EMIm]Cl	[EMIm]Tf_2N	[BMP]Tf_2N
$AlCl_3$	60%	5.5 mol/l	1.8 mol/l
Phases	One	Two	Two

Table 2.2. *The chemical compositions of $AlCl_3$ in the three ionic liquids.*

2.2.1 $AlCl_3$/[EMIm]Cl ionic liquid

The first ionic liquid $AlCl_3$/1-ethyl-3-methylimidazolium tetrachloroaluminate ($AlCl_3$/[EMImCl]) is formed at room temperature (25 ºC) by combining of highly pure anhydrous $AlCl_3$ and highly purified 1-ethyl-3-methylimidazolium chloride salt (see figure 2.1). Only $AlCl_3$ grains were used, as powders (even in 99.998% quality) contain only little amount of electrochemically active $AlCl_3$ due to the presence of inactive basic aluminium chloride. The ionic liquid $AlCl_3$/[EMIm]Cl was prepared by adding carefully sublimed $AlCl_3$ to the EMImCl in a molar ratio of 3:2 ensuring a Lewis acidic composition. This mixing is highly exothermic, therefore care must be taken to ensure that the temperature does not rise above 100 ºC as decomposition may occur. The colour of the ionic liquid changes to pale yellow by the addition of $AlCl_3$. The Lewis acidic composition of this ionic liquid allows Al electrodeposition at room temperature as will be shown in chapter (3).

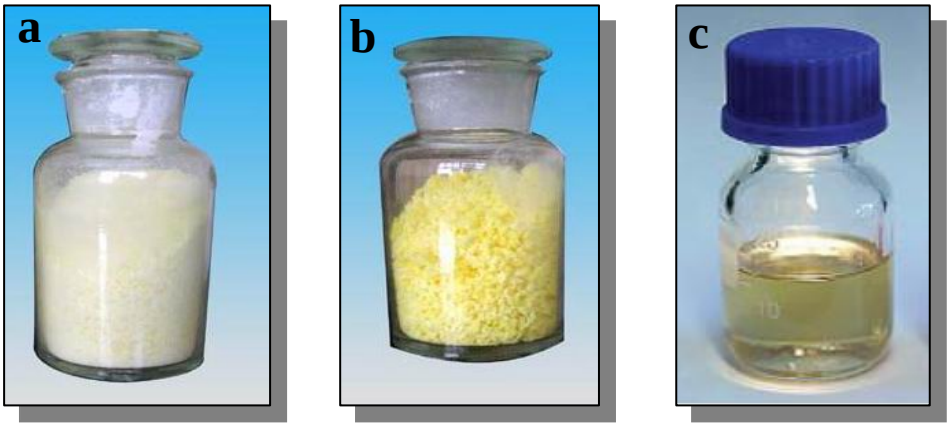

Fig.2.1. *(a) dried 1-ethyl-3-methylimidazolium chloride salt. (b) pure anhydrous $AlCl_3$. (c) The prepared Lewis acidic $AlCl_3$: EMImCl (3:2 molar ratio) ionic liquid.*

2.2.2 $AlCl_3$/[EMIm]Tf_2N ionic liquid

The second used ionic liquid $AlCl_3$/1-ethyl-3-methylimidazolium bis(trifluoro-methylsulfonyl) amide ($AlCl_3$/[EMIm]Tf_2N) shows a biphasic behaviour with increasing concentration of $AlCl_3$: as was also first reported by Endres et al. At a concentration of $AlCl_3$ of more than 2.5 M, a biphasic mixture is formed. Al can't be deposited at concentrations below 2.5 M. Both the upper and the lower phase are liquid. The upper phase of the mixture $AlCl_3$/[EMIm]Tf_2N is clear and colourless while the lower one is pale and more viscous. Upon further addition of $AlCl_3$, the color of the upper phase turns pale yellow and the viscosity of the lower phase increases and it solidifies at an "added" concentration of a bit more than 5 M. The mixture [EMIm]Tf_2N/$AlCl_3$ with a concentration of $AlCl_3$ of 5.5 M was selected as a standard electrolyte for electroplating of Al layers on mild steel in the present experiments. The biphasic mixture also becomes monophasic by heating up to a temperature of about 80°C (see figure 2.2). It was found that Al can only be deposited from the upper phase even at different $AlCl_3$ concentrations, that is, the clear one as will be shown in chapter (3). It must be mentioned here that all of the above descriptions are in agreement with that repeated firstly by Endres et al. **[116,117]**. The present thesis focuses on the electrodeposition of Al from these systems on mild steel. This is also the case for the ionic liquid [BMP]Tf_2N

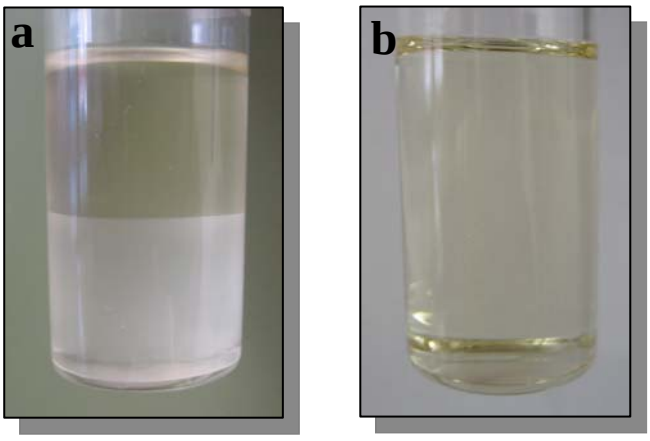

Fig.2.2. *(a) A biphasic mixture of the ionic liquid 1-ethyl-3-methylimidazolium bis(trifluoromethylsulfonyl) amide containing 5.5 M $AlCl_3$ at room temperature. (b) The biphasic mixture becomes monophasic at 80 °C.*

2.2.3 $AlCl_3$/[BMP] Tf_2N ionic liquid

Also, the third used ionic liquid 1-butyl-1-methylpyrrolidinium bis(trifluoro-methylsulfonyl)imide [BMP]Tf_2N shows a biphasic behaviour, above a concentration of $AlCl_3$ of 1.6 M. In this ionic liquid, $AlCl_3$ dissolved less easily than that in [EMIm] Tf_2N ionic liquid. The lower phase is colourless while the upper one is pale and more viscous. By further addition of $AlCl_3$ the volume of the lower phase decreases till reaching a concentration of 2.7 M, then only one solid phase is formed. The mixture [BMP]Tf_2N/$AlCl_3$ with a concentration of $AlCl_3$ of 1.8 M was selected as a standard electrolyte for electroplating of Al layers on mild steel in the present experiments. The biphasic mixture of $AlCl_3$/[BMP] Tf_2N becomes monophasic by heating up to a temperature higher than 80°C (see figure 2.3). It was found that Al can only be deposited from the upper phase of the biphasic mixture as repeated by Endres et al. **[116,117]**.

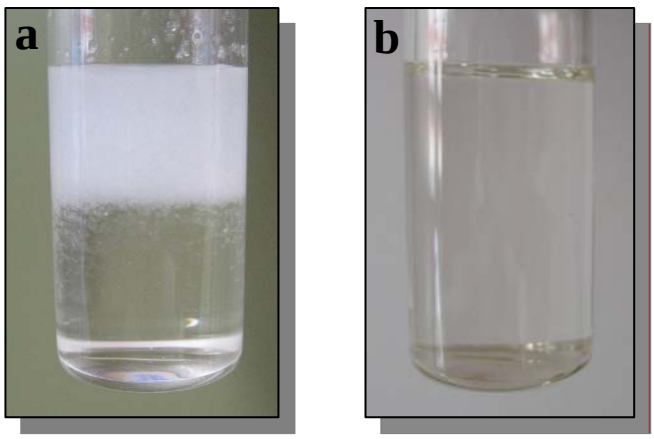

Fig.2.3. *(a) A biphasic mixture of the ionic liquid 1-butyl-1-methyl pyrrolidinium bis(trifluoromethylsulfonyl) amide containing 1.6 M $AlCl_3$ at room temperature. (b) The biphasic mixture becomes monophasic at 80 °C.*

2.3 Electrochemical cells

Figure 2.4 shows the room temperature electrochemical cell used for the electrodeposition experiments: it was made of teflon and clamped over a Teflon covered Viton O-ring onto the substrate yielding a geometric surface area of 0.3 cm^2. For experiments at higher temperature a glass flask with a Teflon cap, as shown in figure 2.5, was used. Prior to use, all parts in contact with the solution were thoroughly cleaned in a mixture of 50/50 vol % of concentrated H_2SO_4 and H_2O_2 (35%) followed by refluxing in bi-distilled water. For fundamental studies, gold substrates from Molecular imaging (gold on glass) were used as working electrodes (WE). Before use, the Au substrates were carefully heated in a H_2 flame for several minutes to remove surface contaminants. After plating, the cathode was withdrawn, washed with isopropanol and dried. For the electrodeposition experiments, the working electrode is a mechanically polished thin mild steel sheet. Prior to use, it was cleaned with acetone in an ultrasonic bath, dried and transferred to the inert gas glovebox to avoid a severe surface oxidation. Pure Al-wire (Alfa, 99.999%) of 0.5 cm diameter and Al-sheet were used as reference (RE) and counter electrodes (CE), respectively. They were mechanically polished to remove the oxide film, rinsed with acetone and dried under vacuum.

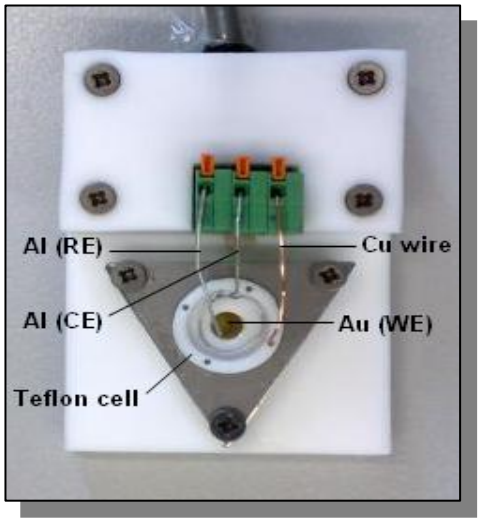

Fig. 2.4. *Electrochemical cell used for Al electrodeposition at room temperature*

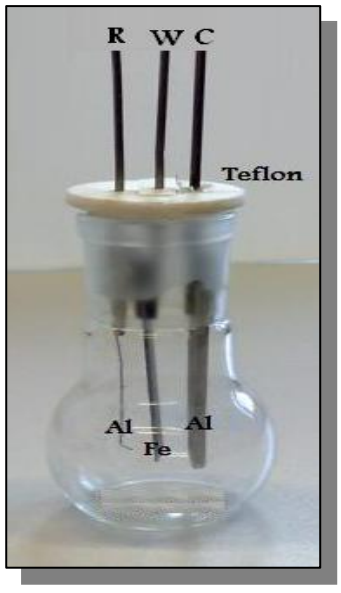

Fig. 2.5. *Electrochemical cell for Al electrodeposition at different temperatures.*

2.4 Methods

2.4.1 Cyclic voltammetry

Cyclic voltammetry is a type of potentiodynamic electrochemical measurement used for providing information about the redox potentials of chemicals and interfacial structures. For the majority of experiments the electroactive species are dissolved in solutions. A potentiostat requires a three-electrode cell with a reference electrode (RE), a working electrode (WE) and a counter electrode (CE). The potentiostat is required to impose on the WE a cyclic potential sweep and to output the resulting current-potential curve.

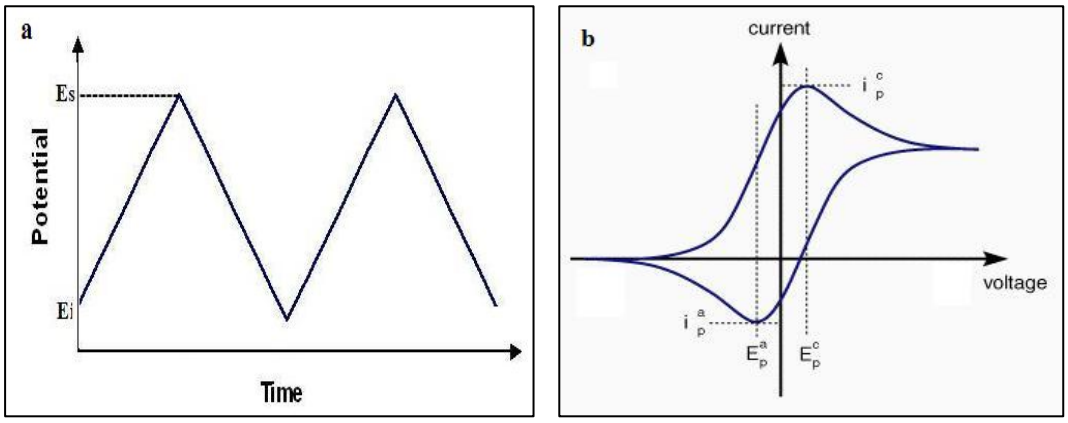

Fig.2.6. *Principle of cyclic voltammetry: (a) potential sweep and (b) redox process.*

As shown in Figure 2.6, there is triangular linear potential sweep as described in the following:

$$E = E_i + vt \qquad \text{(forward sweep)}$$
$$E = E_s - vt \qquad \text{(reverse sweep)}$$

Where E_i, E_s and E, are initial, switching and final potentials in volt, respectively. v and t are sweep (or scan) rate in V s^{-1} and time in sec, respectively. The electrochemical reaction of interest takes place at the WE. Electrical current at the WE due to electron transfer is termed *faradaic current*. A counter electrode (CE) is driven by the potentiostatic circuit to balance the faradaic process at the WE with an electron transfer of opposite direction (i.e., if reduction takes place at the WE, oxidation takes place at the CE).

The process at the CE is typically not of interest, and in most experiments the small currents observed mean that the electrolytic products at the CE have no influence on the process at the WE. The faradaic current at the WE is transduced to a potential at a selected sensitivity, expressed in amperes, and recorded in a digital or analog form. The CV response is plotted as current versus potential. During the forward sweep the oxidized form is reduced, while on the reverse sweep the reduced form near the electrode is reoxidized in case of reversible processes. Chemical reaction coupled to the electrode reaction can drastically affect the shape of the CV response. Cyclic voltammetry is very useful because it helps in understanding the nature of electrodeposition process. For this reason, cyclic voltammograms for Al deposition in [EMIm]Cl, [EMIm]Tf_2N and [BMP]Tf_2N ionic liquids were studied. The cyclic voltammetry measurements were performed in an inert gas glove box using a Parstat 2263 Potentiostat/Galvanostat (Princeton Applied Research) controlled by a Power CV software. The potential was swept in both cathodic and anodic direction with a scan rate of 10 mV s^{-1}.

2.4.2 Scanning electron microscopy (SEM)

Scanning electron microscopy is a standard technique used for giving information about the surface morphology of some selected samples of the electrodeposited aluminium on both gold and mild steel surfaces using a high-resolution field emission scanning electron microscopy (HR-SEM, Carl Zeiss DSM 982 Gemini). The electron beam, with electron's energy up to 50 keV, is generated by heating of a pin-shaped metallic cathode (electron gun; usually a metal, which has a high melting point and a low vapor pressure, for example, tungsten) and accelerated by a high voltage at the anode as shown in Figure 2.7. The beam moves through the column of the microscope by an electrical field. Focusing is achieved by a system of electromagnetic lenses. Primary electrons strike the surface causing a series of elastic and inelastic interactions with the atoms of the sample. The elastic interactions with the nucleus of the atoms produce the backscattered electrons whereas the inelastic interactions with the electrons induce the secondary electrons ejection. Recombination of these electrons with the sample's holes leads to generation of the photons, which have the wavelengths in the visible and infrared region. Inelastic interactions with the

nucleus of the atoms lead to an ionization processes, which, in one's turn, cause the generation of the characteristic X-rays. Besides, interactions between the primary electrons and the sample electrons may induce Auger electrons ejection. Since SEM uses the electrons to obtain an image and the measurement are performed in vacuum, the sample must be dry and electrically conductive. Thus, SEM in combination with an elemental analysis provides good information about topography and morphology of the surface, crystallography and elemental composition of the sample.

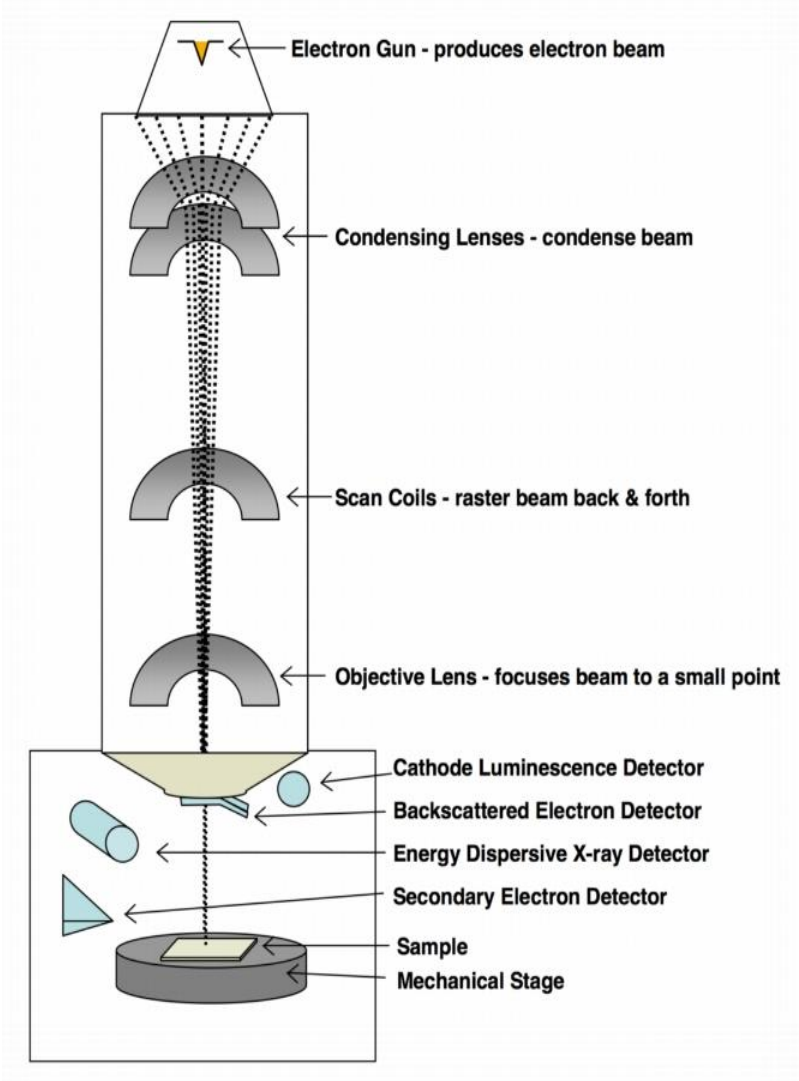

Fig. 2.7. *A schematic view of the scanning electron microscope (SEM) principle.*

2.4.3 Energy dispersive X-ray analysis (EDAX)

This technique is used simultaneously with SEM analysis for determination of the elemental composition of surface films through interactions between the electromagnetic radiation and the substrate, analyzing X-rays emitted by the substrate in response to being hit with charged particles (see Figure 2.8.). At rest, an atom within the sample contains ground state electrons in discrete energy levels or electron shells bound to the nucleus. The incident beam may excite an electron in an inner shell, ejecting it from the shell while creating an electron hole where the electron was. An electron from an outer, higher-energy shell then fills the hole, and the difference in energy between the higher-energy shell and the lower energy shell may be released in the form of an X-ray. The number and energy of the X-rays emitted from a specimen can be measured by an energy dispersive spectrometer. As the energy of the X-rays is characteristic of the difference in energy between the two shells, and of the atomic structure of the element from which they were emitted, this allows the elemental composition of the specimen to be measured. In the present work, SEM and EDX measurements of electrochemically made aluminium films were performed. For this purpose, the working electrode with the electrodeposit on it was removed from the glove box, washed with isopropanol (99.5%, water < 0.05 %) in order to remove the ionic liquid, dried under vacuum and stored in the glove box before analysis.

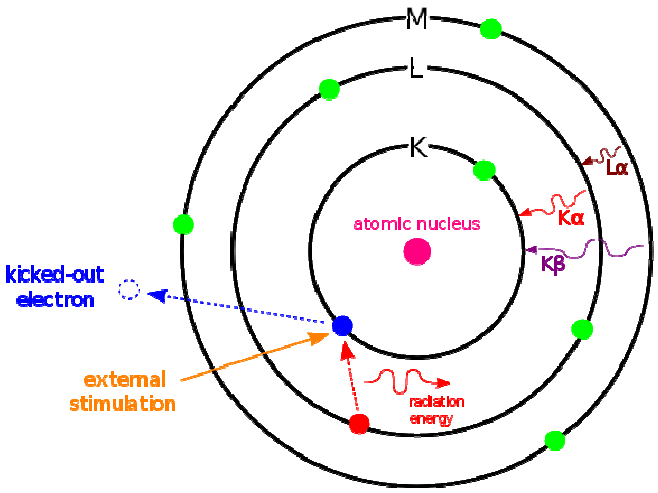

Fig.2.8. *Schematic illustration of energy dispersive X-ray analysis (EDAX) principle.*

2.4.4 X-ray diffraction (XRD)

X-ray diffraction (XRD) is a well-established technique used for the determination of crystallographic structures of solid materials. This technique uses Bragg's Law to determine the type and relative amount of crystalline substances in a bulk sample. As shown in Figure 2.9, the diagram illustrates how crystalline structure (shown diagrammatically as a lattice work of atoms) determined through x-ray diffraction. As the crystal and detector rotate, x-rays diffract at specific angles. The detector reports the intensity (I) of x-ray photons it receives as it moves. Angles of diffraction are marked by peaks. The peak height is a function of the interaction of the x-rays with the crystal and the intensity of the source. In addition, the peaks of the XRD pattern can be used to determine the crystallite sizes. The crystallite sizes can be calculated using standard Sherrer's formula **[122]**:

$$D = 0.9\lambda/\beta\cos\theta$$

where D is the crystallite size in nm, λ is the radiation wavelength, θ is the diffraction peak angle, and β is the line width at half peak intensity. β can be calculated using the formula:

$$\beta^2 = \beta_m^2 - \beta_s^2$$

where β_m is the measured full width at half maxima (FWHM) and β_s is the FWHM of a standard silicon sample. Therefore, the crystal structures of as deposited aluminium on mild steel and gold substrates were examined by X-ray diffraction analysis using a Siemens D-500 diffractometer with CuK_α radiation.

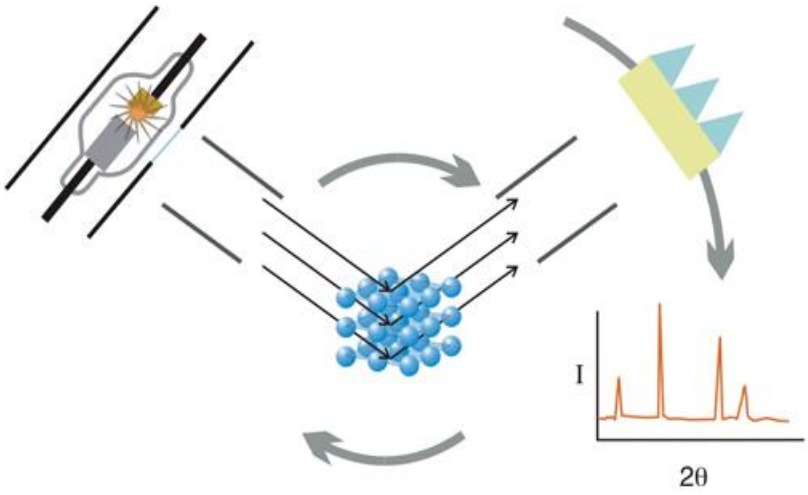

Fig. 2.9. *Schematic illustration of X-ray diffraction (XRD) principle.*

3. Results and discussion

3.1 Aluminium electrodeposition

3.1.1 Electrodeposition of Al from chloroaluminate based ionic liquids

3.1.1.1 Electrodeposition of Al from $AlCl_3$/[EMIm]Cl

In this part of the thesis the electrodeposition of aluminium in Lewis acidic $AlCl_3$/1-ethyl-3-methylimidazolium chloride ($AlCl_3$/[EMIm]Cl) ionic liquid is presented. This system is suitable for the electrodeposition of aluminium and aluminium alloys. One of the most chemically important aspects of chloroaluminate ionic liquids is their adjustable Lewis acidity, which can be altered by varying the molar ratio, $nAlCl_3$: n[EMIm]Cl, where nAl represents the number of moles of $AlCl_3$ and n[EMIm]Cl represents the number of moles of 1-ethyl-3-methylimidazolium chloride salt: Ionic liquids that contain an excess of $AlCl_3$ over [EMIm]Cl are considered Lewis acidic due to the presence of coordinately unsaturated species such as $Al_2Cl^-_7$, whereas those that contain an excess of [EMIm]Cl over $AlCl_3$ are denoted as basic due to the presence of unbound chloride ions. The main acid-base reaction characterizing organic chloroaluminates such as $AlCl_3$/[EMIm]Cl at ambient temperature may be described by the following equilibrium **[100,101]**:

$$2\ AlCl_4^- \longleftrightarrow Al_2Cl_7^- + Cl^-$$

With an equilibrium constant $K = 3.8 \times 20^{-13}$ at 30 °C. In acidic melts, $Al_2Cl_7^-$ ion is the only species from which aluminium can be electrodeposited according to the following reaction:

$$4\ Al_2Cl_7^- + 3e^- \longrightarrow Al + 7\ AlCl_4^-$$

In the presence of excess $AlCl_3$, the following reaction is virtually complete:

$$AlCl_4^- + AlCl_3 \longrightarrow Al_2Cl_7^-$$

It must be mentioned here that the deposition of Al from such systems has been already reported. But for comparison purposes it is studied here. In this study $AlCl_3$ mixes well with the 1-ethyl-3-methylimidazolium chloride salt to a concentration of (60 mol.-%) giving a clear yellowish solution as shown in figure 2.1., from which Al can be deposited. Many studies have been reviewed in details about the preparation and the purification of the chloroaluminate ionic liquid systems by Stafford and Hussey **[123]**. The electrodeposition of Al was investigated from this Lewis acidic chloroaluminate based ionic liquid (3:2 molar ratio) and it was found that at room temperature Al can be easily deposited.

Fig.2.1. *The prepared Lewis acidic $AlCl_3$: EMImCl (3:2 molar ratio) ionic liquid.*

Cyclic voltammetry helps in understanding the nature of the electrodeposition process. For this reason, the cyclic voltammograms for Aluminium deposition in the Lewis acidic $AlCl_3$/EMImCl (3:2 molar ratio) ionic liquid at room temperature were studied. Figure (3.1) shows a typical cyclic voltammogram of the Lewis acidic $AlCl_3$/EMImCl (3:2 molar ratio) ionic liquid at room temperature. The electrode potential was scanned cathodically from the open circuit potential to more negative values with a scan rate of 10 mVs^{-1}. All electrode potentials are referred to Al/Al (III). At a potential of –0.1 V vs. Al/Al (III), the bulk deposition of Al takes place, as shown by the sharp increase of the current, where a clear larger of Al is already seen by naked eye.

The overlapping of the current values in the forward scan with that in the back scan refers to a nucleation process. A wide anodic peak (E`) is recorded on the reverse scan at a potential of about 0.15 V that is correlated to full stripping of the as-deposited aluminium. Here, stripping seems to be kinetically hindered which is a common phenomenon in ionic liquids **[54]**.

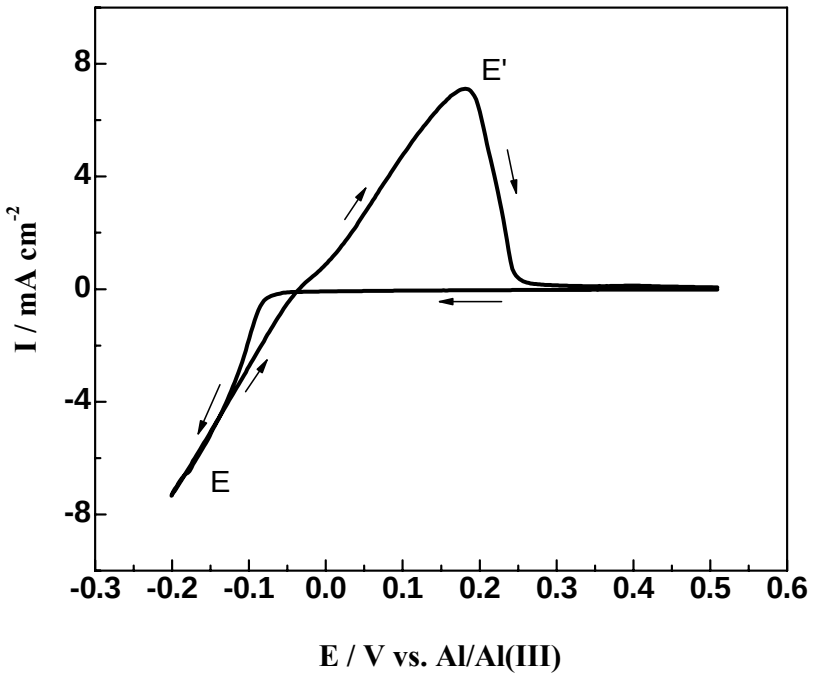

Fig. 3.1. *Cyclic voltammogram recorded at Au (111) substrate in the Lewis acidic $AlCl_3$: EMImCl (3:2 molar ratio) ionic liquid at room temperature. The scan rate was 10 mVs^{-1}.*

Figure (3.2) shows the surface morphology of the as deposited aluminium film produced potentiostatically on Au (111) substrate at -0.2 V vs. Al/Al (III) at room temperature for two hours in the Lewis acidic $AlCl_3$/EMImCl (3:2 molar ratio) ionic liquid. Visually, a dens aluminium film is formed on the surface. The SEM micrograph of such an Al film shows that the layer contains micro crystallites with an average size of about 5 μm with a porous appearance.

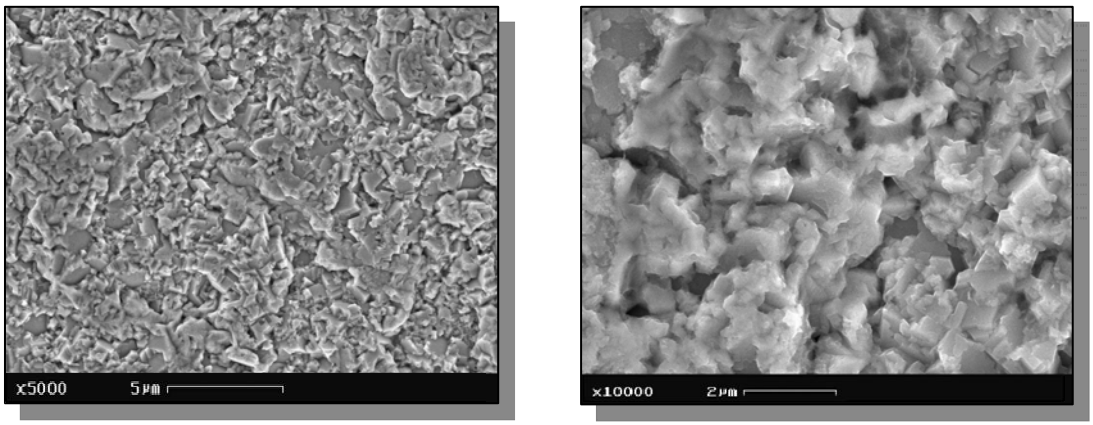

Fig. 3.2. *SEM micrographs of electrodeposited Al films on Au (111) substrate in the Lewis acidic ionic liquid $AlCl_3$/1-ethyl-3-methyl imidazolium chloride (3:2 molar ratio) after potentiostatic polarization (E = –0.2 V) for 2 hours at room temperature.*

Figure (3.3) shows the EDAX profile of the same sample shown in fig. (3.2). It is clearly seen that the EDAX spectrum shows only one characteristic peak of Al. This is consistent with the SEM results, which show that the crystal size is in the micrometer regime. In the light of the mentioned results, it is concluded that in the employed chloroaluminate ionic liquid the Al deposit is always microcrystalline at room temperature.

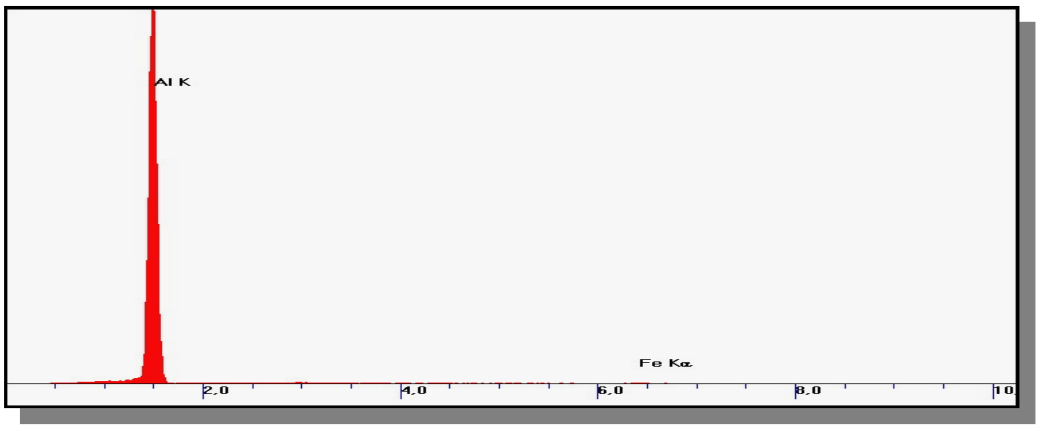

Fig. 3.3. *EDAX profile for the area shown in the SEM micrograph (Fig. 3.2.).*

3.1.1.2 Electrodeposition of Al from [$AlCl_3$/(EMImCl:BzMImCl)]

In this study the electrodeposition of aluminium was carried out in a new system based on the gradual replacement of the 1-ethyl-3-methylimidazolium chloride salt (EMImCl = 40 mol.-%), which contains two alkyl groups, by the 1-benzyl-3-methylimidazolium chloride salt (BzMImCl) which contains one alkyl and one aryl group, (see Fig. 3.4). The concentration of $AlCl_3$ was fixed at 60 mol.-%, during the preparation of the Lewis acidic $AlCl_3$/1-ethyl-3-methylimidazolium chloride ($AlCl_3$/[EMIm]Cl) ionic liquid. This study aims to study the effect of the aromatic group of the imidazolium cation on the electrodeposition of aluminium through EMImCl : BzMImCl molar ratios of: 40:0, 30:10, 20:20, 10:30 and 0:40 mol.-%/ 60 mol.-% $AlCl_3$, respectively.

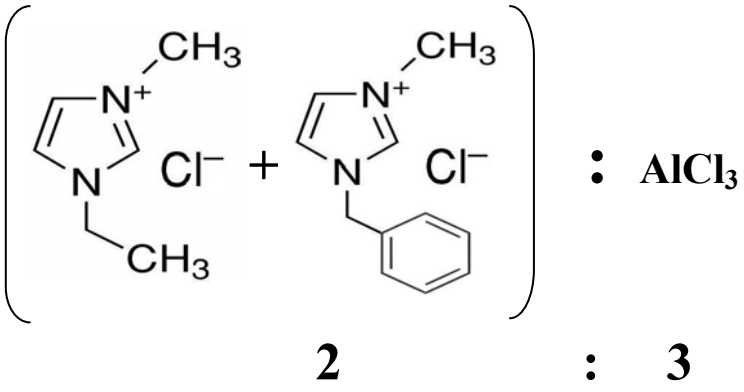

Fig. 3.4. *Simplified scheme for the prepared Lewis acidic $AlCl_3$: (EMImCl/BzMImCl) (3:2 molar ratio) ionic liquid based on 1-ethyl-3-methylimidazolium chloride salt (EMImCl=M.Wt.146.42), 1-benzyl-3-methylimidazolium chloride salt (BzMImCl= M.Wt.208.69) and aluminium chloride ($AlCl_3$= M.Wt.133.35), respectively.*

Figure (3.5) represents the cyclic voltammograms of the Lewis acidic $AlCl_3$:EMImCl/BzMImCl (3:2 molar ratio) ionic liquid mixture at room temperature containing a fixed amount of $AlCl_3$ (60 mol.-%) on gold substrates at different (EMImCl:BzMImCl) molar ratios: 40:0, 30:10, 20:20, 10:30 and 0:40 mol.-%/ 60 mol.-% $AlCl_3$, respectively. As shown from the figure, all cyclic voltammograms exhibit the same general feature of the cyclic voltammogram recorded for the Lewis acidic ionic liquid $AlCl_3$/ EMImCl (3:2 molar ratio). However, it can be clearly seen

that the Al deposition potential shifts gradually to less negative values and the peak currents of both deposition and stripping peaks significantly decrease upon increasing the BzMImCl content. This is ascribed to the decreased mobility of the electroactive species towards the electrode surface due to an increase of viscosity caused by further addition of the more viscous BzMImCl ionic liquid, which, in turn, leads to a lower diffusion rate **[124]**.

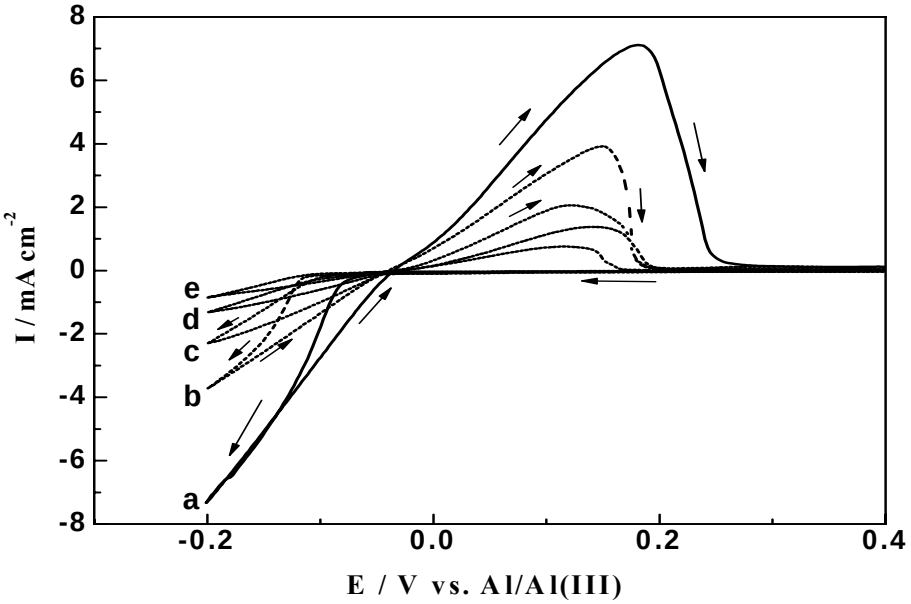

Fig. 3.5*. Cyclic voltammograms acquired on Au substrate in $AlCl_3$ containing ionic liquid mixture of [EMImCl:BzMImCl] at different molar ratios : a) (40:0 mol.-%), b) (30:10 mol.-%), c) (20:20 mol.-%), d) (10:30 mol.-%) and e) (0:40 mol.-%), respectively, the $AlCl_3$ concentration is kept constant (60 mol.-%) in all. The scan rate was 10 mVs^{-1}, at room temperature.*

The SEM micrographs in Fig. 3.6 show the effect of increasing the content of BzMImCl in the ionic liquid mixture (EMImCl:BzMImCl) from 40:0 mol.-% to 0:40 mol.-% with keeping a constant concentration of $AlCl_3$ (60 mol.-%) on the grain size of the deposited Al. The Al deposits were obtained potentiostatically at room temperature and at a potential of – 0.2 V vs. Al/Al (III) for two hours on gold substrates: It is clearly seen that the surface morphology of the deposited aluminium film show gradual change of Al deposites from compact and dense to large coarse cubic-shaped microcrystallites with increasing BzMImCl molar ratio.

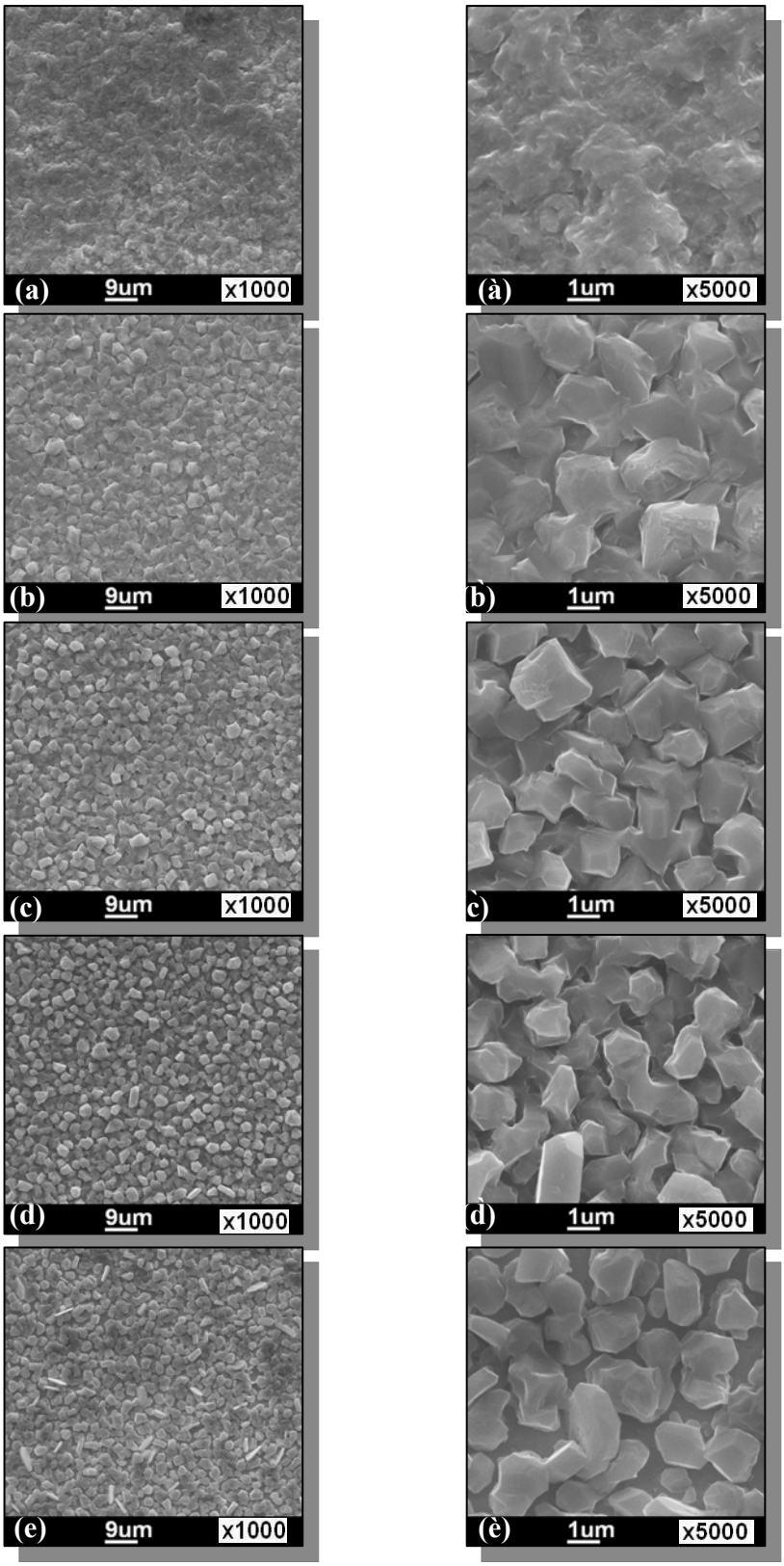

Fig. 3.*6. SEM micrographs of electrodeposited Al films on Au substrates in Lewis acidic ionic liquid consists of a fixed $AlCl_3$ concentration (60 mol.-%) and a mixture of the ionic liquids EMImCl:BzMImCl as follows: , a) (40:0 mol.-%), b) (30:10 mol.-%), c) (20:20 mol.-%), d) (10:30 mol.-%) and e) (0:40 mol.-%), respectively. The deposits were obtained after potentiostatic polarization (E = –0.2 V) for 2 hours at room temperature. a', b', c', d' and e' are higher resolution SEM images of the corresponding a, b, c, d and e images.*

The replacement of the methyl group by a benzyl group in the imidazolium salt in the ionic liquid increases the viscosity of the electrolyte and decreases the mass transport of the electroactive species towards the electrode surface, which, in turn, leads to a slower rate of deposition and hence more chance to form a crystalline deposit. There is an internal stress can originate from intrinsic film stress and from interfacial stress between the deposit and the substrate. In general, this maybe attributed to some factors such as coalescence of the crystallites, inclusion of foreign species or generation of structural defects **[125]**. However, very fine microcrystalline aluminium as coating is an interesting material because by decreasing the particle size an increase in hardness is usually observed. A "hard" aluminium coating on reactive substrates such as mild steel is interesting for corrosion protection.

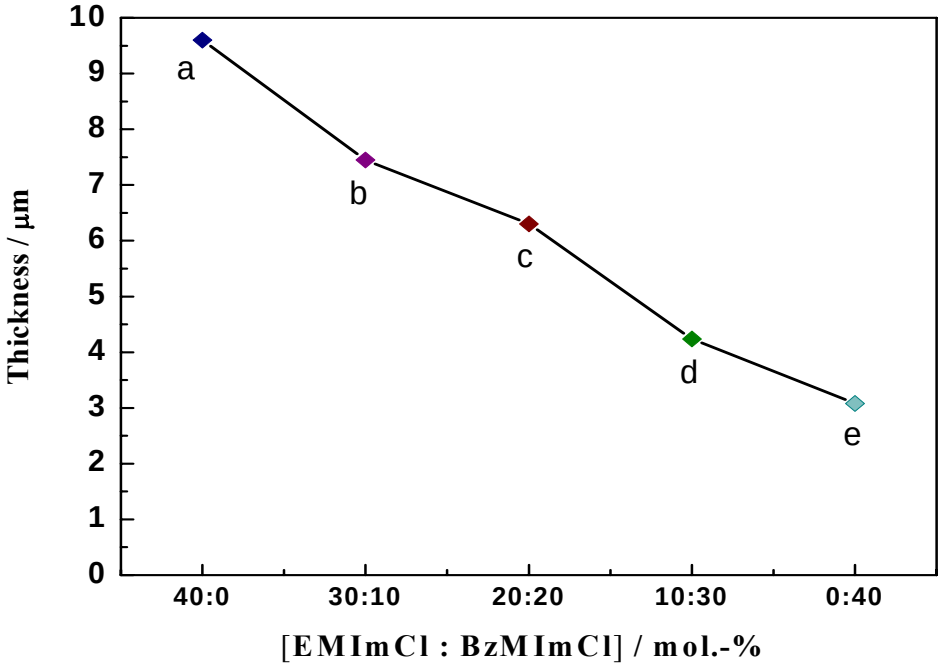

Fig. 3.7. *Adiagram shows the change in thickness of Al deposit obtained from the $AlCl_3$ containing Lewis acidic ionic liquid mixture [EMImCl:BzMImCl] on Au substrates at different molar ratio: a) (40:0 mol.-%), b) (30:10 mol.-%), c) (20:20 mol.-%), d) (10:30 mol.-%) and e) (0:40 mol.-%), respectively. $AlCl_3$ was kept constant (60 mol.-%) in all cases. The deposits obtained after potentiostatic polarization (E = –0.2 V) for 2 hours at room temperature.*

The diagram in figure (3.7) shows the thickness change of the electrodeposited Al films with changing the molar ratio of the ionic liquid mixture [EMImCl:BzMImCl] from 40:0 up to 0:40 mol.-% at the same reaction conditions. The figure shows gradual decrease of Al film thickness with increasing the BzMImCl content at a given constant time of electrolysis. The raising of BzMImCl (at constant $AlCl_3$ concentration) leads to shifting the bulk deposition potential of Al gradually to less negative values, see figure 3.5, and hence to a slower deposition rate at a constant potential. This explains the decrease in thickness.

3.1.1.3 Electrodeposition of Al from [(EMImCl/$AlCl_3$):BzMImCl]

In the present part, Al electrodeposition is carried out in the Lewis acidic $AlCl_3$:EMImCl (3:2 molar ratio) ionic liquid with addition of different weight percents (wt.-%) of 1-benzyl-3-methylimidazolium chloride salt (BzMImCl) compared with weight percent of the Lewis acidic ionic liquid (see Fig. 3.8). The objective of this study is to investigate the effect of increase of the imidazolium salt content and decrease of $AlCl_3$ content at the same time in the ionic liquid on the Al deposites.

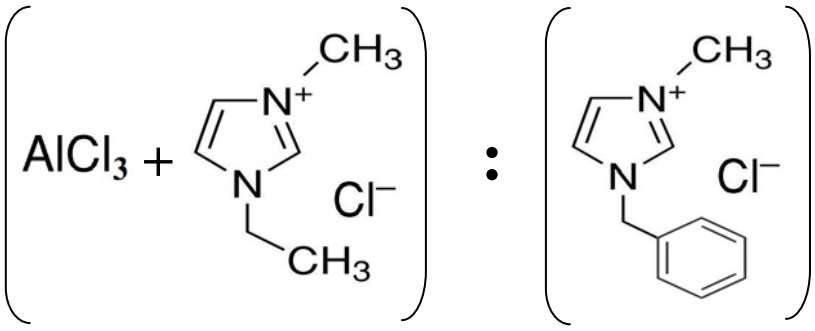

Fig. 3.8. *Simplified scheme for the prepared Lewis acidic $AlCl_3$/[EMIm]Cl ionic liquid with weight percents of 1-benzyl-3-methylimidazolium chloride salt (BzMImCl).*

Figure (3.9) shows the cyclic voltammograms of the Lewis acidic $AlCl_3$/1-ethyl-3-methylimidazolium chloride ($AlCl_3$/[EMIm]Cl) ionic liquid based on different weight percents (wt.-%) of BzMImCl salt: 0, 5, 10, 15 and 20 wt.-%, respectively, on gold substrates after potentiostatic polarization (E = –0.2 V) for 2 hours at room temperature. The figure shows that, the cyclic voltammograms obtained for the BzMImCl (wt.-%) containing ionic liquid exhibiting the same general feature of the cyclic voltammogram of $AlCl_3$/EMImCl (3:2 molar ratio) ionic liquid. By the addition of BzMImCl to the ionic liquid, the deposition potential shifts gradually to less negative values by increasing the cationic imidazolium molar ratio (more than 40 mol.-%) content and decreasing the $AlCl_3$ molar ratio (less than 60 mol.-%) at the same time. Moreover, increasing the cationic salt content, especially containing the aromatic ring, the current value and the peak size of both deposition and stripping significantly decrease. This result is due to increased viscosity and decreased aluminium content as a whole at the same time in the electrolyte caused by further addition of BzMImCl to the ionic liquid. Furthermore, inhibiting the reaction flow

rate of both cathodic deposition and anodic dissolution as result of the few $AlCl_3$ species exist and also decrease the mobility and mass transfer of the electroactive species towards the electrode surface as a result of the presence of branched benzyl group in the imidazolium structure. The ionic liquids with aromatic rings have higher densities and viscosities than the ones having alkyl. So, the physical and chemical properties of these ionic liquid systems strongly dependent on the electrolyte species **[124]**.

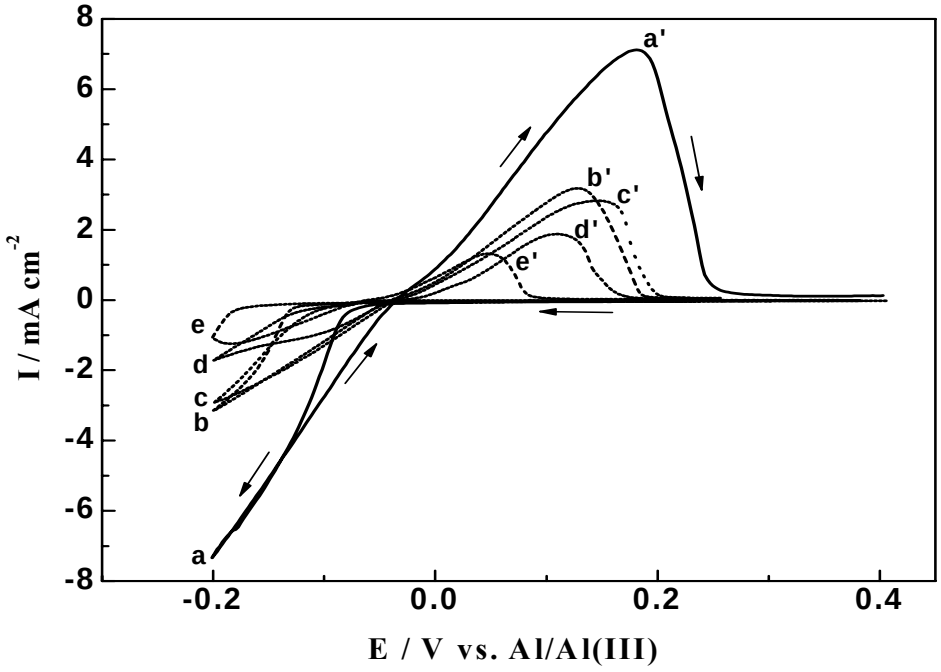

Fig. 3.9*. Cyclic voltammograms acquired on Au substrate in the BzMImCl (wt.-%) containing ionic liquid mixture of $AlCl_3$/EMImCl (3:2 molar ratio) at different weight percents: a=0 wt.-%), b=5 wt.-%), c=10 wt.-%), d=15 wt.-%), e=20 wt.-%), respectively, after potentiostatic polarization (E = –0.2 V) for 2 hours at room temperature. The scan rate was 10 mVs^{-1}.*

The surface morphology of electrodeposited Al films obtained potentiostatically at – 0.2 V for two hours in the Lewis acidic $AlCl_3$/[EMIm]Cl ionic liquid contains weight percents of BzMImCl salt: 0, 5, 10, 15 and 20 wt.-%, respectively, on gold substrates at room temperature are shown in figure 3.10. The SEM micrograph of such Al films shows that the addition of BzMImCl from 0 up to 20 wt.-% to the Lewis acidic ionic liquid affected on the Al electrodeposition. So, it is clearly seen that the deposited aluminium films show gradual change of Al deposits from dense and compact to very fine microcrystallites.

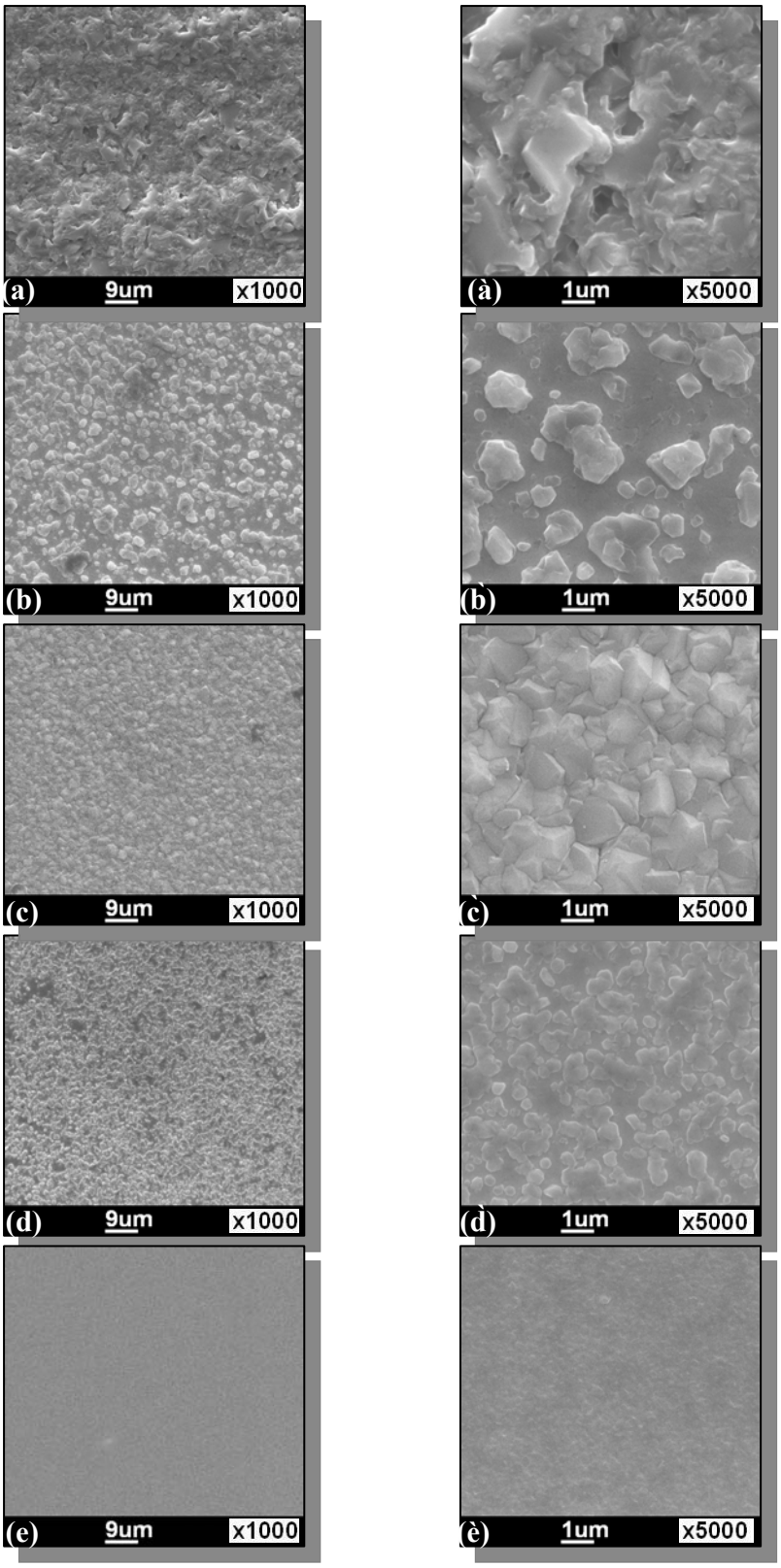

***Fig. 3.10**. SEM micrographs of electrodeposited Al films on Au substrates in the BzMImCl (wt.-%) containing ionic liquid $AlCl_3$/EMImCl (3:2 molar ratio) as follows: a=0 wt.-%), b=5 wt.-%), c=10 wt.-%), d=15 wt.-%) and e=20 wt.-%), respectively. The deposits were obtained after potentiostatic polarization (E = –0.2 V) for 2 hours at room temperature, a', b', c', d' and e' are higher resolution SEM images of the corresponding a, b, c, d and e images.*

This result is due to the $AlCl_3$ molar ratio decreased to less than 60 mol.-% and this decreases grain size of the Al deposited crystallites. Furthermore, excess of the benzyl based imidazolium content increases the viscosity of the ionic liquid and decreases the mobility of the electroactive species towards the electrode surface at the same time, which, in turn, leads to inhibiting the reaction rate of both oxidation and reduction. Figure (3.11) shows the thickness diagram of the electrodeposited Al films obtained in the mentioned ionic liquid with BzMImCl salt from 0 up to 20 (wt.-%), respectively. The figure shows clearly decrease of a Al film thicknesses with increasing the addition of BzMImCl salt. The addition of BzMImCl to the ionic liquid leads to shifting the bulk deposition potential gradually to less negative at the expense of $AlCl_3$ molar ratio. So, the thickness value of Al films, which, in turn, directly proportional with the applied current values and act as a main factor in the calculations decreased.

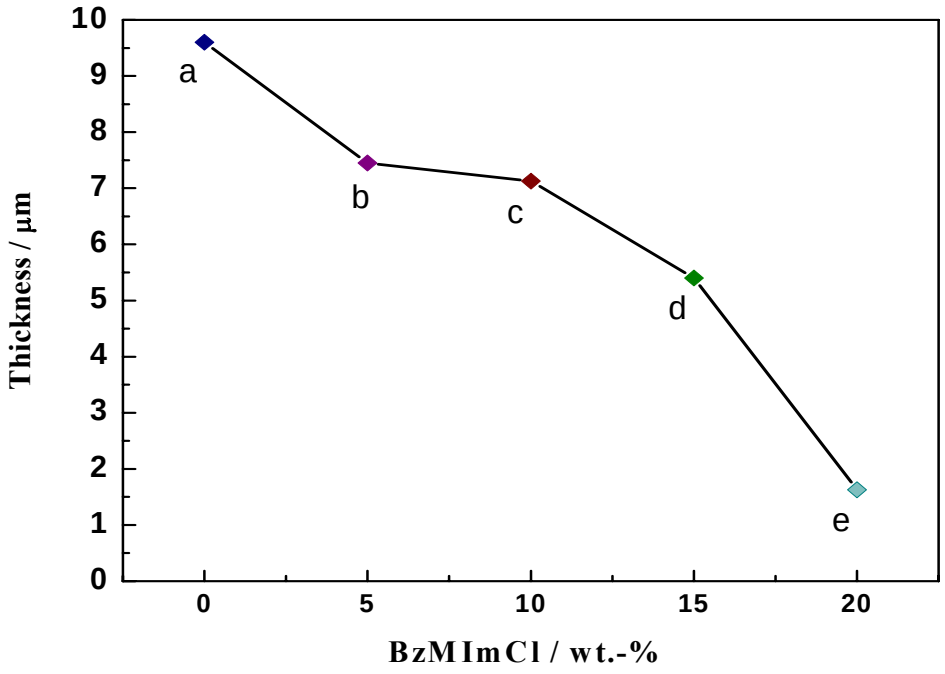

Fig. 3.11. *A diagram shows the change in thickness of Al deposit obtained from the BzMImCl (wt.-%) containing ionic liquid $AlCl_3$/EMImCl (3:2 molar ratio) as follows: a=0 wt.-%), b=5 wt.-%), c=10 wt.-%), d=15 wt.-%) and e=20 wt.-%), respectively. The deposits were obtained after potentiostatic polarization (E = –0.2 V) for 2 hours at room temperature.*

3.1.1.4 Electrodeposition of Al from [$AlCl_3$/(EMImCl:DBzImCl)]

As the presence of a benzyl group in the imidazolium based ionic liquid showed an effect on the morphology and thickness of Al deposit, it was of interest to investigate the effect of "two" aromatic substituents on Al deposition. In this part was carried out by gradual replacement of 1-ethyl-3-methylimidazolium chloride salt (EMImCl = 40 mol.-%) by 1,3-dibenzylimidazolium chloride salt (DBzImCl) (see Fig. 3.12). The concentration of $AlCl_3$ was kept constant (60 mol.-%). The (EMImCl : DBzImCl) molar ratios was changed as follows: 40:0, 30:10, 20:20, 10:30 and 0:40 mol.-%, respectively.

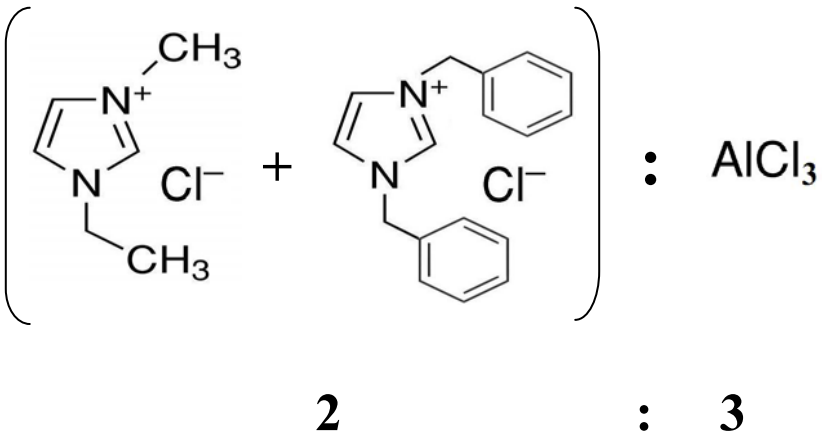

Fig. 3.12. *Simplified scheme for the prepared Lewis acidic $AlCl_3$:(EMImCl/ DBzImCl) (3:2 molar ratio).*

Figure (3.13) represents the cyclic voltammograms of the Lewis acidic $AlCl_3$:EMImCl/DBzImCl (3:2 molar ratio) ionic liquid at room temperature containing fixed amount of $AlCl_3$ (60 mol.-%) on gold substrates at different (EMImCl:DBzImCl) molar ratios: 40:0, 30:10, 20:20, 10:30 and 0:40 mol.-%, respectively. The figure shows, similar to the $AlCl_3$:EMImCl/BzMImCl system that all cyclic voltammograms of $AlCl_3$:EMImCl/DBzImCl mixture have more or less the same general feature of the cyclic voltammogram recorded for the Lewis acidic ionic liquid $AlCl_3$/EMImCl (3:2 molar ratio). The deposition potential shifts rapidly to more negative values with increasing the DBzImCl content over EMImCl. Moreover, the deposition and stripping current peaks significantly decrease.

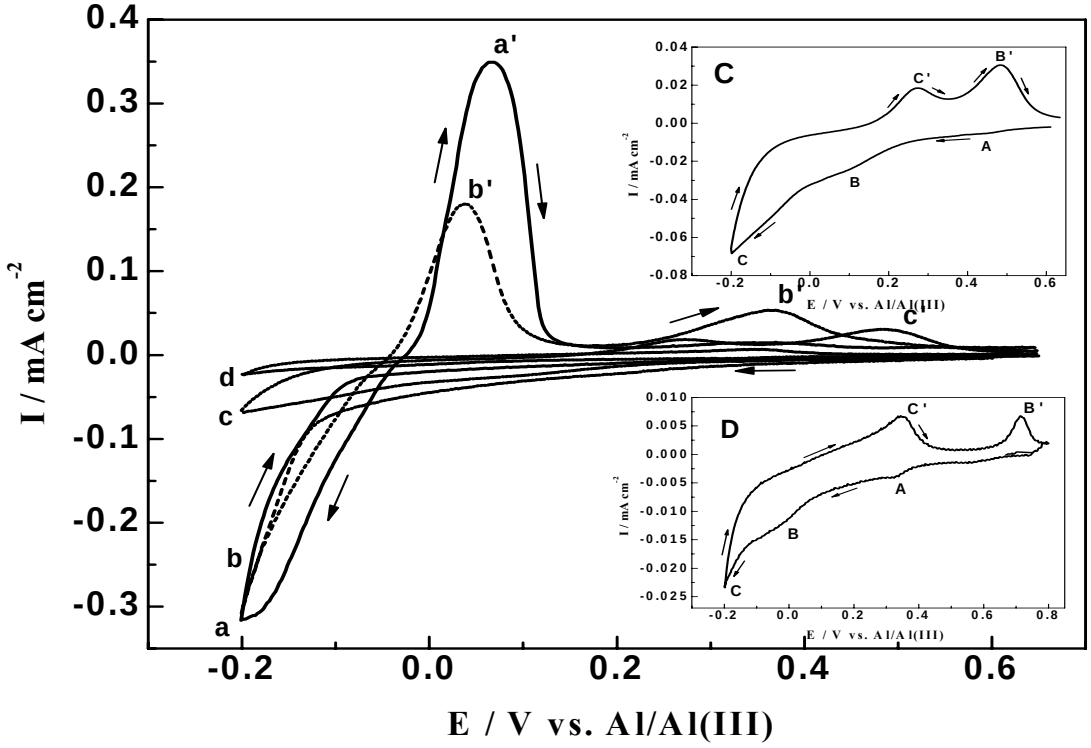

Fig. 3.13*. Cyclic voltammograms acquired on Au substrate in $AlCl_3$ containing ionic liquid mixture of [EMImCl:DBzImCl] at different molar ratios : a) (30:10 mol.-%), b) (20:20 mol.-%), c) (10:30 mol.-%) and d) (0:40 mol.-%), respectively, the $AlCl_3$ concentration is kept constant (60 mol.-%) in all. The scan rate was 10 mVs^{-1}, at room temperature.*

At high DBzImCl content (30 and 40 mol.-%) the cyclic voltammogram of the system showed two cathodic peaks (A and B) (cyclic voltammograms C and D) at potentials of about 0.45 V and 0.12 V and 0.33 V and 0.07 V, respectively. These small cathodic peaks in both cyclic voltammograms (C and D) might be attributed to the aluminium underpotential deposition (UPD) and 3D aluminium cluster formation in the beginning of the OPD regime **[126]**. It is also assumed that the two small cathodic peaks (A and B) in both cyclic voltammograms (C and D) are due to alloying between Au and Al and / or to Al electrodeposition from different Al (III) ion species in the liquid. At potentials of –0.007 and -0.08 V vs. Al/Al (III), a significant overpotential deposition attributed to the nucleation of Al deposit was found, with two small cathodic steps at cyclic voltammograms (C and D) until -0.2 V vs. Al/Al (III), C, that are presumably correlated to two different processes.

The small broad anodic peaks (B` and C`) are corresponding to Al stripping. The two cyclic voltammograms show distinct features both in the forward and reverse scans. There is a direct correlation between processes B and B` and C and C`: The change in the cyclic voltammograms is due to the presence of two aromatic groups in the imidazolium based salt which increase the resistance of the electroactive species towards the electrode surface, as mentioned before, which, in turn, leads to inhibiting the reaction rate of both reduction and oxidation. Also, the imidazolium salt based ionic liquids with two benzyl groups have higher densities and viscosities than the ones having one benzyl group in the same electrolyte. As a result, the viscosity sequence of ionic liquids based on different imidazolium salts will be as the following range Ar-Ar-ImCl > Ar-R-ImCl > R-R-ImCl, respectively. **[124,127]**.

Figure (3.14) shows SEM micrographs of Al deposits obtained from the mentioned system on gold substrate after a potentiostatic polarization at – 0.2 V vs. Al/Al (III) at room temperature for 2 hours. The effect of increasing the concentration of 1,3-dibenzylimidazolium chloride salt (DBzImCl) from 0 up to 40 mol.-%, with taking into consideration that the total molar ratio of the two imidazolium salts to $AlCl_3$ in all cases to be 40 to 60 mol.-%, respectively. It is clearly seen that the surface morphology of the deposited aluminium film shows gradual conversation from compact and dense microcrystallites to small and thin rod-shaped nanocrystallites with increasing DBzImCl content (at constant $AlCl_3$ concentration of 60 mol.-%). On the other hand, the film thickness was decreased from 9 to 0.3 μm in the same trend, see the diagram in figure (3.15). This is due to the increased viscosity upon the increasing DBzImCl content which reduces the deposition rate and hence the grain size of the Al deposited crystallites.

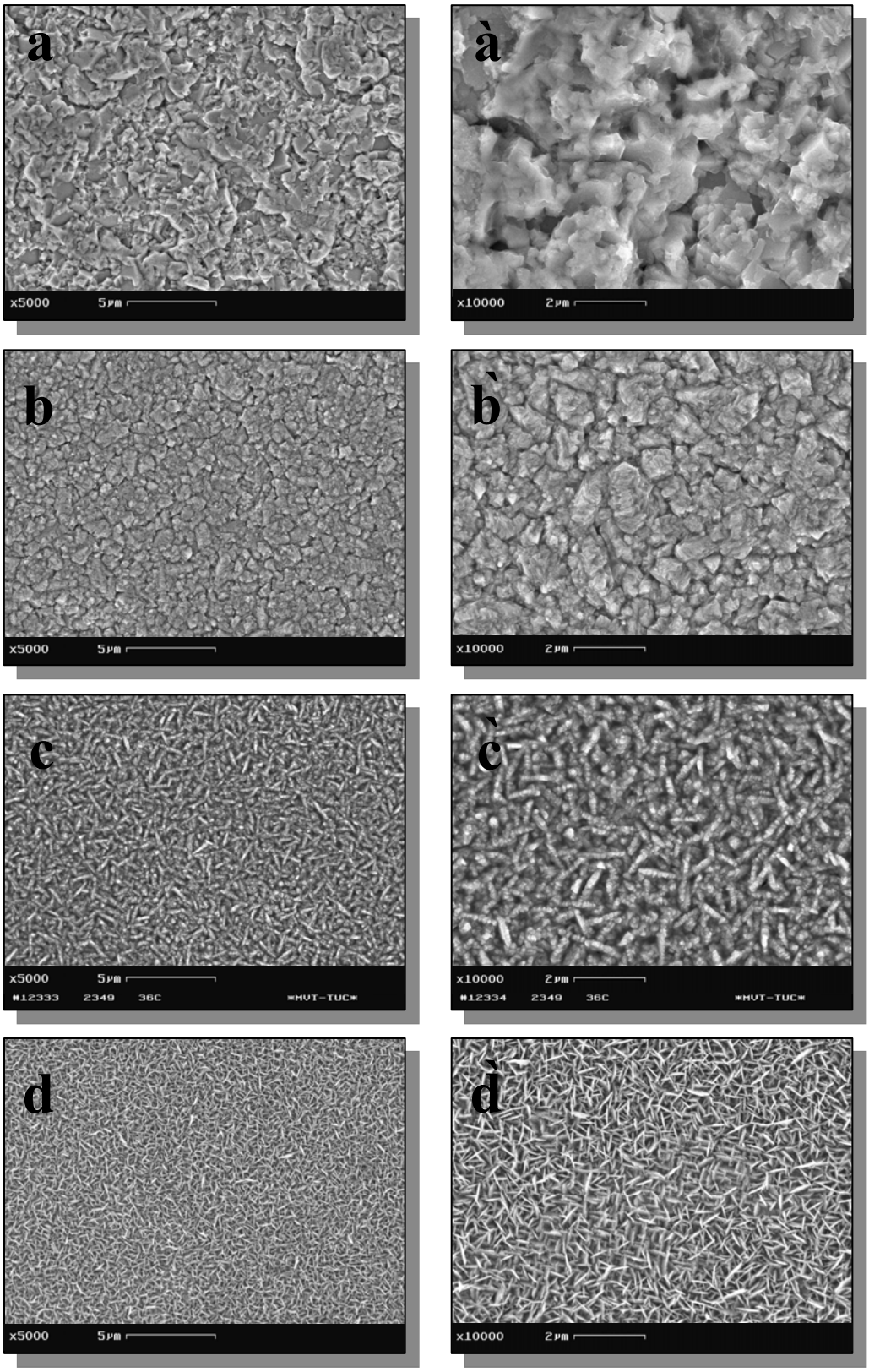

Fig. 3.14*. SEM micrographs of electrodeposited Al films on Au substrates in Lewis acidic ionic liquid consisting of a fixed $AlCl_3$ concentration (60 mol.-%) and a mixture of the ionic liquids EMImCl:DBzImCl as follows: , a) (40:0 mol.-%), b) (30:10 mol.-%), c) (20:20 mol.-%), d) (0:40 mol.-%), respectively. The deposits were obtained after potentiostatic polarization (E = –0.2 V) for 2 hours at room temperature. a', b', c', d' are higher resolution SEM images of the corresponding a, b, c, d images.*

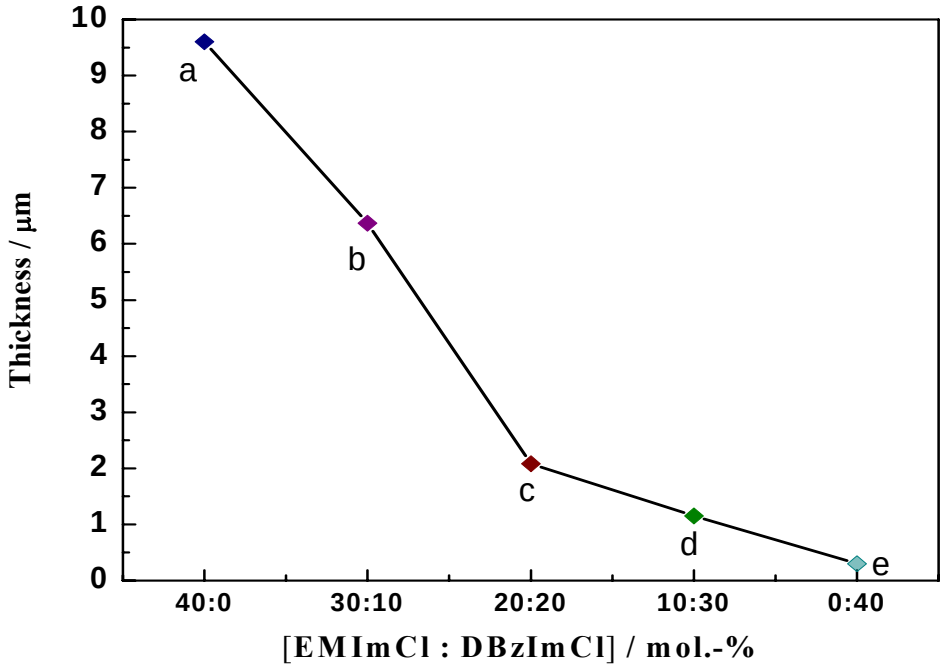

Fig. 3.15. *A diagram shows the change in thickness of Al deposit obtained from the $AlCl_3$ containing Lewis acidic ionic liquid mixture [EMImCl:DBzImCl] on Au substrates at different molar ratio: a) (40:0 mol.-%), b) (30:10 mol.-%), c) (20:20 mol.-%), d) (10:30 mol.-%) and e) (0:40 mol.-%), respectively. $AlCl_3$ was kept constant (60 mol.-%) in all cases. The deposits obtained after potentiostatic polarization (E = –0.2 V) for 2 hours at room temperature.*

3.1.1.5 Electrodeposition of Al from [(EMImCl/$AlCl_3$):DBzImCl]

In the following part, the electrodeposition of aluminium is carried out in the prepared Lewis acidic $AlCl_3$:EMImCl (3:2 molar ratio) ionic liquid with addition of different weight percents (wt.-%) of 1,3-dibenzylimidazolium chloride salt (DBzImCl) compared with weight percent of the Lewis acidic ionic liquid as shown in figure 3.16. The aim of this study is to show the effect of increase the dibenzyl based imidazolium salt molar ratio over $AlCl_3$ molar ratio at the same time in the ionic liquid on the Al deposites.

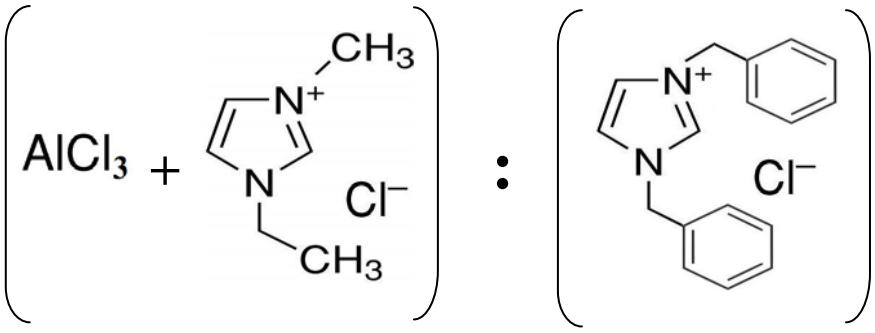

Fig. 3.16. *Simplified scheme for the prepared Lewis acidic $AlCl_3$/[EMIm]Cl ionic liquid with weight percents of 1,3-dibenzylimidazolium chloride salt (DBzImCl).*

Figure (3.17) exhibits the cyclic voltammograms of the Lewis acidic $AlCl_3$/1-ethyl-3-methylimidazolium chloride ($AlCl_3$/[EMIm]Cl) (3:2 molar ratio) ionic liquid containing different weight percents (wt.-%) of 1,3-dibenzylimidazolium chloride salt (DBzImCl): 0, 5, 10, 15 and 20 wt.-%, respectively, on gold substrates after potentiostatic polarization (E = –0.2 V) for 2 hours at room temperature. The figure shows that, the cyclic voltammograms exhibit the same general feature of the cyclic voltammogram of $AlCl_3$:EMImCl (3:2 molar ratio) ionic liquid alone. The deposition potential shifts gradually with the addition of DBzImCl salt to more negative values. Furthermore, with increasing the molar ratio of DBzImCl, the current value and the peak size of both deposition and stripping clearly decrease. The reason of this behaviour is due to increasing of the cationic imidazolium content with the two bulky benzyl groups and decreasing the aluminium content at the same time in the ionic liquid.

Moreover, the deposition and dissolution flow rate decreased as result of the few $AlCl_3$ species exist and also decrease the mobility of the electroactive species towards the electrode surface. So, the ionic liquid contains "two" aromatic substituent based imidazolium salt has a higher viscosity than the imidazolium based on one aromatic substituent **[124]**.

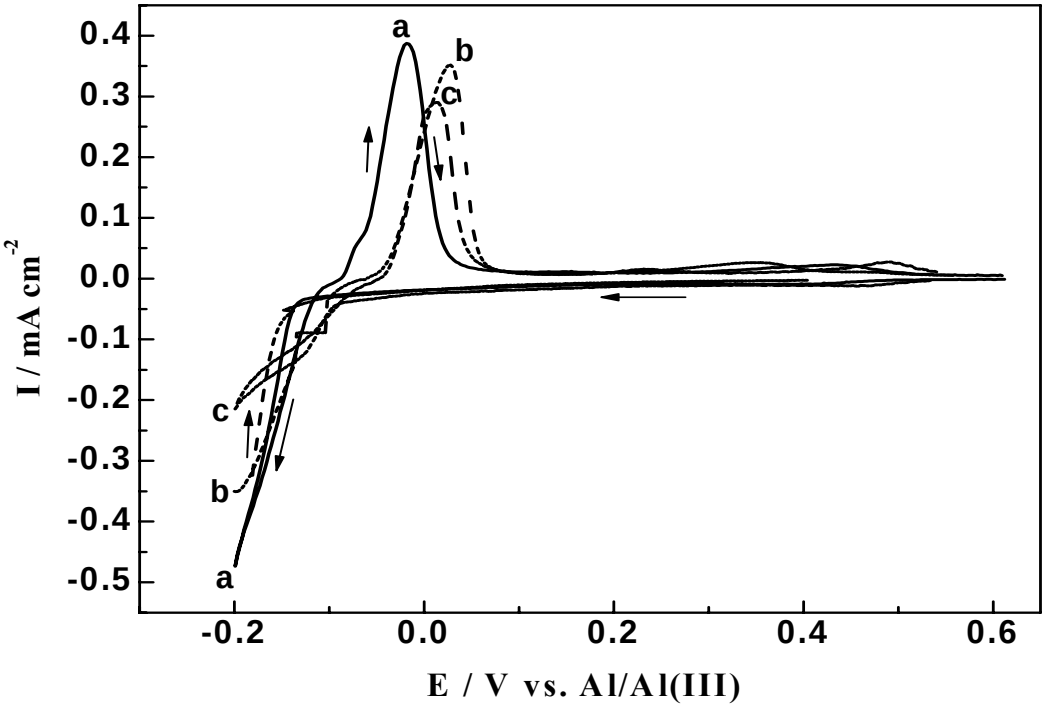

Fig. 3.17*. Cyclic voltammograms acquired on Au substrate in the DBzImCl (wt.-%) containing ionic liquid mixture of $AlCl_3$/EMImCl (3:2 molar ratio) at different weight percents: a=5 wt.-%), b=10 wt.-%) and c=15 wt.-%), respectively, after potentiostatic polarization (E = –0.2 V) for 2 hours at room temperature. The scan rate was 10 mVs^{-1}.*

As seen in figure (3.18), the surface morphology of the aluminium deposits shows gradual change from compact and dense microcrystallites to small and rod-shaped nanocrystallites with increasing the dibenzyl imidazolium salt content over $AlCl_3$ content. On the other hand, the film thickness of the Al electrodeposits was decreased from the micro- to the nanometer regime in the same trend; see the diagram in figure (3.19). This result is due to increasing the viscosity of the reaction medium with the addition of dibenzyl based imidazolium salt, which, in turn, decreasing the deposition rate and the mass transport of the electroactive species towards the electrode surface and this all decreasing the grain size of the Al electrodeposited crystallites.

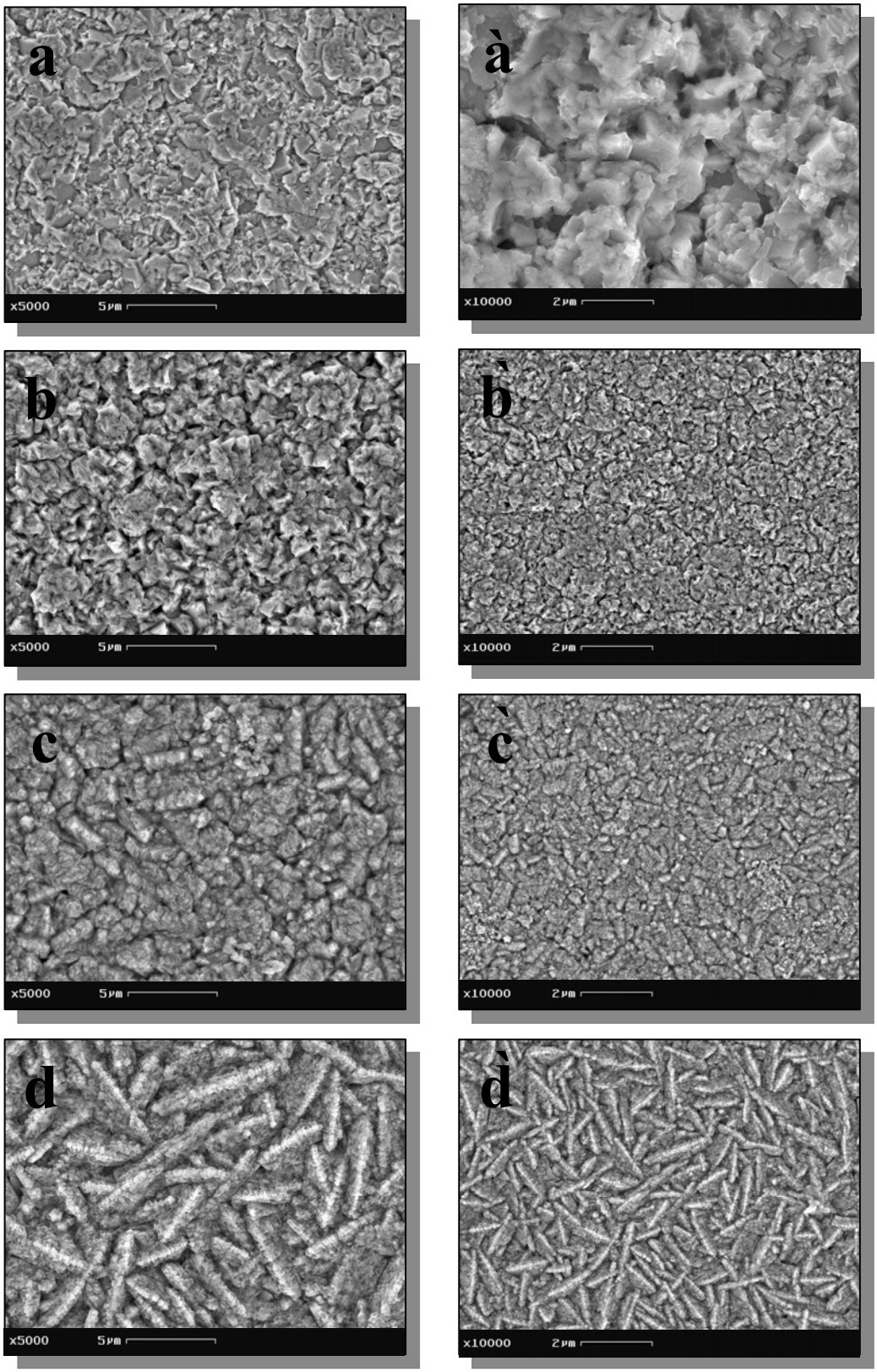

***Fig. 3.18**. SEM micrographs of electrodeposited Al films on Au substrates in the DBzImCl (wt.-%) containing ionic liquid $AlCl_3$/EMImCl (3:2 molar ratio) as follows: a=0 wt.-%), b=5 wt.-%), c=10 wt.-%) and d=15 wt.-%), respectively. The deposits were obtained after potentiostatic polarization (E = –0.2 V) for 2 hours at room temperature, a', b', c' and d' are higher resolution SEM images of the corresponding a, b, c and d images.*

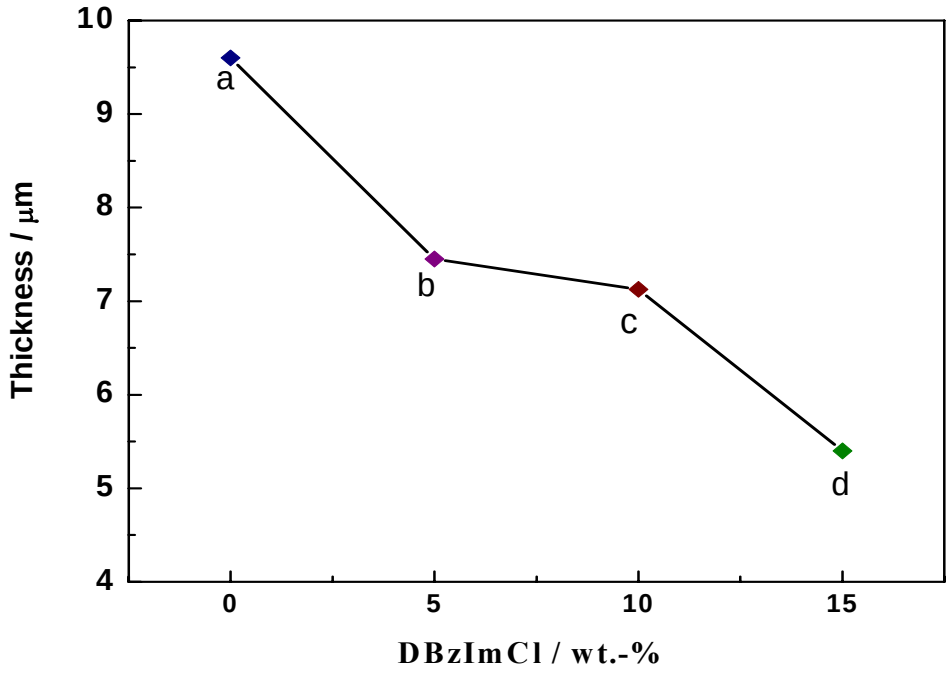

Fig. 3.19. *Thickness diagram shows the change in Al deposits obtained from the DBzImCl (wt.-%) containing ionic liquid $AlCl_3$/EMImCl (3:2 molar ratio) as follows: a=0 wt.-%), b=5 wt.-%), c=10 wt.-%) and d=15 wt.-%), respectively. The deposits were obtained after potentiostatic polarization (E = –0.2 V) for 2 hours at room temperature.*

3.1.1.6 Comparison study between the three $AlCl_3$ based ionic liquids

In the present section, the results obtained from the three prepared acidic ionic liquid systems: $AlCl_3$/1-ethyl-3-methylimidazolium chloride ($AlCl_3$/[EMIm]Cl), $AlCl_3$/1-benzyl-3-methylimidazolium chloride ($AlCl_3$/[BzMIm]Cl) and $AlCl_3$/1,3-dibenzylimidazolium chloride ($AlCl_3$/[DBzIm]Cl), respectively, (figure 3.20) are summarized for better comparison.

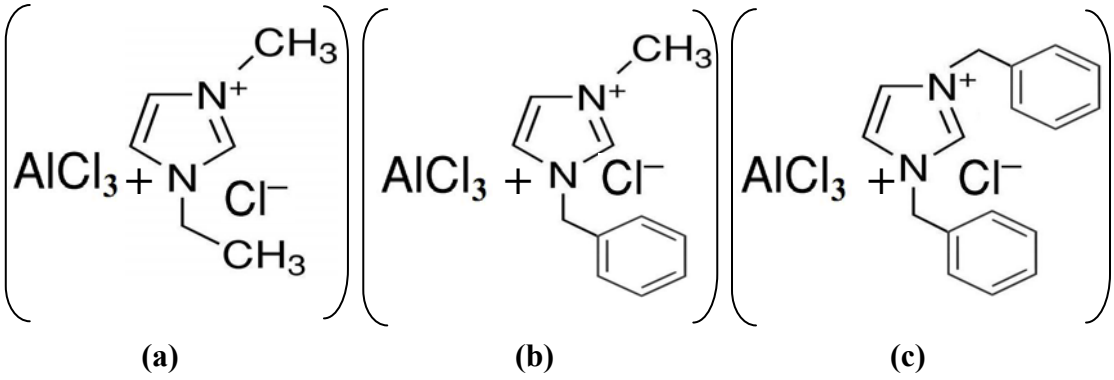

Fig. 3.20. *Simplified scheme for the composition of the three prepared Lewis acidic ionic liquids: a) ($AlCl_3$/[EMIm]Cl), b) ($AlCl_3$/[BzMIm]Cl) and c) ($AlCl_3$/[DBzIm]Cl), respectively.*

Figure (3.21) represents the cyclic voltammograms (on Au substrate) of the three prepared Lewis acidic ionic liquids; $AlCl_3$/[EMIm]Cl, $AlCl_3$/[BzMIm]Cl and $AlCl_3$/[DBzIm]Cl, a, b and c, respectively, at room temperature containing all 60 mol.-% $AlCl_3$. In general, the cyclic voltammograms of [BzMIm]$AlCl_4$ (3:2 molar ratio) ionic liquid (b) and [EMIm]$AlCl_4$ (3:2 molar ratio) ionic liquid are quite similar. On the other hand, the cyclic voltammogram of [DBzIm]$AlCl_4$ (3:2 molar ratio) ionic liquid (c) is different from the other two system. This is apparently due to the much higher viscosity of this liquid. The dialkyl imidazolium based ionic liquid (a) has the lowest viscosity value compared with the two other systems (b and c). Furthermore, in the system (b), the deposition potential shifts to low negative values compared with the values in system (a) due to the presence of one benzyl substituent in the imidazolium cation. Whereas, in the case of (c), the diaryl imidazolium based ionic liquid has the highest viscosity value than two the other systems (a and b), which in turn shifts the deposition potential to more negative values.

The cyclic voltammograms of the systems (b and c) showed two small cathodic peaks (A and B) at potentials of about 0.52 and 0.03 V and 0.44 and 0.12 V, respectively. This might be attributed to the aluminium underpotential deposition (UPD) and 3D aluminium cluster formation in the beginning of the overpotential deposition (OPD) regime, respectively **[127]**. It is also assumed that the two small cathodic peaks (A and B) in both cyclic voltammograms (b and c) are due to alloying between Au and Al and / or to Al electrodeposition from different Al (III) ion species in the liquid. A significant overpotential deposition of the cyclic voltammograms (b and c) attributed to the nucleation of Al deposit at a potentials of -0.1 and –0.006 V vs. Al/Al (III), respectively, was found with small cathodic step to -0.2 V vs. Al/Al (III), that are correlated to two different process. The small broad anodic peaks (C and B) are correlated to Al stripping.

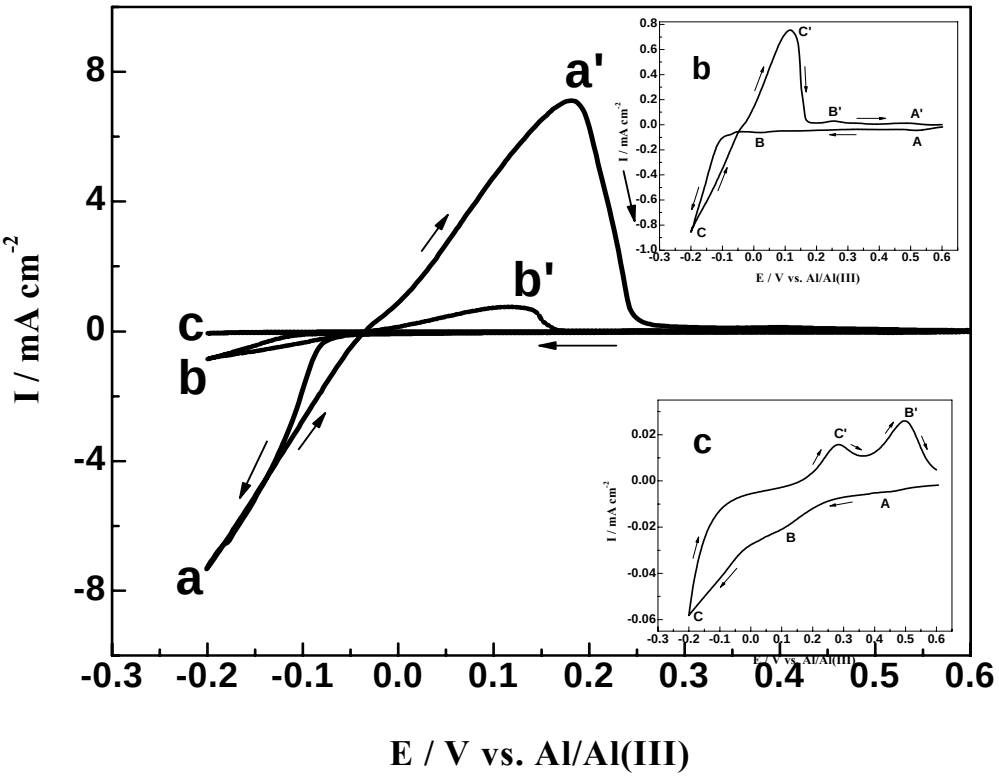

Fig. 3.21*. Cyclic voltammograms acquired at Au substrate from the three Lewis acidic ionic liquids (3:2 molar ratio), a) $AlCl_3$ / EMImCl, b) $AlCl_3$ / BzMImCl and c) $AlCl_3$ / DBzImCl, respectively, after potentiostatic polarization (E = –0.2 V) for 2 hours at room temperature. The scan rate was 10 mVs^{-1}.*

The cyclic voltammogram shows distinct features both in the forward and reverse scans. There is a direct correlation between processes B and B` and C and C`: The main reason for this significantly change in the cyclic voltammogram shapes with BzMImCl and DBzImCl (at fixed concentration of 40 mol.-%) is due to the presence of the benzyl groups in the imidazolium based salt with high concentration which increase the resistance of the electroactive species towards the electrode surface, as mentioned before, which, in turn, leads to inhibiting the reaction rate of both reduction and oxidation. Moreover, imidazolium salt based ionic liquids with two benzyl groups have higher densities and viscosities than the ones having one benzyl group which exist as closed system in the ionic liquid. Finally, the viscosity sequence of the three ionic liquids based on different imidazolium salts will be as the following range DBzImCl > BzMImCl > EMImCl, respectively. **[124,127]**.

Figure (3.22) shows high resolution SEM micrographs (a, b and c) of Al deposits from the three mentioned Lewis acidic ionic liquids: $AlCl_3$/[EMIm]Cl, $AlCl_3$/[BzMIm]Cl and $AlCl_3$/[DBzIm]Cl, respectively. These deposits were obtained after applying a potential of – 0.2 V vs. Al/Al (III) at room temperature for 2 hours. It can be clearly seen that the type of the substituents in the imidazolium cation affects strongly on the surface morphology of deposited Al: The dialkyl substituent imidazolium based ionic liquid $AlCl_3$/[EMIm]Cl gave a compact and dense Al deposit (a). Whereas, the mono aryl-substituted one [BzMIm]$AlCl_4$ gave a coarse and cubic-shaped microcrystalline morphology (b). Interestingly, the diaryl-substituted imidazolium based ionic liquid gave rod-shaped nanocrystallites (c). The average thickness of Al from the three systems a, b and c is 9, 3 and 0.3 µm, respectively, see figure 3.23. This is plausible, because of viscosity increase in the direction from a to c, which in turn, gives rise to a deposition rate decrease in the same direction. Viscosity might be also the key factor in the significant difference in the surface morphology of the Al deposits. However, the effect of solvation layers can not be excluded with bearing in mind the presence of flat benzyl groups which can stack together or be oriented in away that affect the deposition process in a certain manner. This possible supposition may be explain why the presence of one benzyl group in the imidazolium cation gives larger microcrystallites, while the presence of two benzyl groups gives nanocrystallites.

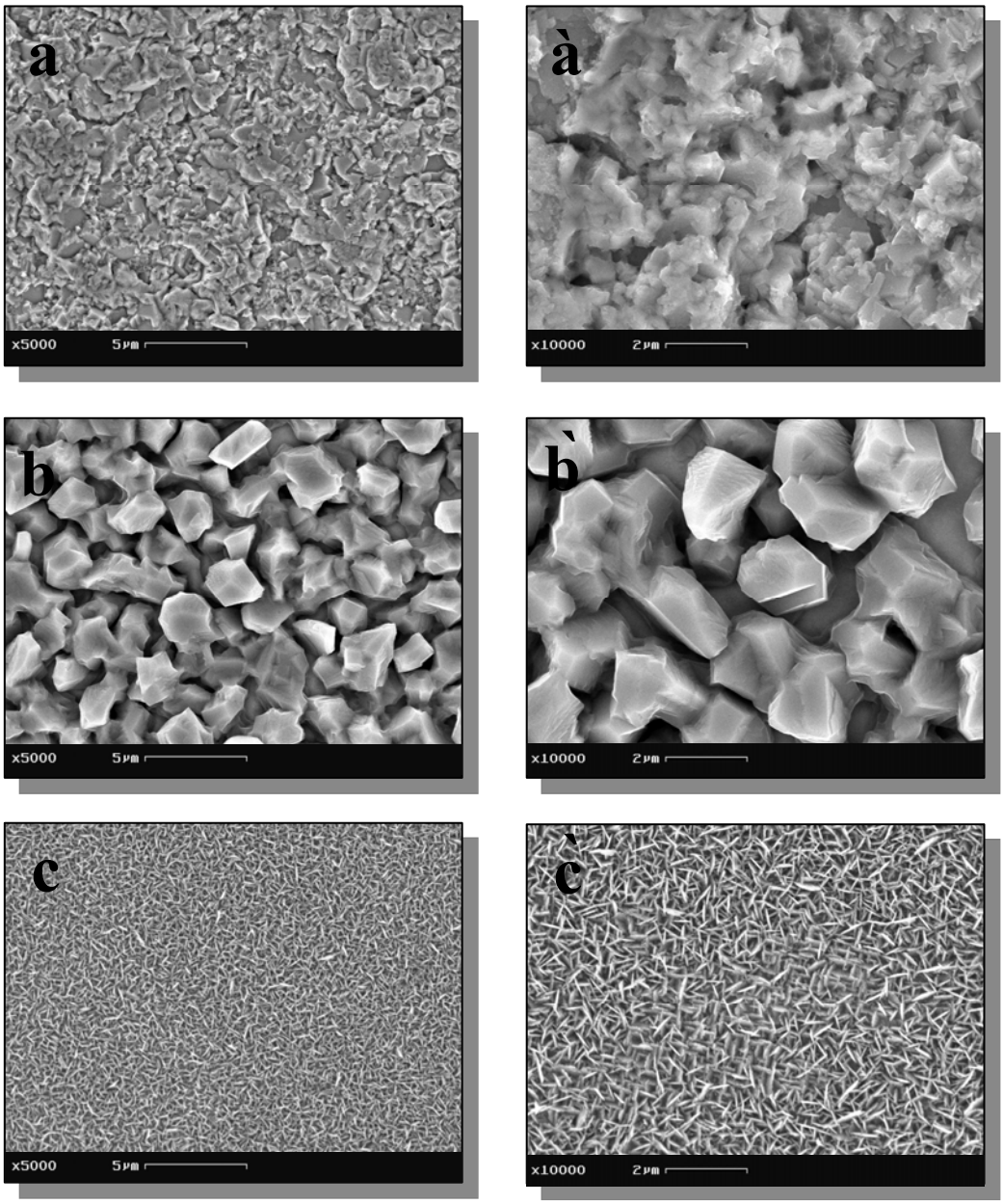

Fig. 3.22. *SEM micrographs of electrodeposited Al films on Au substrates in the three Lewis acidic ionic liquids (3:2 molar ratio): a) $AlCl_3$/EMImCl, b) $AlCl_3$/BzMImCl, c) $AlCl_3$/DBzImCl, after potentiostatic polarization (E = –0.2 V) for 2 hours at room temperature, a', b' and c' are higher resolution SEM images of the corresponding a, b and c images.*

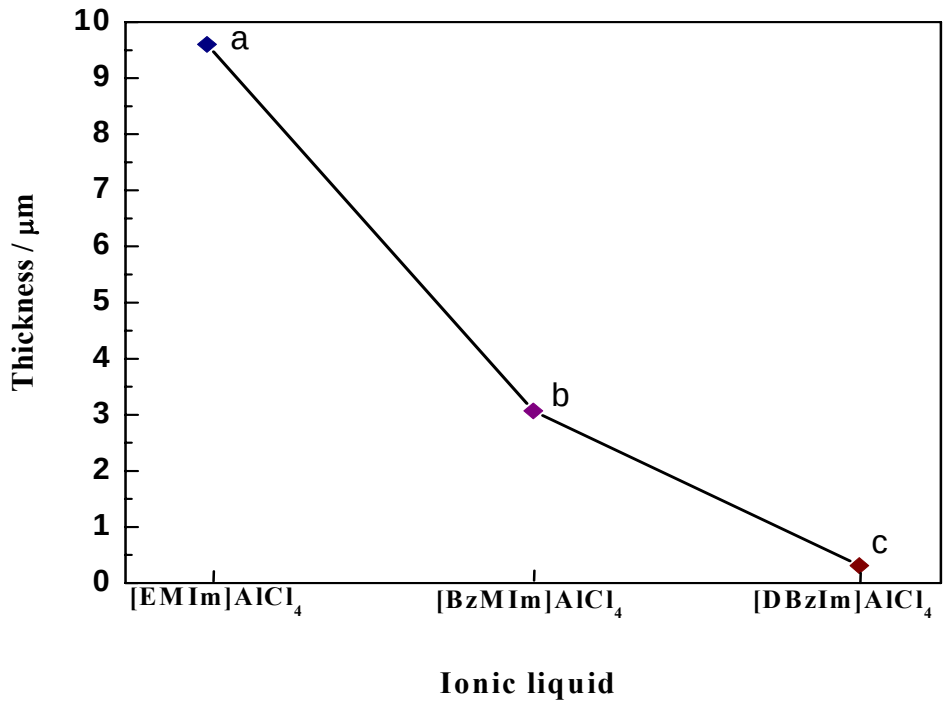

***Fig. 3.23**. Thickness diagram shows the change of Al deposits obtained at Au substrate from the three Lewis acidic ionic liquids, a) $AlCl_3$/[BzMIm]Cl, b) $AlCl_3$/[BzMIm]Cl and c) $AlCl_3$/[DBzIm]Cl, respectively, after potentiostatic polarization (E = –0.2 V) for 2 hours at room temperature.*

3.1.2 Electrodeposition of Al from ($AlCl_3$/[EMIm]Tf_2N)

As the recently reported results of Al deposition on Au (111) from air- and water- stable ionic liquids like 1-ethyl-3-methylimidazolium bis(trifluoromethyl-sulfonyl) amide [EMIm]Tf_2N and 1-butyl-1-methylpyrrolidinium bis(trifluoro-methylsulfonyl) amide [BMP]Tf_2N are quite promising, it is of interest to apply it for Al coating of reactive surfaces like mild steel. In the present section, the Al electrodeposition on mild steel substrates from $AlCl_3$ containing 1-ethyl-3-methylimidazolium bis(trifluoromethylsulfonyl) amide [EMIm]Tf_2N ionic liquid is presented.

As was first reported by Endres et al. **[116,117]** $AlCl_3$ dissolves well in [EMIm]Tf_2N ionic liquid up to a concentration of about 2.5 M, a biphasic mixture is obtained upon further addition of $AlCl_3$ similar to the behaviour of several liquids based on bis(trifluoromethylsulfonyl) amide systems, as firstly described by Wasserscheid **[128]**. Below 2.5 M $AlCl_3$, it is not possible to deposit Al likely because the Tf_2N anion reacts with $AlCl_3$ to form a stable complex that is not reduced within the liquid electrochemical window. In the biphasic $AlCl_3$/ [EMIm]Tf_2N mixture ($AlCl_3$ concentration $\geq$ 2.5 M), the upper phase looks clear and colourless while the lower one is pale and more viscous. Upon further addition of $AlCl_3$, the viscosity of the lower phase increases and it solidifies at a concentration of bit more than 5 M. The biphasic mixture becomes monophasic by heating up to a temperature of about 80 ºC as shown in figure 2.2. As reported in **[116,117],** Al can only be electrodeposited from the upper phase, that is, the clear one. This was ascribed to the presence of mainly [EMIm]$AlCl_4$ and traces of free $[Tf_2N]^-$ and octahedral $Al(Tf_2N)_3$ compound in the upper phase of the biphasic mixture. In the lower phase the amount of $[AlCl_4]^-$ was found to be very small and the main components are free $[Tf_2N]^-$ and octahedral $Al(Tf_2N)_3$ compound. Thus, $[Tf_2N]^-$ can be completely exchanged by $[AlCl_4]^-$ and the lower phase contains only $Al(Tf_2N)_3$. The upper phase does not dissolve the octahedral complex, but some Raman spectroscopic measurements, in combination with quantum chemical calculations, suggest a mixed $[AlCl_x(Tf_2N)_y]^-$ species (x and y are most likely 2) to be the electrochemically active species. These species are supposed to be formed at the phase boundary between $Al(Tf_2N)_3$ and $[AlCl_4]^-$ **[129]**.

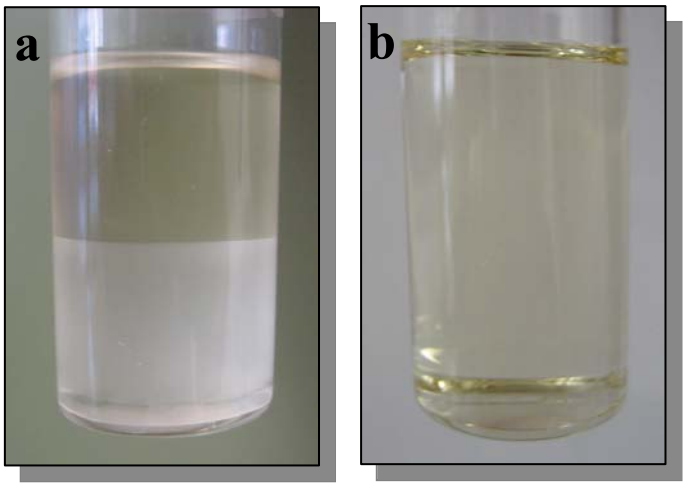

Fig.2.2. *(a) A biphasic mixture of the ionic liquid 1-ethyl-3-methylimidazolium bis(trifluoromethylsulfonyl) amide containing 5.5 M $AlCl_3$ at room temperature. (b) The biphasic mixture becomes monophasic at 80 °C.*

Figure (3.24) shows a typical cyclic voltammogram of the upper phase of the biphasic mixture of $AlCl_3$ / [EMIm] Tf_2N ($AlCl_3$ concentration = 5.5 M) on a mild steel substrate at room temperature. As can be seen, the bulk electrodeposition of aluminium starts at a potential of about – 0.2 V vs. Al/Al (III) as indicated by the reduction peak (A) observed in the forward scan. The small cathodic peak at a potential of about -0.54 V vs. Al/Al (III) is correlated to the over potential deposition (OPD) of Al on Au. As a similar behaviour on Au substrates was reported in **[116,117],** which was proved by scanning tunneling microscopy (STM) to the Al UPD and 3D Al cluster formation in the beginning of the OPD regime **[126,130]**.

The anodic peak (A´) recorded in the back scan at a potential of about 0.27 V vs. Al/Al (III) is correlated to the dissolution of the electrodeposit. The ratio of the anodic to the cathodic charge is equal to unity within the experimental error, suggesting the complete stripping of the Al deposit.

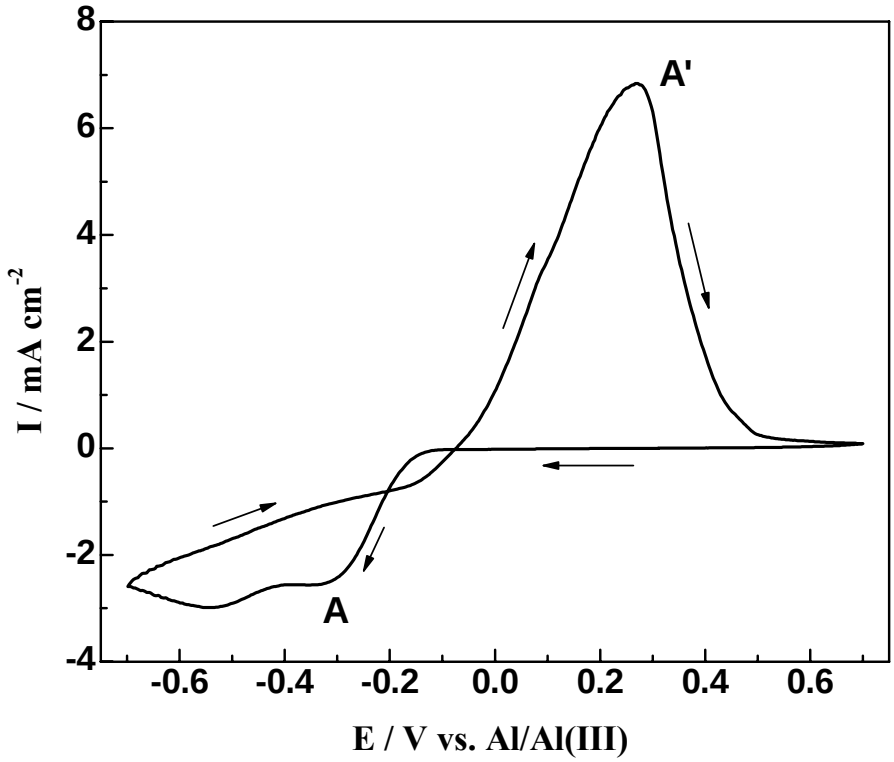

Fig. 3.24. *Cyclic voltammogram recorded on mild steel substrate in the ionic liquid 1-ethyl-3-methyl imidazolium bis (trifluoromethylsulfonyl) amide containing 5.5 M $AlCl_3$ (from the upper phase of the mixture) at room temperature.The scan rate was 10 mVs^{-1}.*

The Al deposits obtained at room temperature were investigated by means of high-resolution field-emission scanning electron microscopy (SEM). Figure (3.25) shows high resolution SEM micrographs of thick Al layers on mild steel substrate electrodeposited potentiostatically (– 0.2 V vs. Al/Al (III)) at room temperature for 2, 6 and 12 hours, a, b and c, respectively. A thickness of 2 to 24 μm was easily obtained. From the SEM images (see Figs.3.25a-c), it can clearly see that the electrodeposits obtained at 2 hours are compact and dense. The Al film made at room temperature sometimes peeled off, forming a cylinder. Internal or residual stress almost always appears during the electrodeposition of metals and alloys. The stress can originate from intrinsic film stress and from interfacial stress between the deposit and substrate. This behaviour might be attributed to some factors such as coalescence of the crystallites, inclusion of foreign species or generation of structural defects **[125]**.

Interestingly, the particle size of the deposit (at room temperature) increases enormously with increasing the duration of the Al electrodeposition up to 6 hours and the deposit apparently became porous and coarse (Fig. 3.25b). Continuous increase of the electrodeposition time up to 12 hours gives spaced porous deposition with coarse crystallites (Fig. 3.25c).

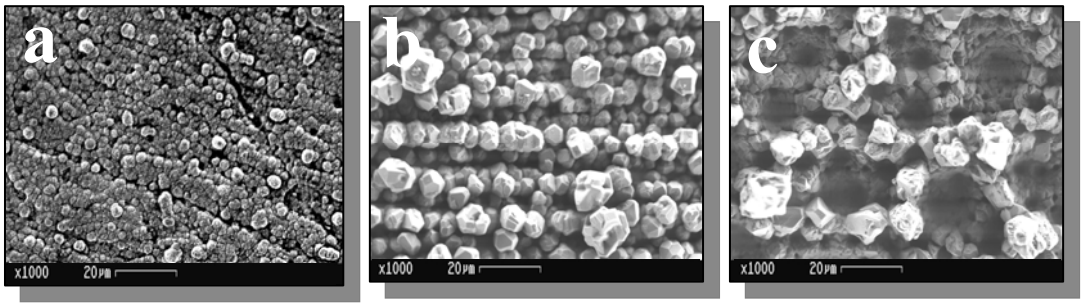

Fig. 3.25. *SEM micrographs of electrodeposited Al films on mild steel substrates formed after potentiostatic polarization at -0.2 V at room temperature in the upper phase of the mixture $AlCl_3$ / [EMIm]Tf_2N for a) 2 hrs., b) 6 hrs. and c) 12 hrs., respectively .*

The EDAX spectrum (figure 3.26) of Al deposit shown in figure 3.25a shows besides Al a small amount of oxygen due to ex situ treatment and very small amount of C, Na and Cl as contaminants.

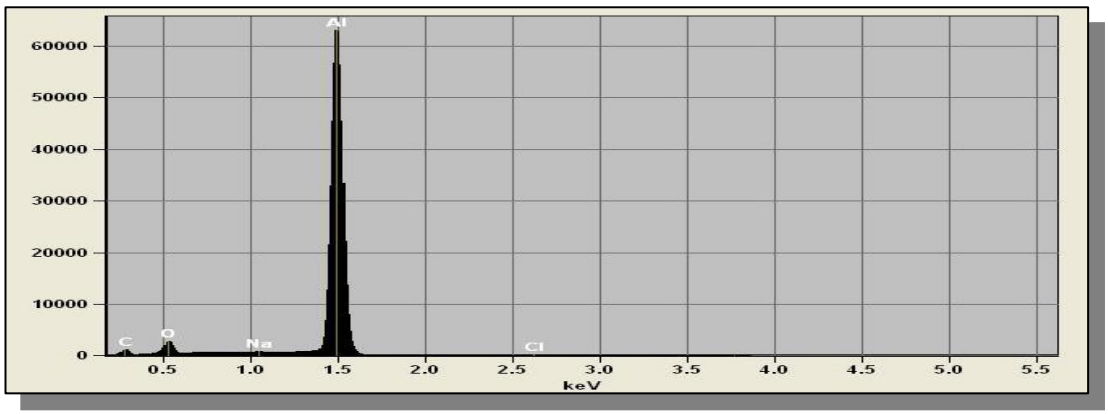

Fig. 3.26. *EDAX profile for the area shown in the SEM micrographs (Fig. 3.25a).*

Therefore it can be concluded that under the applied conditions aluminium is electrodeposited as a microcrystalline metal from the employed imidazolium based ionic liquid [EMIm]Tf_2N with coarse cubic-shaped aluminium particles. This is quite similar to that obtained on Au (111) substrates by Endres et al. **[116,117].**

3.1.3 Electrodeposition of Al from ($AlCl_3$/[BMP]Tf_2N)

It was reported by Endres et al. **[116,117]** the electrodeposition of Al from $AlCl_3$ containing 1-butyl-1-methylpyrrolidinium bis(trifluoromethylsulfonyl) amide [BMP]Tf_2N ionic liquid gave nanocrystalline Al deposits (on Au (111)) with a very fine morphology. This would be very interesting if the same nano- and fine morphology of Al can be also obtained on reactive metal/alloy surfaces like mild steel. The present section aims to investigate this subject.

In view of the previous $AlCl_3$/[EMIm]Tf_2N mixture, $AlCl_3$/[BMP]Tf_2N also shows a biphasic behaviour with increasing the concentration of $AlCl_3$ **[127]**. As mentioned before, $AlCl_3$ dissolves well in the ionic liquid [EMIm]Tf_2N up to a concentration of about 1.5 M, then a biphasic mixture is obtained on further addition of $AlCl_3$. In addition, it is not possible to deposit Al at $AlCl_3$ concentrations below 1.5 M, which implies that the Tf_2N anion reacts with $AlCl_3$ to form a stable complex $[AlCl_x(Tf_2N)_y]^-$ that is not reduced within the liquid's electrochemical window. In contrast to the biphasic mixture of $AlCl_3$/[EMIm]Tf_2N, the upper phase of the mixture $AlCl_3$/[BMP]Tf_2N is pale and more viscous while the lower one is colourless (see Figure 2.3a). By further addition of $AlCl_3$ the volume of the lower phase decreases till reaching a concentration of 2.7 M, then only one solid phase is obtained at room temperature. The biphasic mixture $AlCl_3$/[BMP]Tf_2N becomes monophasic by heating up to a temperature of 80 ºC as shown in Figure 2.3b. As reported in **[129]** Al can only be electrodeposited from the upper phase, that is, the pale viscous one. A recent study was reported on RAMAN and NMR spectroscopic measurements on the reducible aluminium species in order to get more information on the chemical structure of them in these phases. The results showed that the addition of $AlCl_3$ to the employed ionic liquid, [BMP]Tf_2N, leads to the formation of the octahedral compound $Al(Tf_2N)_3$ and the consumed $[Tf_2N]^-$ is increasingly replaced by $[AlCl_4]^-$. At a concentration of $AlCl_3$ of 1.8 M where the system forms two phases, the upper phase containing mainly the viscous [BMP]$AlCl_4$ and traces of free $[Tf_2N]^-$ and $Al(Tf_2N)_3$. In the lower phase the amount of $[AlCl_4]^-$ present is very small. The main components here were found to be free $[Tf_2N]^-$ and $Al(Tf_2N)_3$ species.

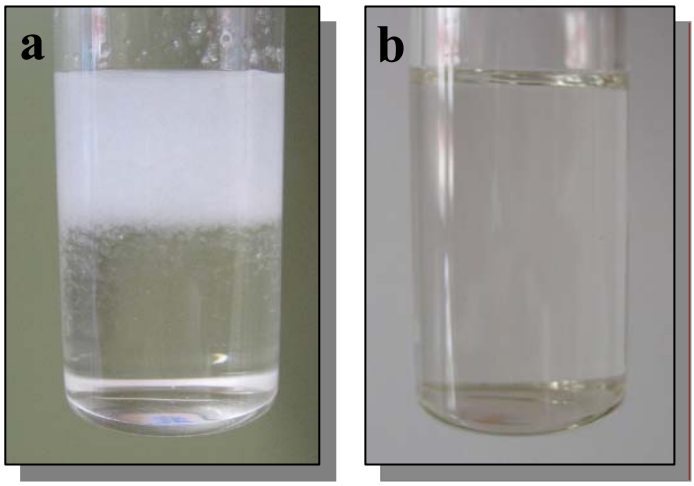

Fig.2.3. *(a) A biphasic mixture of the ionic liquid 1-butyl-1-methyl pyrrolidinium bis(trifluoromethylsulfonyl) amide containing 1.8 M $AlCl_3$ at room temperature. (b) The biphasic mixture becomes monophasic at 80 °C.*

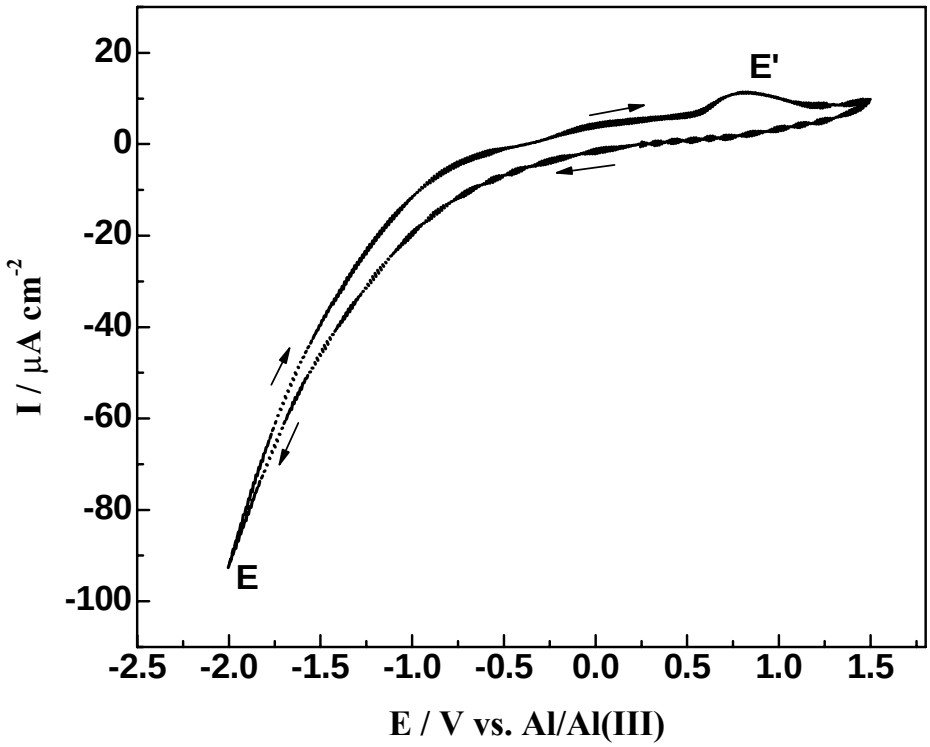

Fig. 3.27. *Cyclic voltammogram recorded on Au substrate in the ionic liquid 1-butyl-1-methyl pyrrolidinium bis(trifluoromethylsulfonyl) amide containing 1.8 M $AlCl_3$ (from the upper phase of the mixture) at room temperature.The scan rate was 10 mVs^{-1}.*

Figure (3.27) shows a typical cyclic voltammogram of the upper phase of the mixture $AlCl_3$/1-butyl-1-methylpyrrolidinium bis(trifluoromethylsulfonyl) amide on Au substrate at room temperature. The electrode potential was scanned cathodically from the open circuit potential to more negative values with a scan rate of 10 mV s^{-1}. The bulk deposition of Al starts at a potential of -0.25 V vs. Al/Al (III). The small anodic peak (E') recorded on the reverse scan at potential of about 0.8 V vs. Al/Al (III) is correlated to small partial dissolution of the deposited aluminium in the employed ionic liquid. Here, stripping seems to be kinetically hindered unlike the [EMIm]Tf_2N ionic liquid. This might be explained by the possible adsorption of some ionic liquid species on the Al deposit.

Figure (3.28) shows the cyclic voltammogram of the same phase on gold substrate at a higher temperature, such as 100 °C and compared it with that at 25 °C. At temperatures around 150 °C the evaporation of $AlCl_3$ slowly begins. It is interesting that the cyclic voltammogram recorded at 25 °C gives stable electrode potentials below -0.1 V vs. Al/Al (III). The cyclic voltammogram recorded at 100 °C exhibits a similar behaviour but with the presence of a nucleation loop at a potential of –0.6 V. At 25 °C the Al deposition rate is very slow due to the high viscosity of the mixture, which, in turn, decreases the deposition rate. Interestingly, no reversible oxidation occurs even at 100 °C. For kinetic reasons, the oxidation of Al is likely to be hindered. Aluminium is passivated in ultrapure and well-dried liquids with the Tf_2N.

Figure (3.29) shows SEM micrographs of thick layers of Al on gold substrate electrodeposited potentiostatically at 25 and 100 ºC at potentials of – 0.9 and – 0.5 V vs. Al/Al (III), respectively, for 2 hours. Visually, the deposits appear to be thick, shiny and well adhering to the gold substrate. The thickness was estimated to be between 2 and 6 μm. Generally, the electrodeposited layers contain very fine crystallites in the nanometer regime. The electrodeposits obtained at 25 ºC are stressed, as also seen by the SEM image (see Fig.3.29a). On occasion, the Al film made at room temperature wrapped up, forming a clumpy shape. This behaviour might be due to internal or residual stress which appears during the electrodeposition of metals and alloys. The stress can originate from intrinsic film stress and from interfacial stress between the deposit and substrate. It is interesting

that the quality of the Al electrodeposit obtained at 100 ºC is improved and there is no stress in the electrodeposited Al film. Furthermore, the crystallites became finer (see Fig. 3.29b).

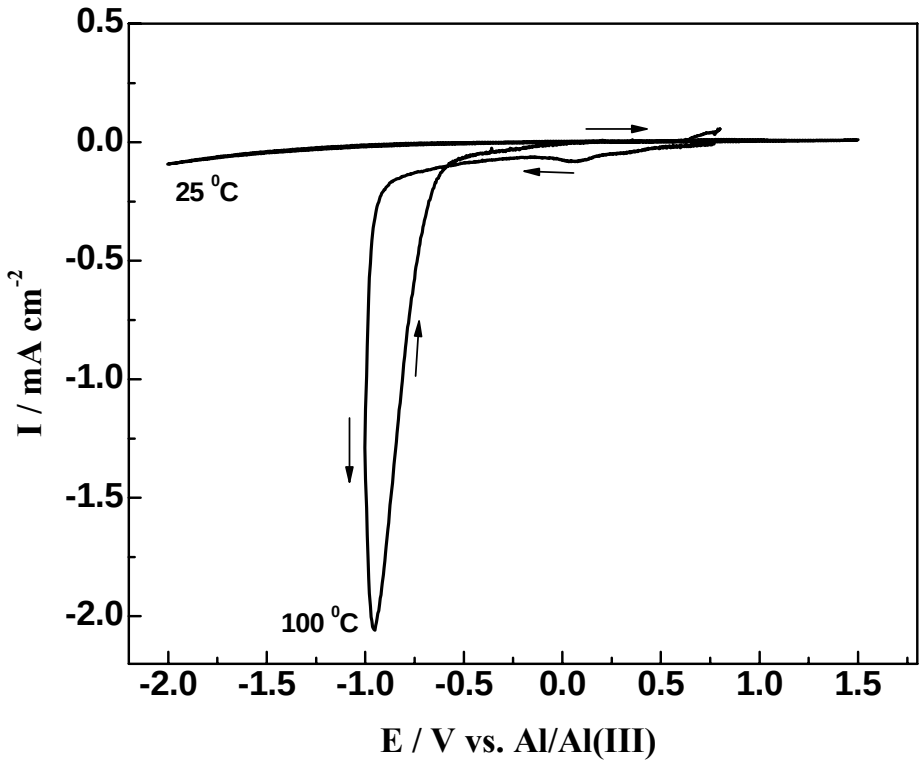

Fig. 3.28. *Cyclic voltammograms recorded on Au substrates in the ionic liquid 1-butyl-1-methyl pyrrolidinium bis(trifluoromethylsulfonyl) amide containing 1.8 M $AlCl_3$ (from the upper phase of the mixture) at different temperatures. The scan rate was 10 mV s^{-1}.*

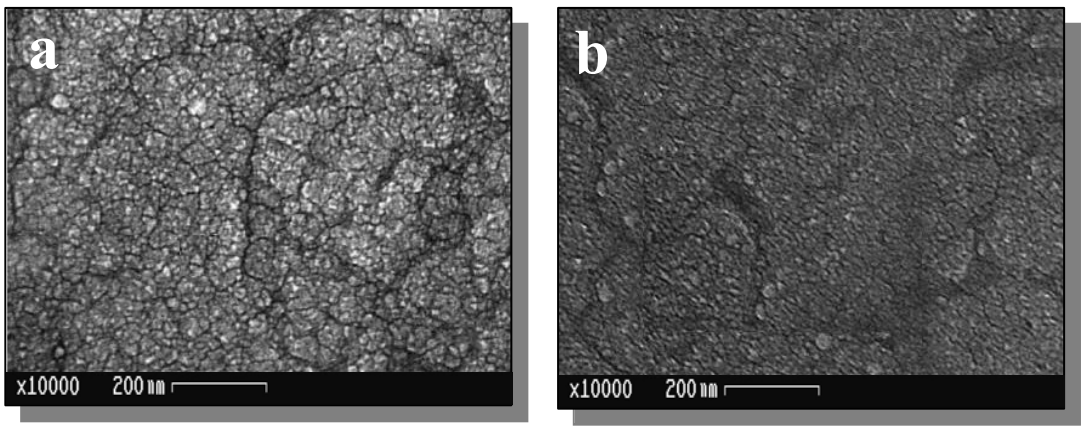

Fig. 3.29. *SEM micrographs of electrodeposited Al films on gold formed in the upper phase of the mixture $AlCl_3$/[BMP] Tf_2N after potentiostatic polarization for 2 hours at a) room temperature (E = –0.9 V, corresponding I = –0.2 mA/cm^2) and b) 100 ºC (E = –0.5 V, corresponding I = –1.0 mA/cm^2).*

Figure (3.30) shows the EDAX profile of Al films obtained potentiostatically in the mentioned ionic liquid on gold substrates at potentials of –0.9 V vs. Al/Al (III) at room temperature which shows pure Al.

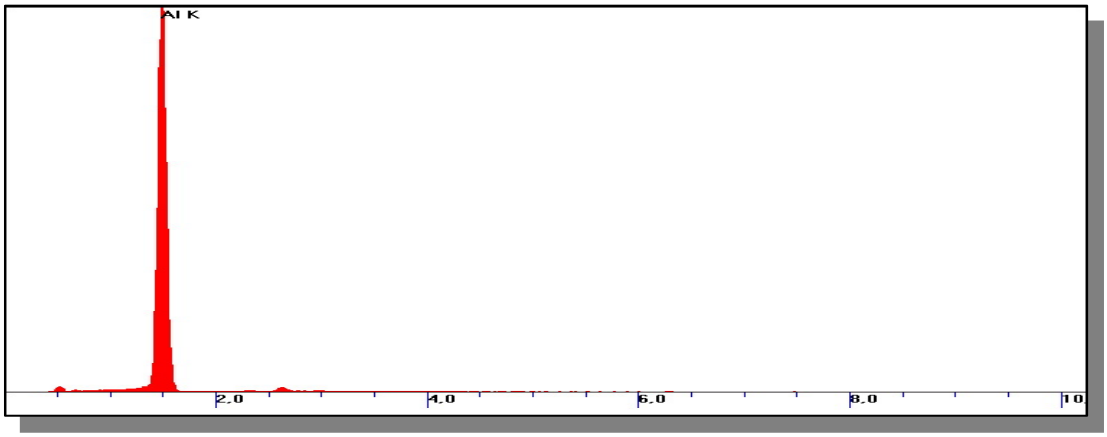

Fig. 3.30. *EDAX profile for the area shown in the SEM micrographs (Fig. 3.29a).*

3.1.4 Electrodeposition of Al-Cu alloy from ($AlCl_3$/[BMP]Tf_2N)

In this chapter, attempts for the electrodeposition of aluminium/copper alloys in 1-butyl-1-methylpyrrolidinium bis(trifluoromethylsulfonyl) amide [BMP]Tf_2N ionic liquid are presented. $AlCl_3$ (1.8 M) was used as Al source. Unfortunately, copper salts have limited solubility in the [BMP]Tf_2N ionic liquid. For this purpose, copper ions can only be introduced in the ionic liquid by anodic dissolution of Cu metal. As a first step, anodic dissolution of Cu from a copper sheet (see experimental part for details) in the $AlCl_3$ containing ionic liquid (that is the upper phase of the mixture: $AlCl_3$+[BMP]Tf_2N, see section 3.1.3) was performed. Unfortunately, no oxidation of copper was obtained even at elevated temperature.

As the cyclic voltammogram of the solution at 100 °C (after the attempts to dissolve Cu) is quite similar to that of the original $AlCl_3$/[BMP]Tf_2N solution, and there are no hints for the presence of a considerable amount of copper ions, (figure 3.31): the reduction peak at –1.5 V is typical for the bulk deposition of Al.

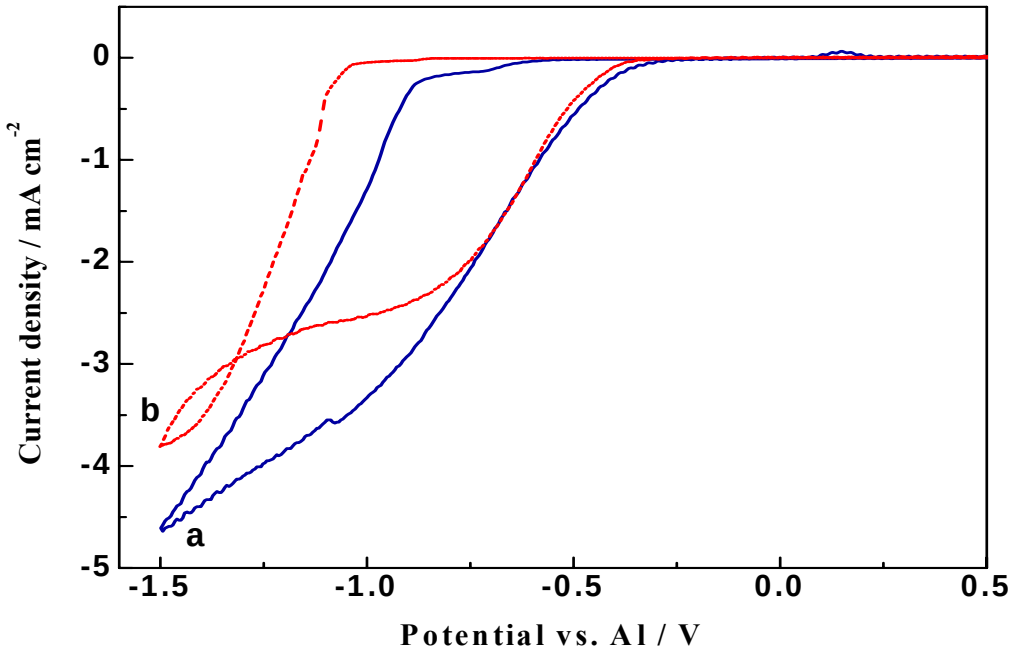

Fig. 3.31. *Cyclic voltammograms recorded on gold substrates in the ionic liquid 1-butyl-1-methylpyrrolidinium-bis(trifluoromethylsulfonyl)imide containing 1.8M $AlCl_3$ at 100°C: a) before (blue) and b) after (red) the attempts to anodically dissolve Cu. The scan reate was 10 mVs^{-1}.*

EDAX analysis of the deposit obtained after applying a potential of –1.0 V vs. Al/Al (III) for 2 hours showed only the presence of Al, see figure (3.32). This reason might be that the surface of the copper sheet was strongly passivated by the $AlCl_3$ containing liquid.

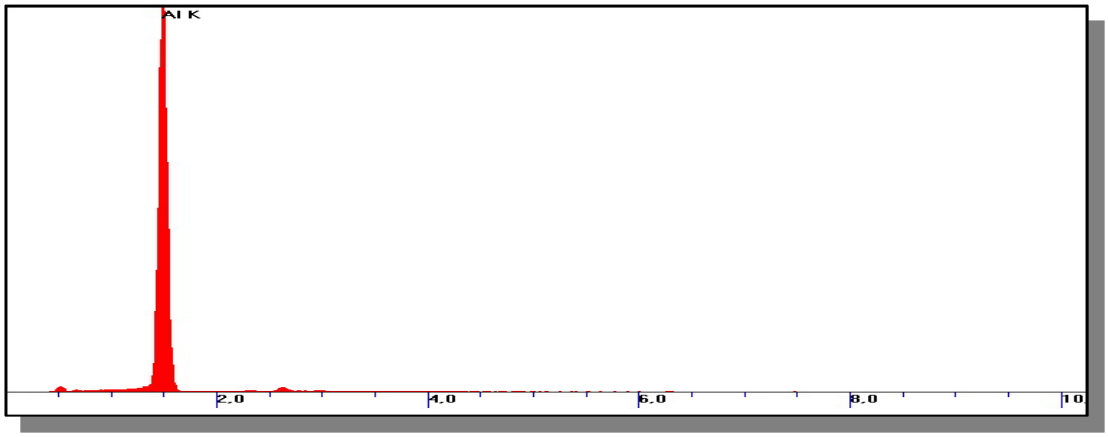

Fig. 3.32. *EDAX profile of the deposit obtained after applying a potential of –1.0 V vs. Al/Al (III) for 2 hours, from anodically treated $AlCl_3$ containing ionic liquid.*

It can be concluded that, there is no evidence in this case for copper ions to be introduced to the ionic liquid under the above mentioned conditions.

In order to exclude the effect of $AlCl_3$, the anodic dissolution of the copper metal was directly performed in the pure [BMP]Tf_2N ionic liquid. For this purpose, a current of 1.3 mA was applied on the freshly polished and cleaned Cu sheet in the ionic liquid. The results showed that a concentration of only 39 mM of Cu^+ ions (as was calculated from weight loss) can be introduced into the liquid at room temperature but only after applying the Cu oxidation current for several days. However, increasing the temperature of the anodic dissolution reaction up to 100 °C, the copper metal ion concentration in the pure [BMP]Tf_2N ionic liquid was increase considerably to about more than 100 mM in only several hours. The ionic liquid turned from colourless to pale orange colour with increasing the duration of the reaction. After the anodic dissolution of Cu metal in the pure [BMP]Tf_2N ionic liquid, 1.8 M $AlCl_3$ added to the Copper ions containing liquid.

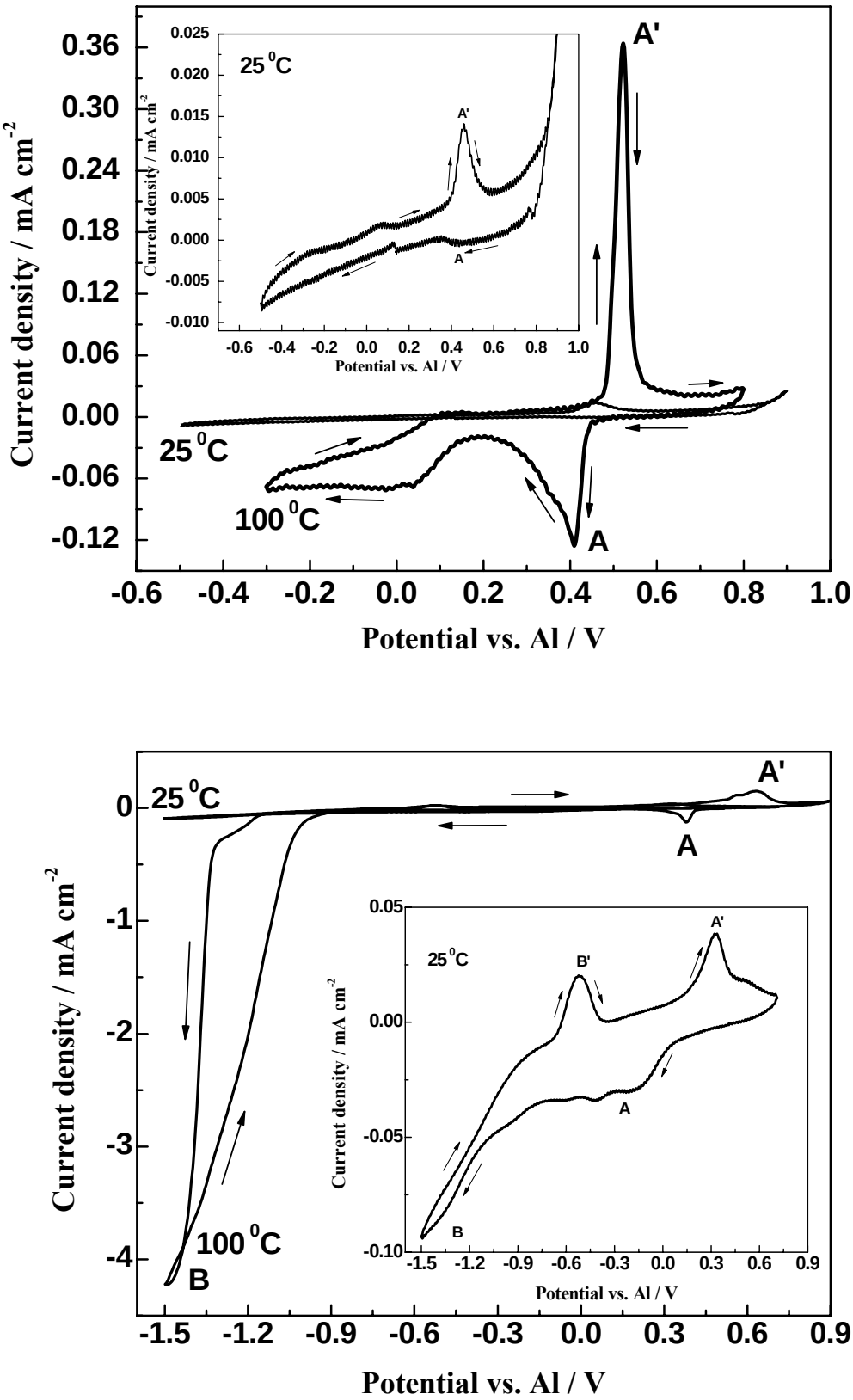

Fig. 3.33a,b). *Cyclic voltammograms recorded on gold substrates in the ionic liquid 1-butyl-1-methylpyrrolidinium-bis(trifluoromethylsulfonyl)imide containing 1.8M $AlCl_3$ and Cu^+ ions at 100°C. The scan rate is 10 mVs^{-1}.*

Figure (3.33a) shows the cyclic voltammograms of the upper phase of the biphasic mixture of $AlCl_3/Cu^+$/[BMP]Tf_2N mixture on gold substrate at different temperatures: 25 and 100 °C. At a potential of 0.38 V vs. Al/Al (III), a small reduction peak (A) appears, which looks sharper at 100 °C. This peak is mainly correlated to the deposition of Cu, as applying a potential of 0.4 V for 2 hours at 100 °C gives a light brown deposit. The anodic peak (A´) recorded in the back scan at a potential of about 0.5 V vs. Al/Al (III) is correlated to the dissolution of the Cu deposit. EDAX analysis of this deposit (Fig. 3.35a) showed that it is Cu with very small amount of Al (from UPD of Al). Au is from the substrate. The sharp increase of the current at a potential of -1 V is correlated to the bulk deposition of Al. The anodic peaks (B̀ and À) observed in the reverse scan of the cyclic voltammograms are due to the partial stripping of the Al and/or Cu deposit at a potentials of about -0.6 V and 0.3 V vs. Al/Al (III), respectively. The available data show that Al (and also Cu) is passivated in ultrapure and well-dried liquids with the Tf_2N anion. The oxidation of Al is dependent on the available anions, which can create a complex or solvated Al (III) species. However, at 150 °C, where $AlCl_3$ can be dissolved up to 6.0 M in [BMP]Tf_2N, the ratio of anodic to cathodic charge is still below 1.

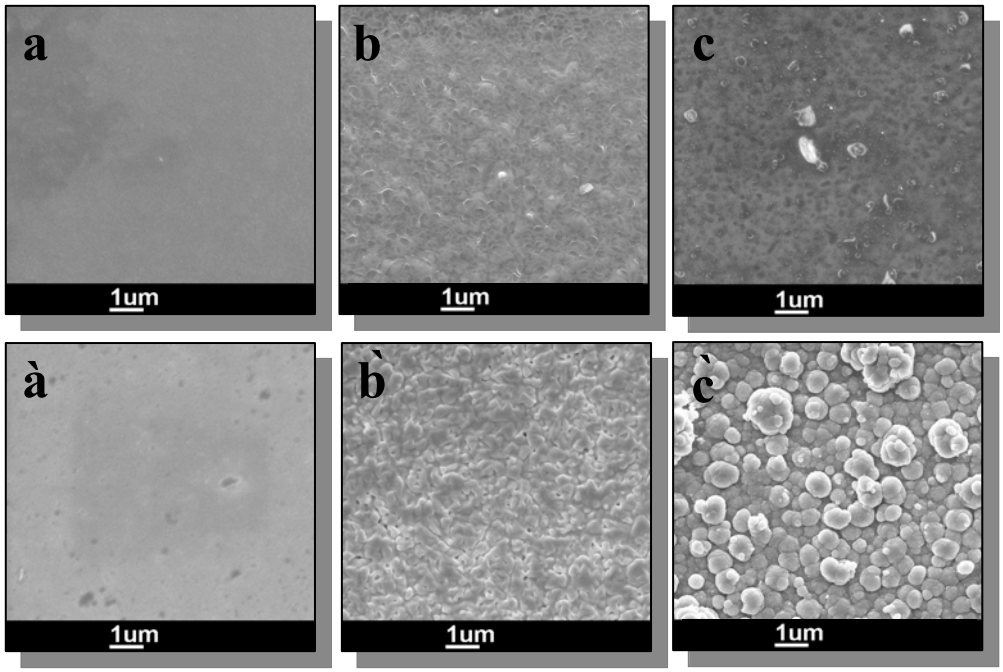

Fig. 3.34a-c. *SEM micrographs of electrodeposited (a) Cu, (b) Al-Cu and (c) Al films on gold formed in the upper phase of the mixture $AlCl_3$/Cu/[BMP] Tf_2N after potentiostatic polarization for 2 hours at a-c)* 25 °C and *a'-c')*100 °C, *E = 0.4, 0.0 and -1.2 V for a, b and c, respectively.*

The Al-Cu electrodeposits obtained at the two different temperatures were investigated by scanning electron microscopy (SEM). Visually, the deposits appear to be shiny and well adhering to the gold substrate. Figures (3.34 a-c) show SEM micrographs of Cu, Al-Cu and Al layers on gold substrate electrodeposited potentiostatically at 25 (a-c) and 100 °C (à-c̀) at potentials of 0.4, 0.0 and – 1.2 V vs. Al/Al (III), respectively, for 2 hours. A thickness of between 2 and 5 µm was obtained. The average grain size of Cu, Al-Cu and Al films is estimated to be 147 nm, 1µm and 8.5 µm, respectively. The electrodeposits obtained at 25 and 100 °C are fine for Cu and coarse for Al, as also observed by visual inspection. This is not too surprising since during the electrodeposition of metals and alloys, internal or residual stress almost always appears. The stress can originate from intrinsic film stress and from interfacial stress between the deposit and substrate. Generally, this may be attributed to some factors such as coalescence of the crystallites, inclusion of foreign species or generation of structural defects **[131]**.

Figure (3.35) shows the EDAX profile of Cu, Al-Cu and Al films shown in Figure (3.34 a'-c'). It is clearly seen that the EDAX profile in Figure (4.34 a) shows a clear peak for Cu metal with maybe some UPD of Al. Furthermore, at potential of 0.0 V a sharp peak of Al and short peak of Cu were appeared. At over potential deposition of Al (-1.2 V) a strong sharp peak of Al is observed with no clear of Cu.

Interestingly, it was observed that during the anodic dissolution of Cu, the solution gets turbid especially when applying relatively high temperatures (≥ 70 ºC). When the dissolution of Cu was performed at such temperatures and for longer time (more than one day) a white precipitate was formed. This white precipitate was isolated and washed carefully with isopropanol to get it as pure powder. Then it was analyzed by XRD, which showed it is CuF_2 salt. This can only be explained by the decomposition of the Tf_2N anion of the ionic liquid. This interesting result has deviated the work from the planned goal (Al-Cu alloy deposition) and is discussed in detail in the following section.

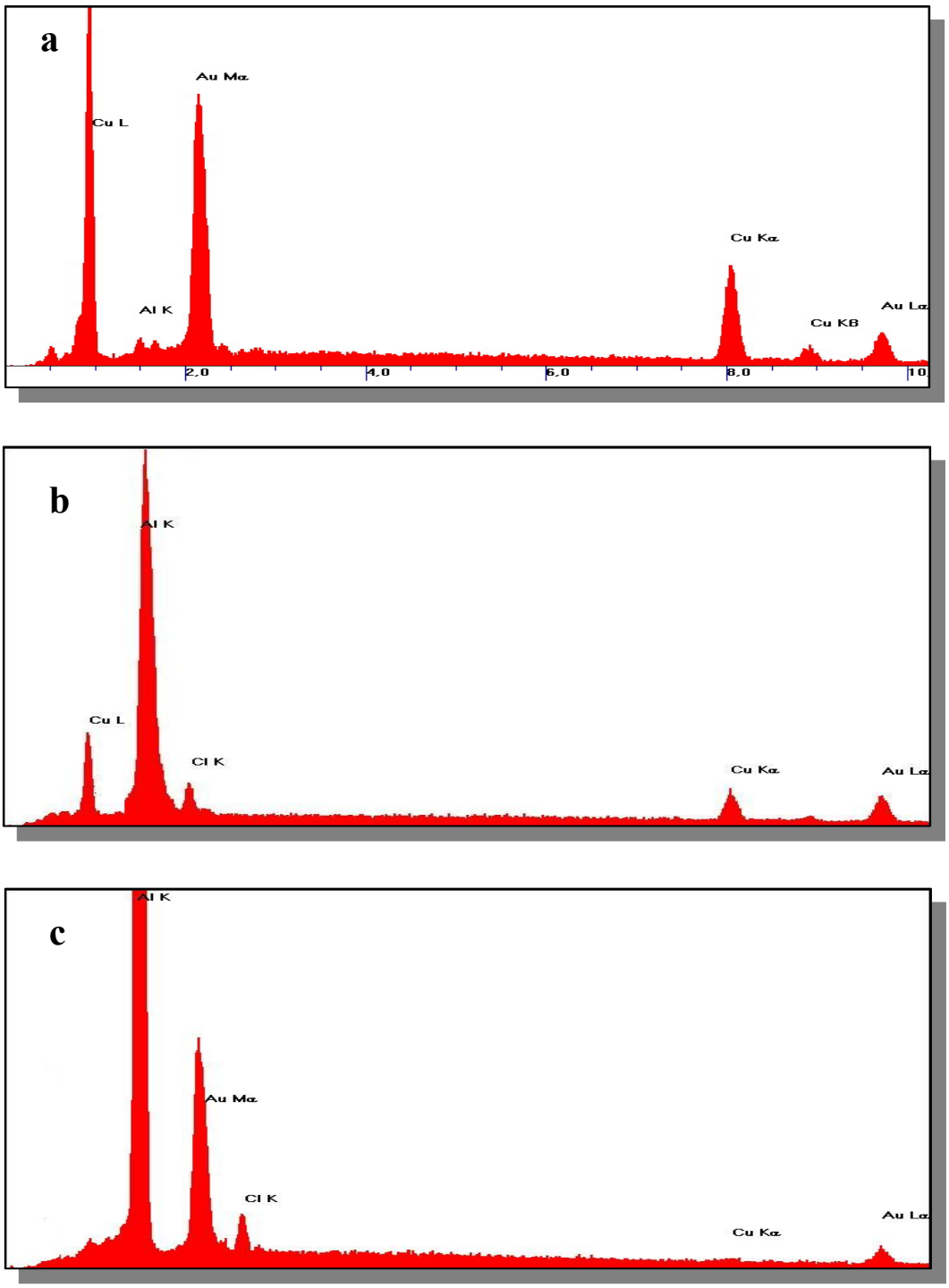

Fig. 3.35a-c. *EDAX profile for the area shown in the SEM micrographs (Fig. 4.34 a'-c').*

3.2. Decomposition of the Tf_2N anion under anodic conditions

The electrochemical stability of ionic liquids is a key factor in their successful applications in various electrochemical processes. Unfortunately, little is known on the cathodic and anodic decomposition reactions of both cations and anions of ionic liquids. To the best of the available knowledge there are no systematic studies available on the anodic decomposition of Tf_2N ionic liquids, but the decomposition of the Tf_2N anion under cathodic conditions was reported **[132,133]**. MacFarlane et. al. **[132]** showed that the Tf_2N anion is subject to an irreversible cathodic breakdown prior to the massive reduction of the [EMIm] cation in the ionic liquid [EMIm]Tf_2N. They reported that the reduction of the Tf_2N can weaken one of the N-S bonds leading to its cleavage to a new anion, $SO_2CF_3^-$, and a reactive radical, $^{\bullet}NSO_2CF_3^-$, as follows:

$$N(SO_2CF_3)_2^- + e^- = N(SO_2CF_3)_2^{2-} = {}^{\bullet}NSO_2CF_3^- + SO_2CF_3^- \quad (1)$$

The reduction products of Tf_2N can undergo further reduction reactions as follows:

$$^{\bullet}NSO_2CF_3^- + e^- = NSO_2^- + CF_3^- \quad (2)$$

$$SO_2CF_3^- + e^- = SO_2^- + CF_3^- \quad (3)$$

In contrast, Passerini and co-workers **[134,135]** reported that the Tf_2N anion is cathodically stable if the ionic liquid is extremely pure and dry, and the reductive decomposition of Tf_2N can only occur in the presence of water and/or other impurities. Furthermore, they showed that the decomposition mechanism taking place in the presence of water traces seems to be different than the one suggested by MacFarlane et. al. **[132].** They suggested that the products of water reduction (OH^- or H_2) are responsible for the Tf_2N reduction **[135]**. It is out of the scope of this work to decide what exactly is the reason for the cathodic instability of the Tf_2N. At a minimum it is clear that this anion is electrochemically less stable than often assumed.

In this part it is shown as a further example that the Tf_2N anion can easily be decomposed at slightly elevated temperatures during anodic oxidation of copper in the ionic liquid [BMP]Tf_2N leading to the formation of CuF_2. Although electrochemically unfavourable with respect to Cu dissolution, the decomposition of

Tf_2N during anodic oxidation of copper might be regarded as a new and facile route for the synthesis of CuF_2.

A two compartment electrochemical cell was used for the anodic oxidation of Cu metal, Fig. 3.36. The counter electrode was separated and connected through an ionic liquid salt bridge. With this setup the contamination of the electrolyte in the working electrode counterpart, via decomposition products from the counter electrode reactions, was avoided.

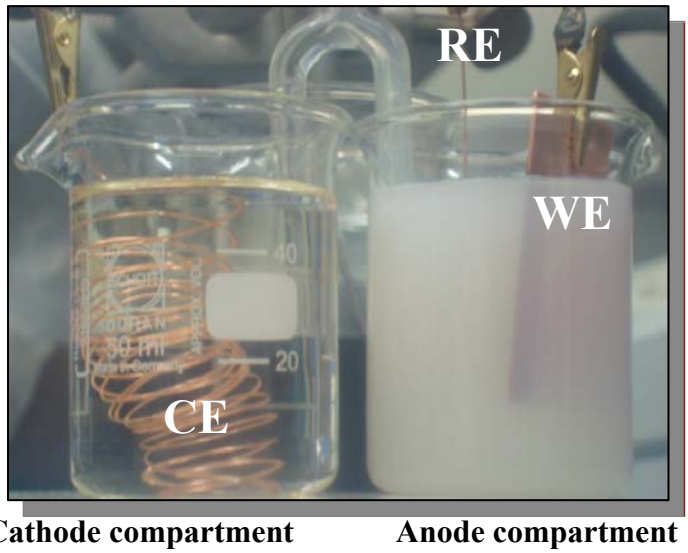

Fig. 3.36. *An optical photo of the electrochemical cell used for the anodic dissolution of copper in the ionic liquid [BMP]Tf_2N at 70°C and under an applied current density of 90 µA cm^{-2}. The photo clearly shows the formation of a white suspension during the anodic dissolution of copper which is due to CuF_2 formation.*

As mentioned in the previous section, the original aim was to anodically dissolve copper in the ionic liquid [BMP] Tf_2N in order to introduce copper ions into the liquid. This is due to the solubility of copper salts in the ionic liquid [BMP]Tf_2N is very limited **[136]**. The anodic dissolution of metals at elevated temperatures is usually kinetically favoured leading to a faster reaction. The cyclic voltammetry behaviour of copper in the ionic liquid [BMP]Tf_2N at two different temperatures, 25 and 70 ^oC (Fig. 3.37) is investigated. The potential was scanned first in the negative direction down to – 0.7 V (vs. Cu) then it was scanned back to + 0.7 V and finally terminated at the open circuit potential. The rapid increase in the anodic current at a potential of + 0.6 V, at 25 ^oC, and at a potential of + 0.5 V, at 70 ^oC, is attributable to the anodic dissolution of copper. The recorded reduction peak

is correlated to redeposition of dissolved copper. Consequently, Cu cations can be anodically introduced into the ionic liquid and the extent of Cu dissolution increases as the temperature increases.

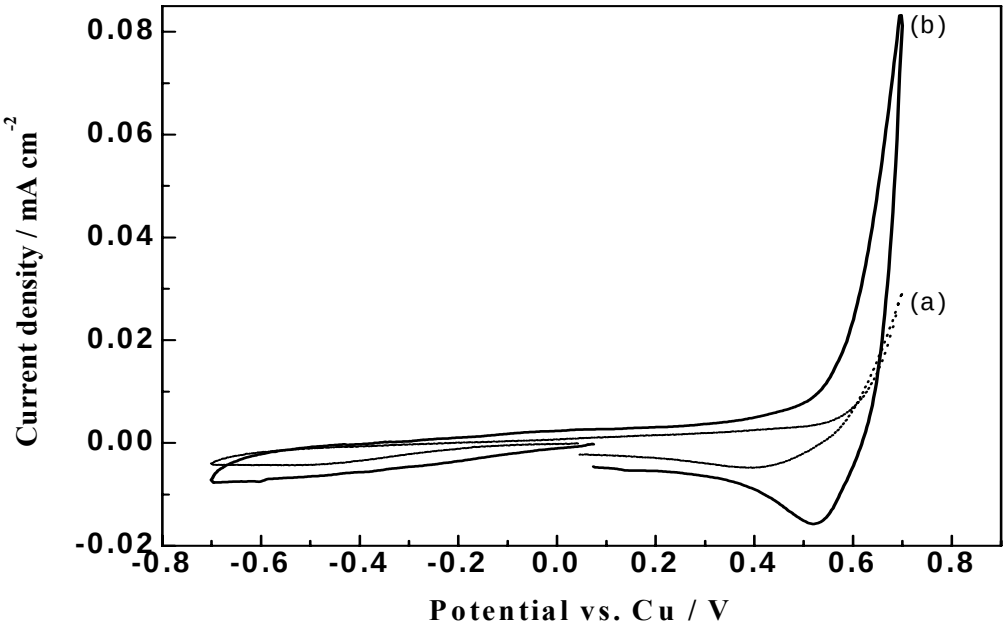

Fig. 3.37. *Voltammetric behaviour of copper electrode in the ionic liquid [BMP] Tf_2N at 25 and 70 ^oC. Scan rate 10 mV/s.*

An anodic current density of 90 μA cm^{-2} (the corresponding potential was about 1 V vs. Cu reference electrode) was applied on the copper electrode in the employed ionic liquid for 1 day at 25 ^oC in order to anodically dissolve copper. Throughout the duration of the experiment no significant change in the solution was observed apart from a slight alteration in its colour to pale yellow due to the anodic dissolution of copper. There is no hint for a side reaction and as shown in **[136]** the oxidation state of the copper species introduced into the ionic liquid [BMP]Tf_2N after anodic dissolution of copper, is 1, thus Cu^+ ions are the electrolysis product.

Quite surprisingly, after applying a current density of 90 μA cm^{-2} at 70 ^oC (the corresponding potential is only about 0.2 V vs. Cu) the ionic liquid became turbid after about 2 hours of electrolysis and the turbidity became more intense with time until a white suspension was obtained after about 6 hours, see Fig. 3.36. After about 12 hours electrolysis a white precipitate was obtained on the bottom of the electrochemical cell.

Subsequently, the ionic liquid containing the electrolysis product was centrifuged to reclaim the precipitate. The white precipitate was then washed several times with isopropanol to remove the residual ionic liquid.

The electrolysis product was investigated by SEM and XRD to explore its morphology and composition, respectively. The SEM micrograph of Fig. 3.38. shows the surface morphology of the obtained powder: it contains fine crystallites with an average size of about 200 nm. The XRD pattern of the obtained powder is shown in Fig. 3.39. Surprisingly, all the diffraction peaks recorded for the obtained powder can be perfectly indexed to the data available in the JPCD (06-0343) diffraction file, thus indicating that pure CuF_2 is the yield of the anodic dissolution of copper in [BMP]Tf_2N at 70 ^oC, which is a clear evidence for the decomposition of Tf_2N anions, the only F^- source. It should be mentioned that anodic oxidation of copper in the ionic liquid [EMIm]Tf_2N, at the same experimental conditions, leads also to the formation of CuF_2. However, the mechanism of the Tf_2N decomposition and the formation of CuF_2 is not clear. At the first glance one might expect that the Tf_2N anion is subject to a direct oxidative decomposition occurring simultaneously with anodic dissolution of Cu to Cu^{2+} leading to F^- which reacts with copper cations to form CuF_2. However, the charge/mass balance is typical for $Cu \rightarrow Cu^+$. Thus, it is excluded that there is at the same time an oxidation of Cu to Cu^{2+} and Tf_2N oxidation liberating F^-. If the Tf_2N anion was anodically decomposed at the copper electrode it would also be decomposed at other electrodes (not only copper) which is not the case. Silver can easily be oxidized to Ag^+ without a clear hint for AgF formation. Thus, what else can it be?

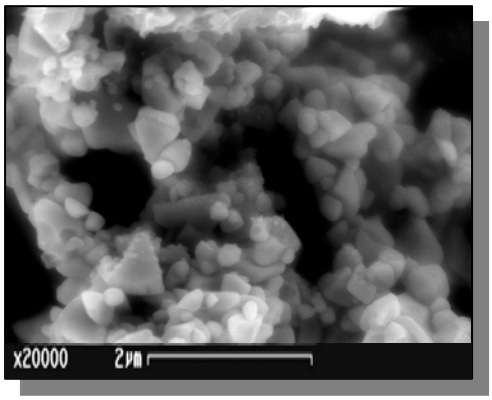

Fig. 3.38 *SEM micrograph of the white powder obtained after anodic dissolution of copper in [BMP] Tf_2N at 70 ^oC under applied current density of 90 µA cm^{-2} for 24 hours.*

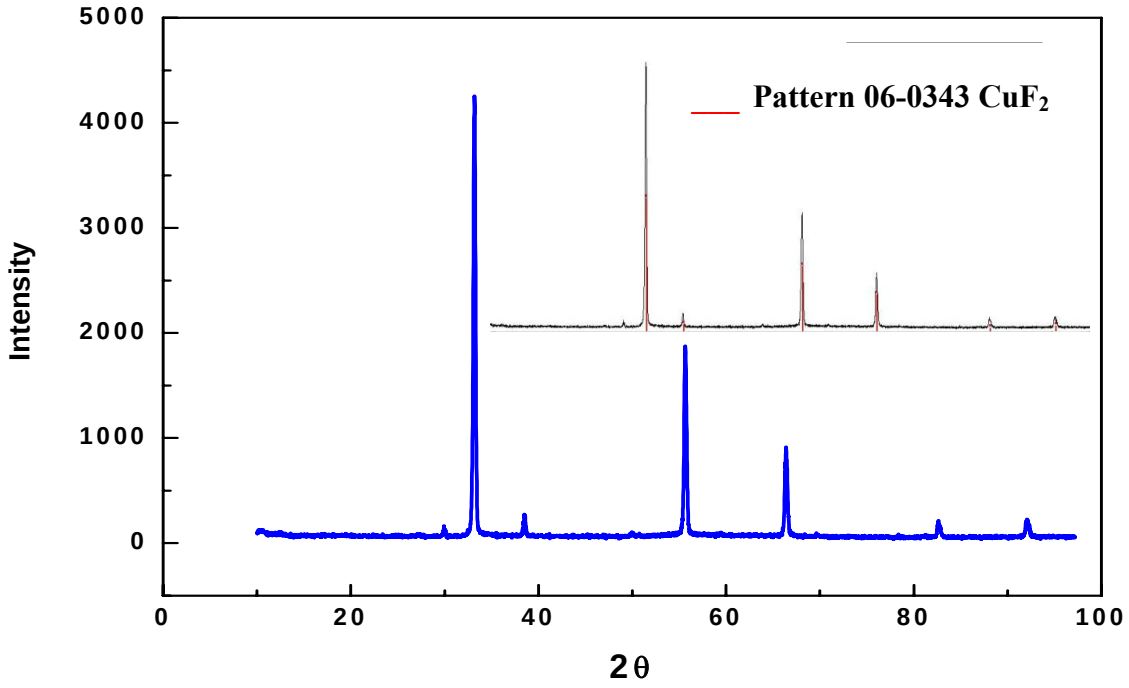

Fig. 3.39. *XRD pattern of the obtained powder.*

As a possible explanation for the formation of CuF_2 it is suggested that anodically dissolved copper cations might chemically reduce the Tf_2N at 70 ^oC, according to the following equation:

$$Cu^+ + N(SO_2CF_3)_2^- = CuF_2 + N(SO_2CF_2)_2$$

Without a detailed spectroscopical analysis the mechanism can not be decided, but it has been reported that the cathodic decomposition of Tf_2N leads to decomposition products like NSO_2, CF_2 and F^-, as described in **[137]**. Thus it is plausible that Cu^+ leads to an irreversible reduction of Tf_2N librates at the same time F^- which reacts with Cu^{2+} to CuF_2. The driving force might be the extreme heat of formation of CuF_2 which is -538.9 kJ/mol **[138]**.

There are some more reports in the literature that make this proposed mechanism reasonable. In **[137]** MacFarlane et. al. have found, using solid-state NMR, that ionic liquids based on Tf_2N anion react with magnesium alloy surfaces to form a metal fluoride rich surface in addition to other organic components. This has been attributed to the decomposition of the Tf_2N anion to SO_2CF_2, CF_2 and F^- species.

The fluoride ions react with the alloy surfaces to form metal fluorides. Furthermore, they have reported that Tf_2N based ionic liquids react with lithium giving an interface composed mainly of decomposition products of the Tf_2N anion with a LiF film close to the lithium surface.

In a corrosion study of Inconel, Brass and commercial steel in [BMIm] Tf_2N Tolstoguzov et. al. **[35]** have found that [BMIm]Tf_2N is subject to a decomposition upon chemical interaction with the alloy surfaces. They have shown by SIMS and XPS that the decomposition products of the ionic liquid are CF_3, C=N and $–SO_2$-groups. All these results support the assumption of the chemical decomposition of Tf_2N anion by the interaction with copper cations at elevated temperature leading to the formation of CuF_2. It can not be commented whether the same result would be obtained by dissolving Cu Tf_2N in [BMP] Tf_2N. A direct comparison would require an extremely pure and fully dissociated Cu(Tf_2N) made in a pure chemical synthesis routine. It can be speculated that Cu^+ "in statu nascendi" is quite a reactive species.

Ionic liquids with the Tf_2N anion have been regarded as potential solvents for many electrochemical applications due to the hydrophobic nature of the Tf_2N anion and due to its great ability to lower the melting point of the ionic liquid. In this thesis it is found that the Tf_2N anion is subject to an unexpected decomposition under quite mild electrochemical conditions during the anodic dissolution of a copper electrode in the ionic liquid [BMP] Tf_2N at 70 ^oC, leading to the formation of CuF_2. Interestingly, at room temperature no such decomposition was obtained. Although the mechanism of this reaction is not clear at all (even raising some questions), one has to be very careful in applying ionic liquids based on Tf_2N for electrochemical experiments: the Tf_2N anion might decompose, depending on the anode material.

4. Summary

In the present thesis the electrodeposition of aluminium on mild steel was investigated in different ionic liquids with the same anion namely: $AlCl_3$/1-ethyl-3-methylimidazolium chloride ($AlCl_3$/[EMIm]Cl), $AlCl_3$/l-benzyl-3-methyl-imidazolium chloride ($AlCl_3$/[BzMIm]Cl), $AlCl_3$/l,3-dibenzyl-imidazolium chloride ($AlCl_3$/[DBzIm]Cl), $AlCl_3$/1-ethyl-3-methylimidazolium bis(trifluoromethylsulfonyl) amide ($AlCl_3$/[EMIm]Tf_2N) and $AlCl_3$/1-butyl-1-methylpyrrolidinium bis(trifluoro-methylsulfonyl) amide ($AlCl_3$/[BMP]Tf_2N). The effect of changing the ionic liquids, like. e.g. changing the organic cation on the properties of the resulting Al-coatings was also studied.

4.1 Aluminium electrodeposition

4.1.1 Electrodeposition of Al from chloroaluminate based ionic liquids

4.1.1.1 Electrodeposition of Al from $AlCl_3$/[EMIm]Cl

The electrodeposition of aluminium in Lewis acidic $AlCl_3$/1-ethyl-3-methylimidazolium chloride ($AlCl_3$/[EMIm]Cl) (3:2 molar ratio) ionic liquid is presented. This system is suitable for the electrodeposition of aluminium and aluminium alloys: Ionic liquids that contains an excess of $AlCl_3$ over [EMIm]Cl are considered Lewis acidic due to the presence of coordinately unsaturated species, whereas those that contain an excess of [EMIm]Cl over $AlCl_3$ are denoted as basic due to the presence of unbound chloride ions. It must be mentioned here that the deposition of Al from such systems is already reported. But for comparison purposes it is studied here. In this study $AlCl_3$ dissolves well with the 1-ethyl-3-methylimidazolium chloride salt to a concentration of (60 mol.-%) giving a clear yellowish solution from which Al can be deposited. The cyclic voltammogram shows a typical cyclic voltammogram of the Lewis acidic $AlCl_3$/EMImCl (3:2 molar ratio) ionic liquid at room temperature. At a potential of –0.1 V vs. Al/Al (III), the bulk deposition of Al takes place where a clear larger of Al is already seen by naked eye and the wide anodic peak is recorded on the reverse scan at a potential of about 0.15 V that is correlated to full stripping of the as-deposited aluminium. The SEM micrograph of Al film shows that the layer contains dense microcrystallites with an average size of about 5 μm with a porous appearance. It is clearly seen that the EDAX spectrum shows only one characteristic peak of Al.

4.1.1.2 Electrodeposition of Al from [$AlCl_3$/(EMImCl:BzMImCl)]

The electrodeposition of aluminium carried out in a new system based on the changing of the EMImCl:BzMImCl molar ratios: 40:0, 30:10, 20:20, 10:30 and 0:40 mol.-%, respectively, to study the effect of the aromatic group of the imidazolium cation on the Al deposit (at fixed $AlCl_3$ concentration of 60 mol.-%). The cyclic voltammograms exhibit the same general feature of the cyclic voltammogram recorded for the Lewis acidic ionic liquid $AlCl_3$/ EMImCl (3:2 molar ratio). However, the Al deposition potential shifts gradually to less negative values and the peak currents of both deposition and stripping peaks significantly decrease upon increasing the BzMImCl content. This is ascribed to the decreased mobility of the electroactive species towards the electrode surface due to increase viscosity caused by further addition of the more viscous BzMImCl ionic liquid, which, in turn, leads to a lower diffusion rate. The surface morphology of the deposited Al film shows gradual change from compact and dense to large coarse cubic-shaped microcrystallites with increasing BzMImCl molar ratio and the Al film thickness was decreased with increasing the BzMImCl content.

4.1.1.3 Electrodeposition of Al from [(EMImCl/$AlCl_3$):BzMImCl]

Al electrodeposition is carried out in the Lewis acidic $AlCl_3$:EMImCl (3:2 molar ratio) ionic liquid with the addition of 1-benzyl-3-methylimidazolium chloride salt (BzMImCl): 0, 5, 10, 15 and 20 wt.-%, respectively, to investigate the effect of increase the imidazolium cation content over $AlCl_3$ content. The cyclic voltammograms exhibit the same general feature of the cyclic voltammogram of $AlCl_3$/EMImCl (3:2 molar ratio) ionic liquid. By the addition of BzMImCl to the ionic liquid, the deposition potential shifts gradually to less negative values by increasing the cationic imidazolium molar ratio. Moreover, the current value and the peak size of both deposition and stripping significantly decrease. This result is due to increased viscosity and decreased aluminium content caused by further addition of BzMImCl to the ionic liquid. It is clearly seen that the deposited aluminium films show gradual change of Al deposites from dense and compact to very fine microcrystallites and the thickness diagram shows clear decrease of Al film thicknesses with increasing the addition of BzMImCl salt.

4.1.1.4 Electrodeposition of Al from [$AlCl_3$/(EMImCl:DBzImCl)]

As the presence of a benzyl group in the imidazolium based ionic liquid showed the effect on the morphology and thickness of Al deposit, it was of interest to investigate the effect of "two" aromatic substituents on Al deposition by changing the (EMImCl:DBzImCl) molar ratios as follows: 40:0, 30:10, 20:20, 10:30 and 0:40 mol.-%, respectively, and the concentration of $AlCl_3$ was kept constant (60 mol.-%). Similar to the $AlCl_3$:EMImCl/BzMImCl system that all cyclic voltammograms of $AlCl_3$:EMImCl/DBzImCl mixture have more or less the same general feature of the cyclic voltammogram recorded for the Lewis acidic ionic liquid $AlCl_3$/EMImCl (3:2 molar ratio). The deposition potential shifts rapidly to more negative values with increasing the DBzImCl content over EMImCl. Moreover, the deposition and stripping current peaks significantly decrease. The surface morphology of the deposited Al film shows gradual change from compact and dense microcrystallites to small and thin rod-shaped nanocrystallites with increasing DBzImCl and the film thichness was decreased from 9 to 0.3 μm in the same trend.

4.1.1.5 Electrodeposition of Al from [(EMImCl/$AlCl_3$):DBzImCl]

The electrodeposition of aluminium is carried out in the prepared Lewis acidic $AlCl_3$:EMImCl (3:2 molar ratio) ionic liquid with the addition of different weight percents (wt.-%) of 1,3-dibenzylimidazolium chloride salt (DBzImCl) to the ionic liquid. The aim of this study is to show the effect of increasing the dibenzyl based imidazolium salt molar ratio over $AlCl_3$ molar ratio. The cyclic voltammograms show the same general feature of the cyclic voltammogram of $AlCl_3$:EMImCl (3:2 molar ratio) ionic liquid alone. The deposition potential shifts gradually with the addition of DBzImCl salt to more negative values. Furthermore, with increasing the molar ratio of DBzImCl, the current value and the peak size of both deposition and stripping clearly decrease. The reason of this behaviour is due to increase of the cationic imidazolium content with the two bulky benzyl groups and decrease the aluminium content at the same time in the ionic liquid. The surface morphology of the Al deposits shows gradual change from compact and dense microcrystallites to small and rod-shaped nanocrystallites with increasing the dibenzyl imidazolium salt content over $AlCl_3$ content and the film thickness of the Al deposits was decreased from the micro- to the nanometer regime in the same trend.

4.1.1.6 Comparison study between the three $AlCl_4$ based ionic liquid systems

The results obtained from the three prepared chloroaluminate ionic liquid systems: ($AlCl_3$/[EMIm]Cl), ($AlCl_3$/[BzMIm]Cl) and ($AlCl_3$/[DBzIm]Cl), respectively, are summarized for better comparison. The cyclic voltammograms of $AlCl_3$/[BzMIm]Cl (3:2 molar ratio) ionic liquid and $AlCl_3$/[EMIm]Cl (3:2 molar ratio) ionic liquid are quite similar, but for $AlCl_3$/[DBzIm]Cl (3:2 molar ratio) ionic liquid is different. The dialkyl imidazolium based ionic liquid has the lowest viscosity value compared with the two other systems. Whereas the diaryl imidazolium based ionic liquid has the highest viscosity value than the two other systems, which in turn shifts the deposition potential to more negative values. It can be clearly seen that the type of the substituents in the imidazolium cation affects strongly the surface morphology of deposited Al: The dialkyl substituented imidazolium based ionic liquid [EMIm]$AlCl_4$ gave a compact and dense Al deposit. Whereas, the mono aryl-substituted one [BzMIm]$AlCl_4$ gave a coarse and cubic-shaped microcrystalline morphology. Interestingly, the diaryl-substituted imidazolium based ionic liquid gave rod-shaped nanocrystallites and the average thickness of Al from the three systems is 9, 3 and 0.3 μm, respectively.

4.1.2 Electrodeposition of Al from ($AlCl_3$/[EMIm]Tf_2N)

From the reported results of Al deposition on Au from [EMIm]Tf_2N ionic liquid, there is interest to apply it for Al coating of reactive surfaces like mild steel. The Al electrodeposition on mild steel substrates from $AlCl_3$ containing [EMIm]Tf_2N ionic liquid is presented. As was first reported by Endres et al., $AlCl_3$ dissolves well in [EMIm]Tf_2N ionic liquid up to a concentration of about 2.5 M, a biphasic mixture is obtained upon further addition of $AlCl_3$, the upper phase looks clear and colourless (which Al can only be electrodeposited) while the lower one is pale and more viscous. The cyclic voltammogram shows that the bulk electrodeposition of Al starts at a potential of about – 0.2 V vs. Al/Al (III) and the small cathodic peak at a potential of about -0.54 V vs. Al/Al (III) is correlated to the over potential deposition (OPD) of Al on Au. The anodic peak recorded in the back scan at a potential of about 0.27 V vs. Al/Al (III) is correlated to the dissolution of the electrodeposit. A thickness of 2 to 24 μm was easily obtained and the particle size of the deposit increases from porous and coarse to spaced porous deposit with increasing the deposition time.

4.1.3 Electrodeposition of Al from ($AlCl_3$/[BMP]Tf_2N)

It was reported by Endres et al., the electrodeposition of Al from $AlCl_3$ containing [BMP]Tf_2N ionic liquid gave nanocrystalline Al deposits on Au with a very fine morphology. This would be very interesting if the same morphology of Al can be also obtained on reactive metal/alloy surfaces like mild steel. In view of the previous $AlCl_3$/[EMIm]Tf_2N mixture, $AlCl_3$/[BMP]Tf_2N also shows a biphasic behaviour with increasing the concentration of $AlCl_3$, the upper phase of the mixture $AlCl_3$/[BMP]Tf_2N is pale and more viscous (which Al can only be electrodeposited) while the lower one is colourless. The cyclic voltammogram shows the bulk deposition of Al starts at a potential of -0.25 V vs. Al/Al (III) and the small anodic peak recorded on the reverse scan at potential of about 0.8 V vs. Al/Al (III) is correlated to small partial dissolution of the deposited Al. The cyclic voltammogram recorded at 100 °C exhibits a similar behaviour but with the presence of a nucleation loop at a potential of –0.6 V. The SEM micrographs of Al deposit was obtained on gold substrate at 25 and 100 ºC appear to be shiny and well adherent very fine crystallites in the nanometer regime and the thickness was estimated to be between 2 and 6 μm. The EDAX profile of Al films on gold substrates shows pure Al.

4.1.4 Electrodeposition of Al-Cu alloy from ($AlCl_3$/[BMP]Tf_2N)

Electrodeposition of Al/Cu alloys in $AlCl_3$ (1.8 M) containing [BMP]Tf_2N ionic liquid is presented. As a first step to introduce the copper ions into the ionic liquid, anodic dissolution of copper metal in the upper phase of the mixture $AlCl_3$/[BMP]Tf_2N was performed. From the obtained result, it is no hints for the presence of Cu ions in the mixture. This may be due to the surface of the copper sheet was strongly passivated by the $AlCl_3$ containing liquid. In order to exclude the effect of $AlCl_3$, the anodic dissolution of the copper metal was directly performed in the pure [BMP]Tf_2N ionic liquid and a current of 1.3 mA was applied. The results showed that a concentration of only 39 mM of Cu^+ ions (as was calculated from weight loss) can be introduced into the liquid at room temperature but only after several days. Whereas, increasing the temperature of the anodic dissolution up to 100 °C, gives more than 100 mM Cu^+ in only several hours with changing the ionic liquid colour from colourless to pale orange colour. After the successful anodic dissolution of Cu in [BMP]Tf_2N, $AlCl_3$ (1.8 M) was added to the Cu^+ containing liquid. From the

electrochemical measurements at different temperatures, the electrodeposition of Cu, Al-Cu and Al, can be obtained. Interestingly, the results shown that during the anodic dissolution of Cu at relatively high temperatures (≥ 70 ºC), the Tf_2N anion of the ionic liquid can be easily decomposed. These results has deviated the work from the planned goal (Al-Cu alloy deposition) and is discussed in detail.

4.2. Decomposition of Tf_2N anion under anodic conditions

Due to the limited solubility of copper salts in the ionic liquid [BMP]Tf_2N, it is worth noting that the aim was to introduce copper cations into the ionic liquid throughout anodic dissolution reaction of copper metal. An anodic current density of 1.3 mA cm^{-2} was applied on the copper electrode in the employed ionic liquid for 1 day at 25 ^oC in order to anodically dissolve copper. Throughout the duration of the experiment, there is no significant change in the test solution at 25 ^oC. It was shown that the oxidation state of the copper species introduced into the ionic liquid [BMP]Tf_2N after anodic dissolution of copper, is 1 and Cu(Tf_2N) is the electrolysis product. Surprisingly, after applying a current density of 1.3 mA cm^{-2} at 70 ^oC an alteration of the ionic liquid was visually observed. The ionic liquid became turbid in the first three hours and the turbidity increased with ongoing time until obtaining a white suspension in about 12 hours. After electrolysis for about 1 day a white precipitate was obtained in the bottom of the electrochemical cell. Afterwards, the ionic liquid containing the electrolysis product was centrifuged to reclaim the precipitate. Finally, the white precipitate was washed several times with acetone to remove the residual ionic liquid. The SEM micrograph shows that the powder contains fine crystallites with an average size of about 200 nm. Interestingly, all the XRD peaks recorded for the obtained powder can be perfectly indexed to the data available in the JPCD diffraction file, thus indicating that pure CuF_2 is the yield of the anodic dissolution of copper in [BMP]Tf_2N at 70 ^oC. The Tf_2N anion can easily be decomposed under mild anodic conditions during anodic oxidation of copper in the ionic liquid [BMP]Tf_2N at 70 ^oC leading to the formation of CuF_2. However, at room temperature no significant decomposition was obtained. Therefore, one has to be very careful in applying ionic liquids based on Tf_2N anions under anodic conditions.

5. Outlook

The present work shows, electrodeposition of adherent nano- and micro- Al layers on mild steel from different ionic liquids were investigated. The employed ionic liquids are, $AlCl_3$/1-ethyl-3-methylimidazolium chloride ($AlCl_3$/[EMIm]Cl), $AlCl_3$/l-benzyl-3-methyl-imidazolium chloride ($AlCl_3$/[BzMIm]Cl), $AlCl_3$/l,3-dibenzylimidazolium chloride ($AlCl_3$/[DBzIm]Cl), $AlCl_3$/1-ethyl-3-methyl-imidazolium bis(trifluoro-methylsulfonyl) amide ($AlCl_3$/[EMIm]Tf_2N) and $AlCl_3$/1-butyl-1-methyl-pyrrolidinium bis(trifluoromethylsulfonyl) amide ($AlCl_3$/[BMP]Tf_2N).

The results obtained here might give rise to further studies:

- Electrodeposition of other Al containing alloys on mild steel by using new types of ionic liquids that are electrochemically more stable such as 1-butyl-1-methylpyrrolidinium tris(pentafluoroethyl)trifluorophosphate ([BMP]FAP) and 1-butyl-1-methylpyrrolidinium trifluoromethylsulfonate ([BMP]TFO).
- Anodic dissolution of Cu and/or other metals in more stable ionic liquids such as 1-butyl-1-methylpyrrolidinium tris(pentafluoroethyl)trifluorophosphate ([BMP]FAP) and 1-butyl-1-methylpyrrolidinium trifluoromethylsulfonate ([BMP]TFO) at different temperatures.
- Decomposition of Tf_2N based ionic liquids throughout the anodic dissolution reaction of different transition metals.
- Morphological examinations, adhesion strength and corrosion performances of such coatings will be employed.

6. References

[1] J. H. Davis, Chem. Lett., **33** (2004) 1072, 1075.

[2] F. Endres and S.Z. El Abedin, Phys. Chem. Chem. Phys., **8** (2006) 2101.

[3] S. T. Handy, M. Okello and G. Dickenson, Org. Lett., **5** (2003) 2513.

[4] S. Fujita, H. Kanamaru, H. Senboku and M. Arai, Int. J. Mol. Sci. **7**(2006) 438.

[5] P. Wasserscheid and W. Keim, Angew. Chem. Int. Ed., **39** (2000) 3772-3776.

[6] H. Ohno, "Electrochemical Aspects ionic liquids", John Wiley&Sons, Inc., New Jersy, (2005) 1,7,27,35,75,111,173,187.

[7] P. Walden, Bull. Acad. Sci. (St. Petersburg), (1914) 405.

[8] F. N. Hurley, T. P. Wier, J. Electrochem. Soc., **98** (1951) 207.

[9] C. G. Swain, A. Ohno, D. K. Roe, R. Brown and T. Maugh II, J. Am. Chem. Soc., **89** (1967) 2648.

[10] H. L. Chum, V. R. Koch, L. L. Miller and R. A. Osteryoung, J. Am. Chem. Soc., **97** (1975) 3264.

[11] J. Robinson and R. A. Osteryoung, J. Am. Chem. Soc., **101** (1979) 323.

[12] J. S. Wilkes, J. A. Levisky, R. A. Wilson and C. L. Hussey, Inorg. Chem., **21** (1982) 1263.

[13] T. B. Scheffler, C. L. Hussey, K. R. Seddon, C. M. Kear and P. D. Armitage, Inorg. Chem., **22** (1983) 2099.

[14] D. Appleby, C. L. Hussey, K. R. Seddon and J. E. Turp, Nature, **323** (1986) 614.

[15] S. E. Fry and N. J. Pienta, J. Am. Chem. Soc., **107** (1986) 6399.

[16] J. A. Boon, J. A. Levisky, J. L. Pflug and J. S. Wilkes, J. Org. Chem., **51** (1986) 480.

[17] Y. Chauvin, B. Gilbert and I. Guibard, J. Chem. Soc. Chem. Commun., (1990) 1715.

[18] R. T. Carlin and R. A. Osteryoung, J. Mol. Catal., **63** (1990) 125.

[19] J. S. Wilkes and M. J. Zaworotko, J. Chem. Soc. Chem. Commun., (1992) 965.

[20] F. Endres, Phys. Chem. Chem. Phys., **3** (2001) 3165.

[21] Y. Chauvin, L. Mussmann, H. Olivier, Angew. Chem. Int. Ed., **107** (1995) 2941.

[22] P. Bonhôte, A. Dias, N. Papageorgiou, K. Kalyanasundaram and M. Grätzel, Inorg. Chem., **35** (1996) 1168.

[23] J. Fuller and R. T. Carlin, in Molten Salts, ed. P. C. Trulove, H. C. De Long, G. R. Stafford and S. Deki, PV 98-11, The Electrochem. Soc. Proceedings Series, Pennington, NJ, (1998) 227.

[24] D. R. MacFarlane, P. Meakin, J. Sun, N. Amini and M. Forsyth, J. Phys. Chem. B, **103** (1999) 4164.

[25] H. Ohno, "Electrochemical Aspects ionic liquids", John Wiley&Sons, Inc., New Jersy, (2005).

[26] M. Koel, "Ionic Liquids in Chemical Analysis", Taylor & Francis Gp., CRC Press LLC, USA, (2009) 1-15.

[27] M. Freemantle, Chem. Eng. News, **76**(1998) 32.

[28] R. D. Rogers and K. R. Seddon, Sci., **302** (2003) 792.

[29] R. Renner, Environ. Sci. Technol., **35** (2001) 410A.

[30] I. Krossing and J. M. Slattery, J. Phys. Chem., **220** (2006) 1343.

[31] J. M. Slattery, C. Daguenet, P. Dyson, T. J. S. Schubert and I. Krossing, Angew. Chem., **119** (2007) 5480.

[32] S. Caporali, A. Fossatia, A. Lavacchia, I. Perissia, A. Tolstogouzova and U. Bardia, Corros. Sci., **50** (2008) 534.

[33] S. Zein El Abedin, J. Phys. Chem., **220** (2006) 1293.

[34] M. Uerdingen, C. Treber, M. Balser, G. Schmitt and C. Werner, Green Chem. **7** (2005) 321.

[35] A. B. Tolstoguzov, U. Bardi and S. P. Chenakin, Bull. Russ. Acad. Sci., Phys., **72** (2008) 605.

[36] M. Yoshizawa, W. Xu, C. A. Angell, J. Am. Chem. Soc., **125** (2003) 15411.

[37] J. G. Huddleston, A. E. Visser, W. M. Reichert, H. D. Willauer, G. A. Broker and R. D. Rogers, Green Chem. **3** (2001) 156.

[38] D. W. Armstrong, L. He and Y.-S. Liu, Anal. Chem. **71** (1999) 3873.

[39] J. G. Huddleston and R. D. Rogers, Chem. Commun., (1998) 1765.

[40] P.-Y. Chen and I. W. Sun, Electrochim. Acta, 45 (1999) 441.

[41] J. D. Holbrey, A. E. Visser and R. D. Rogers, Ionic Liq. Synth., (2003) 68-81.

[42] P. C. Trulove and R. A. Mantz, in Ionic Liquids in Synthesis, ed. P. Wasserscheid and T. Welton, Wiley-VCH, Weinheim, (2003) 56-58,103-126.

[43] Q. Y., D. D. Dionysiou., J. Photochemistry and photobiology A: Chemistry **165** (2004) 229.

[44] A. Elaiwi, P. B. Hitchcock, K. R. Seddon, N. Srinivasan, Y.-M. Tan, T. Welton and J. A. Zora, J. Chem. Soc., Dalton Trans., (1995) 3467-3472.

[45] H. Stegemann, A. Rhode, A. Reiche, A. Schnittke and H. Füllbier, Electrochim. Acta, **37** (1992) 379-383.

[46] J. S. Wilkes, Green Chem. **4** (2002) 73.

[47] J. G. Huddleston, A. E. Visser, W. M. Reichert, H. D. Willauer, G. A. Broker and R. D. Rogers, Green Chem. **3** (2001) 156.

[48] K. N. Marsh, J. A. Boxall and R. Lichtenthaler, Fluid Phase Equilib., **219** (2004) 93.

[49] D. Morgan, L. Ferguson and P. Scovazzo, Ind. Eng. Chem. Res., **44** (2005) 4815.

[50] D. Gerhard, S. C. Alpaslan, H. J. Gores, M. Uerdingenc and P. Wasserscheid, J. Chem. Soc. Chem. Commun., (2005) 5080-5082.

[51] J. Jacquemin, P. Husson, A. A. H. Padua and V. Majer, Green Chem. **8** (2006) 172-180.

[52] K. R. Seddon, A. S. Stark and M.-J. Torres, ed. R. D. Rogers and K. R. Seddon, ACS Symposiom Series 901, Washigton DC, (2004).

[53] S. V. Dzyuba and R. A. Bartsch, ChemPhysChem, **3** (2002) 161.

[54] O. O. Okoturo and T. J. VanderNoot, J. Electroanal. Chem., **568** (2004) 167.

[55] P. A. Z. Suarez, S. Einloft, J. E. L. Dullius, R. F. De Souza and J. Dupont, J. Chim. Phys., **95** (1998) 1626.

[56] U. Shröder, J. D. Wadhawan, R. G. Compton, F. Marken, P. A. Z. Suarez, C. S. Consorti, R. F. de Souza and J. Dupont, New J. Chem., **24** (2000) 1009.

[57] Y. Chauvin, L. Mussmann, H. Olivier, Angew. Chem. Int. Ed., **34** (1995) 2698.

[58] M. A. Klingshirn, G. A. Broker, J. D. Holbrey, K. H. Shaughnessy and R. D. Rogers, Chem. Commun.,(2002) 1394.

[59] S. Park and R. J. Kazlauskas, J. Org. Chem., **66** (2001) 8395.

[60] M. J. Muldoon, C. M. Gordon and I. R. Dunkin, J. Chem. Soc., Perkin Trans. 2, (2001) 433.

[61] H. Olivier and L. Magna, J. Mol. Catal. A, **182-183** (2002) 419.

[62] P. He, H. Liu, Z. Li, Y. Liu, X. Xu and J. Li, Langmuir, **20** (2004) 10260.

[63] C.- C. Tai, F.- Y. Su and I.- W. Sun, Electrochim. Acta, **50** (2005) 5504.

[64] P. Y. Chen and I. W. Sun, Electrochim. Acta, **44** (1999) 441.

[65] P. Y. Chen, M.- C. Lin and I.- W. Sun, J. Electrochem. Soc., **147** (2000) 3350.

[66] P. Y. Chen and I.- W. Sun, Electrochim. Acta, **45** (2000) 3163.

[67] M. H. Yang and I.-W. Sun, J. Appl. Electrochem., **33** (2003) 1077.

[68] M. Schlesinger, M. Paunovic, Eds., "Modern Electroplating", Wiley & Sons, NY, (2000) 483.

[69] A. A. Tikhonov, P. M. Vyacheslavov and G. K. Burkat, Zh. Prikl. Khim., **54** (1981) 364.

[70] F. M. Dzhandubaeva, G. K. Burkat and P. M. Vyacheslavov, Zh. Prikl. Khim., **54** (1981) 2331.

[71] F. M. Dzhandubaeva, G. K. Burkat and P. M. Vyacheslavov, Zh. Prikl. Khim., **54** (1981) 2334.

[72] N.F. Reshetnikova, K.S. Pedan, Zh. Prikl. Khim., **55** (1982) 1996.

[73] P.M. Vyacheslavov, G.K. Burkat, A.A. Tikhonov, F.M. Dzhandubaeva, Zh. Prikl. Khim., **63** (1990) 436.

[74] S.-I. Hsiu , C.-C. Tai and I.-W. Sun, Electrochim. Acta, **51** (2006) 2607.

[75] J. F. Huang and I.-W. Sun, Adv. Funct. Mater., **15** (2005) 989.

[76] J. F. Huang and I.-W. Sun, Chem. Mater., **16** (2004) 1829.

[77] H. Y. Hsu and C. C. Yang, Z. Naturforsch., B, **58b** (2003) 1055.

[78] J. F. Huang and I.-W. Sun, Electrochim. Acta, **49** (2004) 3251.

[79] J. F. Huang and I.-W. Sun, J. Electrochem. Soc., **151** (2004) C8.

[80] J. F. Huang and I.-W. Sun, J. Electrochem. Soc., **150** (2003) E299.

[81] J. F. Huang and I.-W. Sun, J. Electrochem. Soc., **149** (2002) E348.

[82] J. F. Huang and I. W. Sun, Chem. Mater., **16** (2004) 1829.

[83] S. Zein El Abedin, H. K. Farag, E. M. Moustafa, U. Welz-Biermann and F. Endres, Phys. Chem. Chem. Phys., **7** (2005) 2333.

[84] I. Mukhopadhyay, C.L. Aravinda, D. Borissov and W. Freyland, Electrochim. Acta, **50** (2005) 1275.

[85] I. Mukhopadhyay and W. Freyland, Langmuir, **19** (2003) 1951.

[86] A. P. Abbott, G. Capper, D. L. Davies, H. L. Munro, R. K. Rasheed and V. Tambyrajah, Chem. Commun., **7** (2001)1010.

[87] A. P. Abbott, G. Capper, D. L. Davies and R. K. Rasheed, Chem.-Eur. J., **10** (2004) 3769.

[88] A. P. Abbott, G. Capper, D. L. Davies, R. K. Rasheed, J. Archer and C. John, Trans. Inst. Met. Finish., **82** (2004) 14.

[89] M. Galova, Surface Technology, **11** (1980) 357.

[90] W. H. Sanfranek, W. C. Schickner and C. L. Faust, J. Electrochem. Soc., **99** (1952) 53.

[91] R. A. Carpio, L. A. King, R. E. Lindstorm, J. C. Nardi and C. Hussey, J. Electrochem. Soc., **126** (1979) 1644.

[92] P. Singh, R. Singh, K. Rajeshwar and J. DuBow, J. Am. Chem. Soc., **102** (1980) 4676.

[93] P. Singh and K. Rajeshwar, J. Electrochem. Soc., **128** (1981) 1724.

[94] K. Rajeshwar, P. Singh and R. Thapar, J. Electrochem. Soc., **128** (1981) 1750.

[95] R. Thapar and K. Rajeshwar, J. Electrochem. Soc., **129** (1982) 560.

[96] A. R. Brukin, Production of Aluminium and Alumina, Critical reports in Applied Chemistry, Vol. 20. John Wiley, Chichester, U.K. (1987).

[97] Y.Zhao and T. J. VanderNoot, Electrochim. Acta, 42 (1) (1997) 3.

[98] M. W. M. Great, J. Electrochem. Soc., **132** (1985) 1308.

[99] T. Garai, Mater. Chem. Phys., **8** (1983) 399.

[100] R.J. Gale and R.A. Osteryoung, Inorg. Chem.,**18** (1979) 1603.

[101] J. Robinson and R. A. Osteryoung, J. Electrochem. Soc., **127** (1980) 122.

[102] C. L. Hussey, G. Mamantov and A. I. Popov, Eds., VCH Publs., NY, (1994) 227.

[103] T. Tsuda, C. L. Hussey and G. R. Stafford, J. Electrochem. Soc., 151, **6** (2004) C379.

[104] T. Tsuda, C. L. Hussey, G. R. Stafford and J. E. Bonevich, J. Electrochem. Soc., 150, **4** (2003) C234.

[105] T. Tsuda, C. L. Hussey, G. R. Stafford and O. Kongstein, J. Electrochem. Soc., 151, **7** (2004) C447.

[106] Q. Zhu, C. L. Hussey and G. R. Stafford, J. Electrochem. Soc., 148, **2** (2001) C88.

[107] T. Tsuda, C. L. Hussey and G. R. Stafford, J. Electrochem. Soc., 152, **9** (2005) C620.

[108] T. Jiang, M. J. C. Brym, G. Dube, A. Lasia and G. M. Brisard, Surface and Coatings Technol., 201, **1-2** (2006) 1.

[109] Q.X. Liu, S. Z. El Abedin and F. Endres, Surface and Coatings Technology, 201, 3-4 (2006) 1352.

[110] Q. Zhu and C. L. Hussey, J. Electrochem. Soc., 148, **5** (2001) C395.

[111] Q. Zhu and C. L. Hussey, J. Electrochem. Soc., 149, **5** (2002) C268.

[112] F. Endres, M. Bukowski, R. Hempelmann and H. Natter, Angew. Chem. Int. Ed., **42** (2003) 3428.

[113] D. FIoreani, D. Stech, J. Wilkes, J. Williams, B. Piersma, L. King and R. Vaughn, Proc. Power Sources Symp., **30** (1982) 84.

[114] P. K. Lai and M. Skyllas-Kazacos, J. Electroanal. Chem., 248 (1988) 413.

[115] R. T. Carlin, W. Crawford and M. Bersch, J. Electrochem. Soc., 139, **10**, (1992) 2720.

[116] S. Zein El Abedin, E. M. Moustafa, R. Hempelmann, H. Natter and F. Endres, Electrochem. Commun., **7** (2005) 1111.

[117] S. Zein El Abedin, E. M. Moustafa, R. Hempelmann, H. Natter and F. Endres, J. Phys. Chem., **7** (2006) 1535.

[118] E. M. Moustafa, S. Zein El Abedin, A. Shkurankov, E. Zschippang, A. Y. Saad, A. Bund and F. Endres, J. Phys. Chem. B, **111** (2007) 4693.

[119] A. B. McEwen, E. L. Ngo, K. LeCompte, J. L.Goldman, J. Electrochem. Soc., **146** (1999) 1687.

[120] H. Tokuda, S. Tsuzuki, M. A. B. H. Susan, K. Hayamizu, M. Watanabe, J. Phys. Chem. B, **110** (2006) 19593.

[121] N. V. Ignat'ev, U. Welz-Biermann, A. Kucheryna, G. Bissky, H. Willner, J. Flour. Chem., **126** (2005) 1150.

[122] P. Scherrer, Göttinger Nachrichten, **2** (1918) 98.

[123] G. R. Stafford and C. L. Hussey, in "Advances in Electrochemical Science and Engineering, Volume 7", Ed. by R. C. Alkire and D. M. Kolb, WILEY-VCH Verlag GmbH, Weinheim, GE, (2002) 275-281.

[124] P. S. Kulkarni, L. C. Branco, J. G. Crespo, M. C. Nunes, A. Raymundo, and C. A. M. Afonso, Chem. Eur. J., **13** (2007) 8484.

[125] F. Czerwinski, J. Electrochem. Soc., **143** (1996) 3327.

[126] F. Endres, in "Ionic Liquids in Synthesis", by P. Wasserscheid and T. Welton (Eds.), Wiley- VCH, 294 (2002).

[127] O. O. Okoturo, T. J. VanderNoot, J. Electroanal. Chem., **568** (2004) 167.

[128] N. Brausch, A. Metlen, P. Wasserscheid, Chem. Commun., **13** (2004) 1552.

[129] P. Eiden, Q. Liu, S. Zein El Abedin, F. Endres and I. Krossing, Chem. Eur. J., **15** (2009) 3433.

[130] E. Budevski, G. Staikov and W. J. Lorenz (Ed), "Electrochemical phase formation and growth", Wiley-VCH, Weinheim, (1996).

[131] L.E. Simanavicius and A. M. Levinskiene, Elektrokhimiya, **2** (1966) 353.

[132] P.C. Howlett, E. Izgorodina, M. Forsyth, D.R. MacFarlane, *Z. Phys. Chem.* **220** (2006) 1483.

[133] P. C. Howlett, N. Brack, A. F. Hollenkamp, M. Forsyth, and D. R. MacFarlane, *J. Electrochem. Soc.* **153** (2006) A595.

[134] S. Randström, G.B. Appetecchi, C. Lagergren, A. Moreno, S. Passerini, *Electrochim. Acta* **53** (2007) 1837.

[135] S. Randström, M. Montanino, G.B. Appetecchi, C. Lagergren, A. Moreno, S. Passerini, *Electrochim. Acta* **53** (2008) 6397

[136] S. Zein El Abedin, A.Y. Saad, H.K. Farag, N. Borisenko, Q.X. Liu and F. Endres, *Electrochim. Acta* **52** (2007) 2746.

[137] M. Forsyth, W.C. Neil, P.C. Howlett, D.R. MacFarlane, B.R.W. Hinton, N. Rocher, T.F. Kemp, and M.E. Smith, *Appl. Mat. Interf.* **1** (2009) 1045.

[138] V.S. Pervov, V.Ya. Leonidov, L.I. Klynev, A.G. Muravina, *Dokl. Akad. Nauk SSSR* **214** (1974) 1088.

Curriculum Vitae

Personal Information:

Name:	Amr Sayed Emam Ismail
Nationality:	Egyptian
Marital Status:	Married with three children
Sex:	Male
Date of Birth:	25th. Dec. 1979
E.mail:	amrchem@yahoo.com or amr.s.e.ismail@tu-clausthal.de
Languages:	Arabic (mother language), English and German

Current Address: Institut für Mechanische Verfahrenstechnik, Abteilung für Grenzflächenprozesse (Prof. Endres), der Technischen Universität Clausthal, Arnold-Sommerfeld-Straße 6, 38678 Clausthal-Zellerfeld, Germany.

Permanent Address: Department of Petrochemicals, Egyptian Petroleum Research Institute (EPRI),Cairo, Egypt.

Scientific Degrees:

1. M.Sc. (Organic Chemistry), 2004, M.Sc. Thesis examined "Synthesis and study of some modified polyesters" Helwan University, Egypt. Rank: first

2. B.Sc. (Chemistry) May 2000 with general estimation of "Very Good", Cairo University, Egypt. Rank: fourth

Academic Experience:

2000-2001:	Teaching Assistant: Helwan University, Chemistry Department (practical chemistry), Cairo, Egypt.
2001-2005:	Researcher Assistant: Egyptian Petroleum Research Institute, Petrochemicals Department, Cairo, Egypt.
2005-2006:	Assistant Researcher: Egyptian Petroleum Research Institute, Petrochemicals Department, Cairo, Egypt.
2006-present:	Assistant Research: Institute of Particle Technology, Clausthal University of Technology, Clausthal- Zellerfeld, Germany

Certificates and Scholarships:

- **December 2006-Present:** PhD scholarship from the Egyptian Government in Germany.
- **July 2006:** Germany Language Certificate, Goethe Institute (9th Primary Levels).
- **July 2006:** International Computer Driving Licence (ICDL) , UN - Eg - 0034.

Publications within the framework of this thesis

1. H. K. Farag, **A. S. Ismail**, N. Borisenko, S. Zein El Abedin and F. Endres, "On the electrodeposition of reactive metals from ionic liquids", *In Press*.

2. **A. S. Ismail**, S. Zein El Abedin, O. Höfft and F. Endres, "Unexpected decomposition of the bis (trifluoromethylsulfonyl) amide anion during electrochemical copper oxidation in an ionic liquid", Electrochem. Commun., **12** (2010) 909.